SYNAPTIC:

Structural, Functional and Chemical Assessments of the Visual Pathway in Retinal Disease

Rachel L.W. Hanson

Doctor of Philosophy

Cognitive Neuroscience and Neuroimaging

University of York

Department of Psychology

July 2020

Abstract

Retinal diseases including age-related macular degeneration (AMD) and retinitis pigmentosa (RP), have been associated with significant secondary structural changes to the posterior visual pathway. What has yet to be established is whether such cortical changes reflect atrophy (cortical shrinkage), demyelination (reduced axon myelination) and/or degeneration (cell death). Understanding the effects of retinal disease on the entire visual pathway and how this may differ with the type of retinal disease, will aid future techniques aimed to restore visual input and patient selection for such treatments

In this thesis, novel magnetic resonance imaging (MRI) and magnetic resonance spectroscopy (MRS) protocols were employed to quantify changes to the posterior visual pathway, specifically whether there is evidence of cortical atrophy, degeneration, or demyelination in retinal disease. Outcome measures from the anterior and posterior visual pathways were correlated to investigate potential biomarkers of disease progression. The penultimate chapter investigated how the Argus® II retinal prosthesis affects the structure and function of the visual cortex.

Chapters two and three reveals that significant cortical atrophy of the entire occipital cortex is observed in long-term unilateral and bilateral AMD. Pilot data from a small cohort of long-term bilateral RP patients, suggest some patients show signs of atrophy whilst other do not, although a larger sample is needed to draw definitive conclusions. Moreover, there were no significant signs of cortical degeneration or demyelination were observed in either retinal disease.

Chapters four and five reveal that reduced macular thickness, specifically the ganglion cell layer (GCL), is observed in both retinal diseases suggesting degeneration of the retina. Monitoring GCL thickness may be a sensitive biomarker of disease progression. This thesis also revealed that reduced cortical thickness in the occipital pole significantly predicts visual acuity performance in AMD, the first study to report such a finding.

Finally, in an individual AMD patient implanted with the Argus® II, 13-months post-surgery there was a very modest increase in cortical thickness of the occipital cortex yet diminished stimulus-driven responses. The success of restoring visual input in this case may well have been limited by the substantial cortical atrophy observed pre-surgery.

<u>Contents</u>

List of Tables

<u>List of Figures</u>

<u>Acknowledgements</u>

I would like to express my sincere gratitude to my academic supervisor Dr Heidi Baseler and clinical supervisor Professor Richard Gale for their unlimited guidance, support and encouragement throughout the course of this research.

My appreciation also goes to my TAP members, Professor Antony Morland and Dr Mark Hymers, for their support and guidance along with the ophthalmology research team at York Teaching Hospital, Dr Archana Airody, Alison Grice-Holt and Carol Sarginson, for their help and expertise.

Whilst I thank the wider research team at York Neuroimaging Centre, especially Dr Andre Gouws, Rebecca Lowndes and Martin Scott, a special thank you goes to my 'lab family' Holly Brown, Dr Richard Vernon and Dr Samuel Lawrence. The four of us united (albeit following copious amounts of cheese for one individual!) and helped each other survive our PhD's. Through thick and thin, you were there to cheer me up, listen to my struggles and ultimately provided the daily silliness which kept me on track. I could not have wished for a better lab family.

To my husband Dave, thank you for enduring the horrid person you have had to live with at times during the past 3 years! Along with our two dogs Winston and Edison, your patience, encouragement, and belief that I could finish this work has meant everything.

Finally, this research would not have been possible without all the enthusiastic and dedicated participants involved, both patients and control participants. I thank each and every one of you from the bottom of my heart for agreeing to take part in my research and especially for coming back time and time again!

Author Declaration

I declare that this thesis is a presentation of original work. This work has not previously been presented for an award at this, or any other, University. All sources are acknowledged as References.

Chapter 2. I was the principle investigator in this follow-up clinical research study led by Professor Antony Morland. Follow-up data was collected at a mean of 5 years following the original study. I was responsible for collecting all MRI data at York Neuroimaging Centre and for conducting all microperimetry assessments at York Teaching Hospital. All other clinical data (visual acuity and optical coherence tomography assessments) was collected by Professor Richard Gale and his ophthalmology research team at York Teaching Hospital. I was responsible for analysing all data, neuroimaging and clinical. Data, both neuroimaging and clinical, relating to the original study were collected by both Professor Antony Morland and his research team at York Neuroimaging Centre and Professor Richard Gale and his ophthalmology team at York Teaching Hospital.

Chapters 3, 4 and 5. I was the principle investigator in this clinical research study supervised by Professor Richard Gale and Dr Heidi Baseler. All MRI and MRS data was collected by myslef whilst clinical data was collected by myself (microperimetry assessments only) or Professor Richard Gale and his ophthalmology research team at York Teaching Hospital (visual acuity, optical coherence tomography and Humphrey visual field assessments). I was responsible for all data analysis. The MRS package was developed by Gülin Öz and Dinesh Deelchand for the semi-LASER sequence and provided by the University of Minnesota under a C2P agreement.

Chapter 6. Patients were recruited by the research team at Manchester Royal Eye Hospital under the supervision of Professor Paulo Stanga for their independent clinical trial study. In a separate study at the University of York, led by Dr Heidi Baseler, I was the lead researcher. Patient details were provided by Prof. Stanga and his team for those

who consented to hear more about the study at York. My role in this study was to contact and consent the patients, perform and analyse all MRI data.

The contents of this thesis have resulted in the following dissemination:

<u>Publications</u>

Chapter 2 is a direct replication of the following publication:

- **Hanson, R.L.W**., Gale, R.P., Gouws, A.D., Airody, A., Scott, M.T.W., Akthar, F., Waterson, S., Wells, M.T., Wright, A.J., Bell, K., Silson, E., Baseler, H.A and Morland, A.B. (2019). Following the status of visual cortex over time in patients with macular degeneration reveals atrophy of visually deprived brain regions. Investigative Ophthalmology and Visual Science, 60(15), 5045-5051.

<u>Conference abstracts and Invited talks</u>

Chapter 2:

- 2018 - The Association for Vision Research and Ophthalmology (ARVO). **R Woodall**, R Gale, A Gouws, M Scott, E Silson, K Bell, M Wells, A Wright, S Waterson, F Akthar, H Baseler and A Morland. Investigative Ophthalmology and Visual Science, 59(9), 5021. Reductions in primary visual cortex volume in patients receiving long-term treatment for neovascular age-related macular degeneration.
- 2017 - Symposium on Learning to see: From retinal to brain computations. The Rank Prize Fund. **Rachel L. Woodall**, Andre D. Gouws, Richard P. Gale, Antony B. Morland and Heidi A. Baseler. Using MRI to assess the benefit of ranibizumab treatment for age-related macular degeneration.
- 2016 – European Conference on Visual Perception (ECVP). **RL Woodall**, AD Gouws, RP Gale, AB Morland and HA Baseler. Perception, 45, 303-304. Using MRI to assess visual function during treatment for wet age-related macular degeneration.

Chapter 3:

- 2020 - Women in Vision UK/100% Optical. **Rachel L.W. Hanson,** Richard P. Gale, Archana Airody, Antony B. Morland and Heidi A. Baseler. SYNAPTIC: Structural, functional and chemical assessments of the visual pathway in vision loss.

Chapter 6:

- 2020 - Vision Sciences Society (VSS). **Rachel L.W. Hanson,** Richard P. Gale, Archana Airody, Paulo E. Stanga, Emmanouil Tsamis, Irene Siso-Fuertes, Jessy D. Dorn, Andy Fisher, Fiona I.J. Crawford, Mark Humayun, Robert J. Greenberg, Antony B. Morland and Heidi A. Baseler. Structural, functional and neurochemical assessments of visual cortex before and after implantation with the Argus II ® retinal prosthesis.

<u>**Chapter 1**</u>

Overview of the Human Visual System and Retinal Disease

1.1. The Human Visual System

Vision is the primary sense in humans and as such, vision processing is a multifaceted system. Understanding how vision is processed is vital when it comes to retinal disease or disorders which cause vision loss. Knowing how the system breaks down in these circumstances may help to inform new treatment strategies. Typically, ophthalmologists assess changes to the eye or the 'anterior visual pathway' however, the visual system includes both the eye and the brain, or the 'posterior visual pathway' and both elements of the visual pathway need to be intact for vision processing to take place. Therefore, it is essential that the entire visual pathway is assessed and considered when determining causes and effects of vision loss.

1.1.1. Anterior Visual Pathway

The anterior visual pathway encompasses the eyes, optic nerve, optic chiasm and optic tract. To begin, the basic concept of the anatomy of the eye is like a camera; at the optical surface, primarily the lens and cornea, light rays are refracted and focused on the light sensitive tissue of the retina. Between the lens and the retina lies the transparent vitreous gel which is attached to the retina at the pars plana.

Light energy is transduced into electrical signals by the retinal photoreceptor cells in the photo-transduction cycle. There are two types of photoreceptors, rods and cones. Rods, of which there are 130 million in the retina (Snell & Lemp, 1998), are more sensitive than cones. Rods are responsible for low light (scotopic) vision and are located principally in the peripheral part of the retina. The central part of the retina is called the macula, with a diameter of 5.5mm representing 18 degrees of the visual field, and the central part of the macula is called the fovea, with a diameter of 1.5mm representing 5 degrees of the visual field. It is the fovea where seven million cone cells (Snell & Lemp, 1998) are located which are responsible for vision in high illumination settings (photopic vision), allowing high acuity.

Information from rods and cones are received by bipolar cell dendrites with the body of bipolar cells forming the inner nuclear layer of the retina. Axons of bipolar cells

then contact the dendrites of retinal ganglion cells. Horizontal and amacrine cells are classed as interneurons of the retina, responsible for processing visual input from bipolar and retinal ganglion cells (Joukal, 2017).

Retinal ganglion cell axons run toward the posterior pole of the eye, passing through the wall of the eyeball at the optic papilla. The axons then constitute the optic nerve which emerges from each eye in the middle cranial fossa and meet in the optic chiasm. Here, fibres of the nasal hemiretinae cross to the contralateral optic tract while axons of the temporal hemiretinae remain uncrossed (Joukal, 2017). These axons then form the lateral root of the optic tract and continue to the lateral geniculate nucleus (LGN).

1.1.2. Posterior Visual Pathway

The posterior visual pathway commences at the LGN, which comprises of six cellular layers; three layers (layer 1, 4 and 6) receive information from the contralateral nasal hemiretinae, whilst the remaining layers (layers 2, 3 and 5) receive information from the ipsilateral temporal hemiretinae (Swienton & Thomas, 2014). Neurons of the LGN send their axons to the cortex via the optic radiations (Figure 1). Inferior fibres contain information relating to the superior visual field which travel anteriorly as the Meyer Loop, passing through the temporal lobe and terminating below the calcarine fissure of primary visual cortex in the medial surface of the occipital lobe. Superior fibres contain information relating to the inferior visual field which pass through the parietal lobe, terminating above the calcarine fissure in the superior part of primary visual cortex, V1 (Joukal, 2017; Swienton & Thomas, 2014).

The posterior visual pathway contains multiple maps of the visual world, including 'early' visual areas V1, V2 and V3. Early visual cortex occupies the medial wall of the occipital cortex; primary visual cortex (V1) occupies the calcarine sulcus, with V2 and V3 bordering V1 both dorsally and ventrally. The central part of our visual field (where visual acuity is highest) is located posteriorly at the occipital pole and has a much larger representation in visual cortex; this is referred to as cortical magnification. Approximately, 50% of the occipital lobe is dedicated to processing the central 5 degrees visual field. The focus of this thesis will be on retinal disease affecting the central and/or peripheral visual field. As such, references to the posterior visual pathway will refer to

primary visual cortex, V1, specifically the occipital pole and calcarine sulcus which are known to represent the central and peripheral retina respectively.

Figure 1: *Cross-sectional view of the visual pathway. Visual information travels from the left (L) or right (R) visual field onto the corresponding retinal wall. This information then travels along the optic nerve to the corresponding lateral geniculate nucleus (LGN), along the axons of the optic radiations (OR), terminating in the primary visual cortex (PVC).*

1.2. Classification of Retinal Disease

Vision loss can also be characterised functionally by the region of the visual field affected. Throughout this thesis, vision loss will be categorised as either affecting the central visual field, or peripheral visual field and in some cases, both. Here, some of the most commonly diagnosed causes of vision loss will be described.

1.2.1. Central Retinal Disease

Age-related macular degeneration (AMD) is a progressive form of blindness affecting the central visual field. AMD is currently the leading cause of vision loss in developed countries; in the UK, 12% of all people over the age of 80 are affected (H. D. H. Brown, Woodall, Kitching, Baseler, & Morland, 2016). There are two types of this condition: dry-AMD, the early and most common form, which is less severe but so-far untreatable; and wet-AMD, an advanced, treatable, and less common form.

Dry-AMD results in progressive atrophy of the retinal pigment epithelium (RPE), choriocapilliaris and photoreceptors. A central scotoma, caused by a build-up of drusen in the RPE, damages the photoreceptor cells leading to central blindness. Roughly 10% of dry-AMD cases progress into wet-AMDknown clinically as neovascular-AMD (nvAMD), which is characterised by choroidal neovascularisation (CNV), which is a process involving the growth of abnormally fragile blood vessels under and through the layers of the retina. These blood vessels leak, allowing the build-up of fluid in the macula, a region of the retina responsible for central vision. This fluid, along with accumulated cellular waste (drusen) causes the detachment and scarring of the macula, damaging its delicate photoreceptor cells, resulting in a growing blind spot, known as a scotoma (Holz, Pauleikhoff, Klein, & Bird, 2004)**.** The treatment often used for nvAMD in the UK is the intravitreal injection of one of a group of drugs known as anti-vascular endothelial growth factor (anti-VEGF), which work by perturbing the function of the protein VEGF responsible for CNV, to reduce leakage (Nowak, 2006)**.** In the UK, nvAMD accounts for more than half of all cases of registered sight and severe sight impairment (Rostron & McKibbin, 2012).

1.2.2. Peripheral Retinal Disease

Retinitis pigmentosa (RP) is the most common inherited retinal degeneration worldwide (Shintani, Shechtman, & Gurwood, 2009). Characterised by the progressive loss of rod and cone photoreceptors, RP affects about 1 in 4000, with around 1 million individuals affected (Hartong, Berson, & Dryja, 2006). Typically, manifestations arise between adolescence and early adulthood, but the range of onset can vary considerably, along with disease severity even within the same family (Berson, 2007). Peripheral vision loss is typically associated with night blindness, but as the disease progresses, patients develop tunnel vision as the far peripheral vision is lost, finally losing central vision by the age of 60 years (Hartong et al., 2006).

1.3. Clinical Assessments of Retinal Disease

Performance of the anterior visual pathway is often assessed within the eye clinic using a multitude of techniques. The methods used throughout this thesis have been split into those assessing structural and functional performance of the anterior visual pathway.

1.3.1. Structural Assessments

Optical coherence tomography (OCT) is a relatively quick examination of the eye, providing cross-sectional 3D images of the retina, optic disc and anterior segments. OCT is widely used to aid diagnosis and management of many ocular diseases, such as AMD, glaucoma, RP, central serous retinopathy, and macular oedema.

Numerous morphologic parameters can be assessed including central retinal thickness (CRT), which is ranked the most readily available and most intuitive to interpret (Ou, Brown, Payne, & Wykoff, 2017). Many clinical trials use CRT as a complementary outcome to visual performance. OCT is particularly useful is assessing nvAMD, providing information on whether excess fluid is present in the retina. nvAMD is primarily treated in form of anti-VEGF ocular injections. OCT-measured CRT has revealed significant decreases in retinal fluid with the anti-VEGF agent ranibizumab (Airody, Venugopal, Allgar, & Gale, 2015), a result confirmed by other studies albeit over shorter time periods for groups treated with both ranibizumab and aflibercept anti-VEGF agents (Keane et al., 2008; J. H. Kim, Lee, Chang, Kim, & Kim, 2016).

OCT assessments can also provide additional measurements to CRT. For example, retinal diseases including RP , OCT is used to assess differences in thickness of the retinal layers, including the retinal nerve fibre layer (RNFL), ganglion cell complex (GCCx) and ganglion cell layer (GCL). In RP, OCT is also used to evaluate the structural integrity of the inner and outer retinal layers, including peripapillary RNFL. Whilst studies have reported high variability in RP patients, with peripapillary RNFL thickness either increasing, decreasing or remaining within normal limits (Anastasakis, Genead, McAnany, & Fishman, 2012; Walia, Fishman, Edward, & Lindeman, 2007), evaluating these changes would appear prudent if patients are to be considered for therapeutic trials.

1.3.2. Functional Assessments

Visual acuity (VA) has been established as the most important outcome for clinical trials for new ophthalmic pharmaceutical agents (Ou et al., 2017). Therefore, VA is considered a primary endpoint in clinical research with the most common method of assessment being the Early Treatment Diabetic Retinopathy Study (ETDRS) letter chart (ETDRS, 1985). ANCHOR and MARINA were two early clinical trials reporting the effects of anti-VEGF treatment for nvAMD. These studies revealed significant increases in VA by 15 letters or more following ranibizumab injections; a benefit which was maintained at 24-month follow-up (D. M. Brown et al., 2006; Rosenfeld et al., 2006). These were the first reports to show vision loss prevention in nvAMD with ranibizumab treatment. Many research studies have since reported similar findings with other types of anti-VEGF treatment such as aflibercept (J. H. Kim et al., 2016). More importantly, studies have also reported that stabilisation of vision is maintained in nvAMD patients longitudinally, assessed over a 5 year period (Airody, Venugopal, Allgar, & Gale, 2015). In RP patients who have a small area of preserved retinal function in the central macula, visual acuity can remain normal whereas in other cases, visual acuity can be lost earlier in the disease (Hartong et al., 2006).

Visual field assessments are another common measure of functional vision, covering wide-field peripheral functioning and more central assessments to capture the macula. Typically, RP research employs wide-field assessments to capture retinal function using Goldmann perimetry or the Humphrey visual field analyser. Studies have shown that midperipheral scotomas with asymmetrical visual field loss is associated with RP, with initial preservation of the central visual field (S. Grover, Fishman, Anderson, Alexander, & Derlacki, 1997; Sandeep Grover, Fishman, & Brown, 1998). Progressive loss of visual function has also been linked with significant loss of the central visual field (Hirakawa, Iijima, Gohdo, Imai, & Tsukahara, 1999; Holopigian, Greenstein, Seiple, & Carr, 1996). Microperimetry is a more focused assessment of central macular functioning and is regularly used in retinal disease including AMD, revealing decreased retinal sensitivity with disease severity (Dinc, Yenerel, Gorgun, & Oncel, 2008; Vujosevic et al., 2011).

Both structural and functional assessments are often conducted in vision loss research to observe correlations following treatment and to compare outcomes from different techniques. For example, changes in RNFL and GCL appear to vary considerably with RP, appearing thinner (Humayun, Prince, et al., 1999; Oishi et al.,

2009; Vámos et al., 2011) and thicker (Hood et al., 2009; Vámos et al., 2011) compared to sighted controls. In a larger review of six prospective clinical trials of AMD patients, no correlations were observed between measures of CRT and BCVA (Ou et al., 2017), with similar findings observed across other studies (Ristau et al., 2014; SPAIDE et al., 2006).

Whilst this section has summarised just a few techniques used within the eye clinic to measure visual performance; these techniques are only assessing the anterior visual pathway. As previously mentioned, vision processing requires the entire visual system to work in synchrony. Therefore, when assessing cases of visual disease and loss, it is vital to consider potential changes occurring to the posterior visual pathway.

1.4. Neuroimaging Assessments of Retinal Disease

Magnetic resonance imaging (MRI) is a non-invasive technique for measuring the function, structure, and neurochemistry of the human brain. Approximately 20% of cortex in the human brain is dedicated to visual processing, spanning the occipital lobe (Wandell, Dumoulin, & Brewer, 2007). MRI of this posterior visual pathway can therefore allow for correlations with clinical assessments of the anterior visual pathway to allow further understanding of underlying mechanisms in different clinical presentation (H. D. H. Brown et al., 2016).

1.4.1. Functional Magnetic Resonance Imaging

Functional MRI (fMRI) has been used extensively to record how our visual world is mapped in the brain. In doing so, the variation in these maps in both health and disease can be determined. Before neuroimaging was available, (Holmes, 1918) outlined key features of how visual space is represented in human visual cortex using brain lesions caused by gunshot wounds. Neuroimaging research has since supported these original findings, demonstrating that visual cortex is topographically organised; spatial information is preserved, meaning neighbouring areas in the visual world are represented by neighbouring neurons in visual cortex (Holmes, 1918).

When visual input is diminished following sight loss via retinal disease or damage, research has shown that regions of cortex dedicated to processing parts of the affected visual field are subject to change (Baker, Dilks, Peli, & Kanwisher, 2008;

Baker, Peli, Knouf, & Kanwisher, 2005; Baseler, Gouws, et al., 2011). However, there is a debate in the literature regarding the definition of cortical reorganisation, but also the mechanism by which it may occur (Dilks, Baker, Peli, & Kanwisher, 2009). Cortical reorganisation frequently refers to functional brain changes whereby patterns of neural activation differ from those observed in healthy individuals. It has been proposed that the term 'reorganization' should be used only when the absence of visual input, combined with known properties of the normal visual system, cannot explain the pattern of activity observed in patients with visual loss (Dilks et al., 2009; Morland, 2015).

Central vision loss due to AMD for example, has generated much research into this area of reorganisation. Some researchers have evidenced cortical reorganisation occurs as the cortical region representing the lesioned retina (lesion projection zone; LPZ) takes on a new function and processes visual information from the cortical region representing intact retina (intact projection zone; IPZ) (Baker et al., 2008, 2005; Dilks et al., 2009; Dilks, Julian, Peli, & Kanwisher, 2014). Other researchers argue that the region of visual deficit must be absolute and include the fovea to generate reorganisation, because some patients with foveal sparing do not exhibit reorganisation (Baker et al., 2008). Additionally, the spread of activation in the LPZ is not always large-scale; in some cases, only part of the occipital pole is activated by stimuli presented to a small, intact part of the retina, suggesting a smaller, more local reorganisation is occurring in these individuals (Dilks et al., 2014). Other studies reporting LPZ activity in AMD suggest this is evidence of feedback from extrastriate visual areas and as such, this task-specific 'reorganisation' reveals existing feedback pathways (Masuda, Dumoulin, Nakadomari, & Wandell, 2008; Masuda et al., 2010).

AMD patients have also been shown to develop a preferred retinal locus (PRL) in part of the peripheral retina still intact. Typically, a PRL will develop in a region abutting the scotoma, but the location depends on the size and extent of the damaged retina (Cheung & Legge, 2005; Schumacher et al., 2008). It is thought that the establishment of a PRL may trigger reorganisation as it essentially takes on the function of the formerly intact fovea (Schumacher et al., 2008). Whilst some have shown greater LPZ activity to stimuli presented to the PRL compared to a peripheral location of equal eccentricity (Schumacher et al., 2008) others have argued there is no difference between peripheral locations (Dilks et al., 2009).

Comparatively, fewer studies have assessed functional changes resulting from peripheral vision loss such as retinitis pigmentosa (RP). Similarly to AMD studies, some researchers have reported evidence of reorganisation in RP, revealing task-dependent activity in the LPZ (Masuda et al., 2010), a shift of central retinal representations to more peripheral locations (Ferreira et al., 2017) whilst others have reported no evidence of reorganisation in the LPZ (Goesaert, Van Baelen, Spileers, Wagemans, & Op De Beeck, 2014). A lack of reorganisation, reported in AMD (Baseler, Crossland, et al., 2011; Smirnakis et al., 2005; Sunness, Liu, & Yantis, 2004) and RP (Goesaert et al., 2014) may be positive news with respect to treatment restoring retinal function; if cortex has not taken on a new role it is theoretically ready to resume processing incoming information.

1.4.2. Structural Magnetic Resonance Imaging

Structural MRI can reveal associated changes in the brain to several visual disorders, evidence of cortical atrophy due to diminished visual input. Primarily, research focuses on changes to cortical grey and white matter using analysis methods to measure changes in mean cortical thickness and volume. However, new novel acquisitions allowing the quantification of cortical myelination may provide additional information on how the visual cortex may change over time.

Structural abnormalities have been observed in a variety of studies assessing central vision loss from diseases such as AMD. These reports suggest significant reductions in grey and white matter within the posterior visual pathway, including the occipital pole, LGN, optic radiations and optic tract in AMD patents compared to age-matched sighted controls (Boucard et al., 2009; Hernowo et al., 2014; Malania, Konra, Jägle, Werner, & Greenlee, 2017; Plank et al., 2011). Some suggest this supports the transneuronal degeneration idea, whereby retinal degeneration at the fovea propagates back along the visual pathway causing atrophy in the retinotopically corresponding areas of cortex (Boucard et al., 2009; Hernowo et al., 2014). Significant thinning of primary visual cortex in macular degeneration has also been reported alongside significant increases in peripheral cortical representations (Burge et al., 2016). Here it is believed that compensatory recruitment of spared vision in those with central vision loss may explain the increase in cortical thickness of intact retinal representations.

Volumetric reductions of white matter in other non-visual cortical regions has been reported in AMD patients suggesting a potential link between AMD and Alzheimer's disease, although this warrants further investigations (Keenan, Goldacre, & Goldacre, 2014; Ohno-Matsui, 2011; Sivak, 2013).

Alterations to the posterior visual pathway associated with RP are not well researched. Of the few studies which have assessed such structural changes, no difference in cortical thickness has been reported compared to sighted control participants (Cunningham, Weiland, Bao, Lopez-Jaime, & Tjan, 2015; Ferreira et al., 2017), although one study has reported that as the disease advances, cortical volume decreases (Rita Machado et al., 2017). Another study concluded there is no evidence of cortical atrophy in RP due to a lack of correlation between cortical thickness decreases and visual sensitivity (Castaldi, Cicchini, Falsini, Binda, & Morrone, 2019). Considering that RP participants are generally targeted in trials assessing success of restorative treatments (Ahuja et al., 2011; Castaldi et al., 2016, 2019; da Cruz et al., 2016; Humayun et al., 2009; Luo, Davagnanam, & Dacruz, 2013; Luo, Zhong, & da Cruz, 2015; Rizzo et al., 2014), understanding how the visual cortex may change as a result of long-term vision loss is imperative to such devices working.

Myelin is essential for a healthy functioning nervous system as it expedites conduction of electrical signals along axons. Whilst myelinated fibres are abundant within the cortical white matter, significant amounts are also found within cortical grey matter (Shafee, Buckner, & Fischl, 2015). Myelin content is believed to covary with the intensity of T1-weighted (T1w) and T2-weighted (T2w) images, but in the opposite direction, and recent work has outlined a method to quantify cortical grey matter myelin content using a ratio of T1w and T2w images acquired during a normal MRI session (Glasser & Van Essen, 2011). A significant correlation has been found between myelination content and the retinotopic organisation of the visual cortex, with high myelin density in early visual areas, V1-V3 (Abdollahi et al., 2014; Sereno, Lutti, Weiskopf, & Dick, 2013). However, it is not known how myelin content may change in relation to other structural changes, associated with long-term vision loss. One could hypothesise that myelin content may reduce along with cortical thickness and volume, potentially indicating cortical atrophy due to diminished visual input but current research has not yet assessed this.

1.4.3. Magnetic Resonance Spectroscopy

Magnetic resonance spectroscopy (MRS) is an inherently quantitative technique since the signal intensity of a resonance is directly proportionate to a specific metabolite concentration. MRS data can therefore be analysed in conjunction with MRI to correlate anatomical and physiological changes in the brain. For this reason, MRS is a potential tool for studying the metabolic changes in visual cortex in vivo, providing direct clinical applications for studying brain plasticity and adaptive changes following sight loss (Bernabeu, Alfaro, García, & Fernández, 2009).

γ-aminobutyric acid (GABA) is the principle inhibitory neurotransmitter believed to be involved in a homeostatic balance between excitatory, inhibitory and modulatory pathways. Reduced resting GABAergic inhibition has been shown to trigger ocular dominance plasticity, modulating both the onset and offset of the critical period (H. D. H. Brown et al., 2016). Therefore, measuring GABA in response to visual stimulation following deprivation could be a sensitive indicator of plasticity.

Retinal damage is in continuous progress in glaucoma, RP and AMD. A number of mechanisms have been invoked to explain the effects of glaucoma, including reactive oxygen species, excitotoxicity, defective axon transport, trophic factor withdrawal and loss of electrical activity (Chang & Goldberg, 2012). These pathophysiological actions lead to a series of biochemical compound changes in brain tissue. For example, transsynaptic damage caused by excitotoxicity of glutamate (Glu) (as can be assessed by levels of the glutamate/glutamine complex (Glx)) is an important mechanism of glaucomatous central visual pathway injury. Using MRS to investigate metabolic concentrations in the striate area and geniculocalcarine tract, significant decreases in N-Acetyl-Aspartate:Creatine (NAA:Cr) and Choline:Creatine (Cho:Cr) ratios were detected, although there were no reported differences in concentrations of Glx:Cr in a group of glaucoma patients compared with sighted controls (Yan Zhang, Chen, Wen, Wu, & Zhang, 2013). These results suggest that within the central visual pathway in glaucoma, neurodegeneration is an ongoing process. If progressive visual deprivation affects the metabolism of the adult visual brain, lower concentrations of the metabolite NAA would be expected in occipital cortex, given the association between NAA and neuronal activity. However, one study reported no difference in either Cho, Cr or NAA absolute concentrations in the striate area in a group of glaucoma patients compared to AMD patients, relative to sighted controls (Boucard, Hoogduin, van der Grond, & Cornelissen, 2007). This indicates that within the visual pathways of the brain, progressive

retinal visual field defects do not always induce a measurable decrease in metabolite concentration.

A single MRS voxel of interest (VOI) can in theory be positioned anywhere in the brain as long as there is limited interference with the metabolic signal. One theory proposed as a factor in glaucoma is the apoptosis theory (programmed cell death). Therefore, one would expect to see an increase in metabolic concentrations of Glu in the vitreous humour and lateral geniculate body (LGB) regions due to the known neurotoxic effects of Glu. MRS was performed using a VOI in these two regions in a group of glaucoma patients. Analysis revealed significantly greater levels of Glx:Cr in both VOIs for the glaucoma patients compared to sighted controls, supporting the apoptosis theory in the aetiopathogenesis of glaucoma (Boucard et al., 2007). MRS could therefore move the diagnosis of glaucoma forward enhancing the understanding and diagnosing of glaucoma at the cellular level (Boucard et al., 2007).

1.4.4. Summary

To summarise, structural MRI investigating the effects of vision loss on the brain reveal significant alterations to cortical structure, with reductions to both white and grey matter in multiple regions along the posterior visual pathway. Correlating these observed alterations with clinical measures of the anterior visual pathway can aid our understanding of disease progression and ultimately, vision restoration. In addition to ophthalmological measures, including visual acuity, perimetry, optical coherence tomography and physical examination of the retina, fMRI aids our understanding of how the entire visual system is affected with eye disease, from the eye to the brain (Baker et al., 2008, 2005; Haak, Morland, & Engel, 2015; Masuda et al., 2008). Lastly, MRS can provide which neurochemical constituents change in the posterior visual pathway as a result of brief and long-standing visual deprivation.

1.5. Aims of the Thesis

Vision loss is of growing concern in our aging population; by 2020, it is estimated that 2.7 million people will be registered with sight loss. This estimation is believed to double to over 4 million by 2050 (RNIB, 2018). Therefore, understanding how the entire visual pathway, from the eye to the brain, is affected by visual disease, is essential.

A growing body of vision research is investigating techniques aimed at restoring visual input to those affected by such conditions outlined above, including retinal prostheses (Weiland & Humayun, 2014). Treatments have also been developed to help limit disease progression in the eye, including anti-VEGF for wet-AMD (D. M. Brown et al., 2006; Rosenfeld et al., 2006). However, success of such treatments depends on the posterior visual pathway remaining viable to receive and process restored visual input. Neuroimaging literature has revealed significant structural reductions of the posterior visual pathway in patients with vision loss, reporting decreased cortical volume of brain regions representing damaged retina (Boucard et al., 2009; Hernowo, Boucard, Jansonius, Hooymans, & Cornelissen, 2011; Hernowo et al., 2014). If these reductions in volume of the posterior visual pathway result from degeneration due to significant cell death, restoration techniques may be unsuccessful in patients with vision loss. However, if vision loss results in temporary atrophy of the posterior visual pathway; a shrinkage of the cortex, this may suggest a potential ability for the brain to return to processing visual information once input has been restored (Hensch & Fagiolini, 2005). Therefore, understanding how the posterior visual pathway responds to different types of vision loss will ultimately aid our understanding of how this pathway might respond once/if vision is restored.

The aim of this thesis is to examine the effects of long-term vision loss on both the anterior and posterior visual pathways. In a group of patients diagnosed with bilateral vision loss resulting from either central or peripheral retinal damage, or both, clinical assessments of the anterior visual pathway will be compared with neuroimaging measures of the posterior visual pathway. Neuroimaging research has revealed significantly decreased cortical volume of brain regions representing damaged retina. What has yet to be established is 1) whether this reduction represents a) atrophy: condensed cortex that remains plastic to restored visual input, b) demyelination: a reduction in myelin density or c) degeneration: reduced cortical volume due to cell death and 2) to what extent do changes in the anterior visual pathway influence changes in the posterior visual pathway.

1.5.1. Objectives

The primary objective will measure how the posterior visual pathway changes due to diminished visual input following vision loss. The hypotheses will be 1) reduced visual input due to retinal disease will result in reductions in cortical volume and thickness

which will represent evidence of cortical atrophy 2) reduced visual input may result in reduced myelin density evidencing demyelination 3) reduced visual input may result in cell death evidencing cortical degeneration via necrosis and/or apoptosis due to decreased Choline and increased Glutamate. Whilst it is hypothesised that cortical changes may be the result of either atrophy, demyelination or degeneration, it is important to note that long-term retinal disease may in fact result in a combination of these three possibilities.

The secondary objective will measure changes to the anterior visual pathway following vision loss and the relationship between changes in the brain and the retina. Here, the hypotheses will be 1) increased disease duration and reduced visual function will correlate with reduced cortical volume, thickness and myelin density; evidence of cortical atrophy and 2) scotoma size will correlate with decreased visual performance and amount of brain atrophy.

Chapter 2

Following the status of visual cortex over time in patients with macular degeneration reveals atrophy of visually deprived brain regions

2.1. Introduction

It has recently emerged that eye disease can result in secondary structural changes within primary visual cortex. This is true whether the eye disease is congenital, for example in ocular albinism (Von Dem Hagen, Houston, Hoffmann, Jeffery, & Morland, 2005), or acquired, for example in age-related macular degeneration (Boucard et al., 2009). Most commonly, atrophy demonstrated by a reduction in cortical thickness or volume, is reported in the retinotopic representation of the lesions that are a consequence of the disease (Aguirre et al., 2016; Boucard et al., 2009; Hernowo et al., 2014; Malania et al., 2017; Neveu, von dem Hagen, Morland, & Jeffery, 2008; Plank et al., 2011; Prins et al., 2016; Von Dem Hagen et al., 2005). Conversely, some studies have reported atrophy in retinotopic representations of intact but not lesioned retina in monocularly blind (Prins, Jansonius, & Cornelissen, 2017) and age-related macular degeneration (AMD) patients (Prins et al., 2016), whereas others revealed significant thickening of cortical representations of the intact retina, believed to be a compensatory phenomenon (Burge et al., 2016). Controversy therefore remains over the exact nature of the response of visual cortex to retinal disease and furthermore the timing of such changes.

AMD is an excellent model to study the consequences of vision deprivation as it leads to a loss of retinal input to the cortical representation of the central visual field. However, the most common form of the disease progresses slowly, and onset of visual loss is a challenge to pinpoint in time. However, the neovascular (nvAMD) form of the disease, characterised by fluid leakage and haemorrhage in the central macula, has an acute onset, therefore visual loss is well-defined (Lim, Mitchell, Seddon, Holz, & Wong, 2012). NvAMD generally manifests unilaterally, with disease onset in the second eye occurring in 50% of patients within 3-years following unilateral loss (A. Y. Lee et al., 2015).

To assess the time course of structural changes to visual cortex resulting from a loss of input, we recruited individuals recently diagnosed with onset of acute unilateral

nvAMD who had established bilateral retinal disease. As a result, a significant unilateral change of input to visual cortex was well-defined in time.

NvAMD affects 40,000 new people in the UK every year (NICE, 2018) and when left untreated, leads to severe sight impairment. Current treatment involves regular intraocular Anti-Vascular Endothelial Growth Factor (anti-VEGF) injections which restore around half the initially lost visual acuity (D. M. Brown et al., 2006a; J. H. Kim et al., 2016; Rosenfeld et al., 2006) by halting leakage, therefore decreasing central retinal thickness (Airody et al., 2015; Keane et al., 2008; J. H. Kim et al., 2016). Following an initial improvement of visual acuity by month 3, a long-term slow decline in visual acuity can be observed (Airody et al., 2015; Rofagha, Bhisitkul, Boyer, Sadda, & Zhang, 2013; Singer et al., 2012). The patients we tested received standard treatment to preserve and stabilize vision.

This study aimed to observe the short- and long-term nature of visual cortical changes in the context of unilateral visual loss due to nvAMD. Previous studies focussed on testing patients with established bilateral disease, between 1-42 years post-onset (Boucard et al., 2009; Burge et al., 2016; Hernowo et al., 2014; Malania et al., 2017; Prins et al., 2016). Therefore, our first objective was to determine whether cortical changes occurred over a short timescale of 3 months. The second objective, met by the opportunity to follow-up patients long-term, was to determine what changes occurred several years following the acute onset of unilateral nvAMD. The third objective was to establish whether cortical changes were atrophic and if they were specific to the cortical representation of the retinal lesion.

2.2. Materials and Methods

2.2.1. Participants

Written informed consent was obtained from all participants. This study followed the tenets of the Declaration of Helsinki with approval granted by York Neuroimaging Centre Research, Ethics and Governance Committee and the NHS Research Ethics Committee (IRAS: 27966, 199112).

Ten participants were recruited from York Teaching Hospital NHS Foundation Trust. Inclusion criteria was onset of acute unilateral nvAMD following progression from bilateral dry-AMD based on clinical examination. Thus, a significant reduction in input to visual cortex from unilateral disease was well-defined in time. Recruitment took place between January 2011 and November 2013. Routine clinical treatment was

administered in accordance with guidance from the National Institute of Health and Clinical Excellence (NICE, 2008).

Initial assessments and magnetic resonance imaging (MRI) were carried out prior to commencing routine anti-VEGF treatment for nvAMD, with short-term assessments taking place a mean of 3.5 months (range, 3-4 months) later in all 10 participants. Long-term assessments were carried out a mean of 4.8 years (range, 3.8 – 6.1 years) post-diagnosis in 7 participants in this group, because 2 participants did not join the follow-up component of the study for long-term assessments and 1 died. Our analysis was therefore restricted to assessing those 7 patients in whom we had measures at all time points. The mean age of participants at baseline was 73.5 years (range = 67.1 – 81.5 years), increasing to 77.9 years (range = 73.1 – 86.1 years) at follow-up (Table 1).

Table 1: Participant demographics.

Participant	Gender	Treated eye	Age (y, m)		MRI Visit	
			Baseline	Long-term assessment	Short-term assessment	Long-term assessment
P3	Male	Right	67, 11	73, 10	3 months	6.01 years
P5	Female	Right	75, 01	79, 09	3 months	4.08 years
P6	Male	Right	81, 05	86, 01	4 months	4.08 years
P7	Male	Right	71, 04	75, 09	3 months	4.05 years
P8	Female	Right	70, 00	73, 10	4 months	3.10 years
P9	Female	Right	70, 07	74, 03	4 months	4.10 years
P10	Male	Left	79, 00	82, 08	3 months	3.08 years

2.2.2. Design

In this longitudinal study, structural MRI was acquired at three intervals, a baseline assessment took place prior to participants receiving the first anti-VEGF treatment (month 0), a short-term assessment took place a mean of 3.5 months post-baseline with a long-term assessment occurring a mean of 4.8 years post-baseline (Table 1). Routine clinical assessments, detailed below, coincided with the MRI visits.

2.2.3. Procedures

2.2.3.1. MRI. Structural MRI was acquired using an eight-channel phased-array head coil tuned to 127.4 MHz, on a GE Healthcare 3 Tesla Signa HD Excite scanner. One T1-weighted anatomical volume was acquired (TR, 8ms; TE, 3ms; TI, 450ms; voxel size,

1.13 x 1.13 x 1mm^3, flip angle, 20^0; 256 x 256 matrix; FOV, 290mm). All participants were instructed to lie as still as possible during the scan. Foam padding was used around the head to minimise movement, with earplugs provided to protect against scanner noise.

2.2.3.1.1. Analysis. Cortical reconstruction and volumetric segmentation were performed using the Freesurfer analysis suite (version 5.3, available at: http://surfer.nmr.mgh.harvard.edu/). This process includes removal of non-brain tissue, intensity normalisation (Sled, Zijdenbos, & Evans, 1998), tessellation of the grey/white matter boundary, automated topology correction (Fischl, Liu, & Dale, 2001; Ségonne, Pacheco, & Fischl, 2007) and surface deformation following intensity gradients to optimally place the grey/white matter and grey/cerebrospinal fluid boundaries at the location where the greatest shift in intensity defines the transition to the other tissue class.

Cortical anatomy was assessed in two ways with the following rationale. We first assessed grey matter volume of occipital cortex. This coarse measurement has the advantage of not being susceptible to individual differences in the cortical representations of the visual field whilst also capturing representations outside primary visual cortex. At the same time, however, analysis of the whole occipital cortex does not allow hypotheses concerning the retinotopic nature of cortical changes. We turned therefore, to a more focussed region of interest (ROI) analysis, gathering information explicitly testing regions of primary visual cortex representing lesioned and intact retina. The occipital pole and calcarine sulcus were selected as they coincide with the lesion and intact projection zones for individuals with central visual loss. In defining such regions on the cortical surface, cortical thickness offers a sensible way to gauge the status of the visual representation that can be compared over time. Our target areas of the brain were defined using Freesurfer's Destrieux Atlas using the following parcellations; occipital cortex: 2, 11, 19, 20, 22, 42, 44, 51, 57, 58, 59, 65; lesion projection zone: 42; intact projection zone: 44 (Destrieux, Fischl, Dale, & Halgren, 2010) (see Figure 2A).

Mean grey matter volume was extracted from each parcellation within the occipital cortex ROI, from both the left and right hemispheres. An average across hemispheres was then calculated for each participant, creating the final entire occipital cortex ROI. A paired-samples t-test assessed changes in cortical volume between the three intervals. Mean cortical thickness was extracted following this same procedure for the lesion and intact projection zones, calculated as the shortest distance between the

grey/white matter boundary and the grey/cerebrospinal fluid boundary at each vertex across the cortex in millimetres (mm), averaged over all vertices within each ROI (see Figure 1). A paired-samples t-test assessed changes in cortical thickness within each ROI between the same three intervals.

2.2.3.2. Routine clinical assessments. Best corrected visual acuity and central retinal thickness were acquired in all 7 participants at all time points

2.2.3.2.1. Best Corrected Visual Acuity. Standard clinical visual acuity was measured in an illuminated room at 4 meters, with the participant's spectacle correction in each eye using an ETDRS (Early Treatment Diabetic Retinopathy Study) letter chart (ETDRS, 1985). If participants were able to read four or more of the five letters on the first line of the chart they were asked to continue reading down the chart until they could read fewer than three letters on a single line. At this point, the total number of letters read correctly was recorded and an additional 30 letters were added to the total. If participants were unable to read 4 letters correctly on the first line, they were brought to 1 meter and asked to continue reading down the chart until they could read fewer than three letters on a single line. Thirty letters were not added to the final ETDRS score in this circumstance.

2.2.3.2.2. Central retinal thickness. Effectiveness of anti-VEGF treatment in reducing the consequence of choroidal neovascularisation over time can be measured using central retinal thickness. A reduction in central retinal thickness will indicate resolution of the oedema due to treatment. This was measured using $1mm^3$ subfield central retinal thickness with spectral-domain optical coherence tomography (Cirrus OCT, Carl Zeiss Meditec, Dublin, CA). A standard macular cube (128 x 256 x 518) assessment took place in an illuminated room, acquiring retinal images through dilated pupils for the treated and untreated eyes of each participant.

2.2.3.2.3. Analysis. Changes in best corrected visual acuity and central retinal thickness were analysed for the treated and untreated eyes at each session. As ETDRS letter scores and central retinal thickness values did not pass tests for normality (Shapiro-Wilk, $p < 0.001$ 0.000), a Wilcoxon signed rank test assessed changes over time.

Figure 1. T1-weighted MRI image showing the boundary between the white and gray matter surface, referred to as the white surface (yellow line) and the gray matter and CSF, referred to as the pial surface (red line). The distance between the white and pial surfaces gives the thickness at each location of cortex (white line).

A Region of Interest

B Occipital Cortex

C Intact Projection Zone
(Calcarine sulcus)

D Lesion Projection Zone
(Occipital pole)

Figure 2. *Regions of interest (ROIs) and their anatomical properties.* *A:* *Surface reconstruction of a template brain with the occipital lobe (blue), lesion projection zone (red) and intact projection zone (green). Note that the latter two ROIs constitute elements of the larger occipital lobe ROI.* *B:* *Volume of grey matter measured in the occipital lobe ROI at the three times of measurement. T1 refers to the baseline measure, T2 refers to the short-term assessment and T3 refers to the long-term assessment. Also plotted is the cortical thickness of grey matter detected within the intact projection zone* *(C)* *and lesion projection zone* *(D)* *ROIs at three times of measurement. Line graphs for B-D represent individual changes in cortical structure for each participant at each time point. In panels B-D statistically significant differences at p<0.05 are indicated with an * and error bars represent +/- one standard error of the mean.*

2.3. Results

2.3.1. MRI

Our first and second objectives set out to determine whether cortical changes occurred within the initial treatment period following the onset of unilateral nvAMD (short-term) and what cortical changes occurred over time (long-term). Compared to baseline, we reveal no significant changes in cortical volume at the short-term assessment (31,580mm^3, t(6) = 0.757, p = 0.478) however, there is a significant reduction in cortical volume at long-term follow-up (31,767mm^3 versus 28,639mm^3, t(6) = 3.033, p = 0.023) - indeed 6 of the 7 participants showed a reduction in volume. There was also a significant difference in cortical volume between the short-term and long-term assessments (t(6) = 2.689, p = 0.036) (Figure 2B).

We next asked whether changes in volume were reflected by cortical atrophy: a thinning of cortex in identifiable retinotopic representations of the retinal lesion. The two regions we selected showed different results (Figure 2C&D). In the intact projection zone, mean cortical thickness changed very little (Figure 2C); neither short-term (1.81mm, t(6), 1.218, p = 0.269) nor long-term (1.76mm, t(6) = 1.021, p = 0.347) assessments yielded significant differences compared to baseline (1.82mm). There was also no significant difference between the short- or long-term assessments (t(6) = 0.793, p = 0.458). In contrast, the lesion projection zone was significantly thinner at the long-term (1.94mm, t(6) = 2.389, p = 0.027, one-tailed), but not short-term (2.08mm, t(6) = 1.857, p = 0.113) assessments compared to baseline (2.11mm), with a significant difference between the short- and long-term assessments (t(6) = 2.467, p = 0.025). Although there is not a significant interaction between timepoint and ROI, these data are suggestive that cortical atrophy is a feature present at long-term follow-up and larger in the cortical representation of the lesioned retina.

While results indicate anatomical changes in visual areas of the brain are atrophic and retinotopic, we wanted to check whether age-dependent changes in the whole brain explained any effects detected. Cortical thinning associated with natural aging is well documented, although there is some discrepancy whether cortical thinning of primary visual cortex occurs with increasing age (Fjell et al., 2009; McGinnis, Brickhouse, Pascual, & Dickerson, 2011) or not (Lemaitre et al., 2012; Thambisetty et al., 2010). Griffis et al. reported age-dependent cortical thinning specific to peripheral but not central representations of visual cortex (Griffis, Burge, & Visscher, 2016). To

investigate whether reductions in mean thickness observed in this study are not simply a consequence of natural aging, a linear regression analysis investigated changes to the lesion and intact projection zones in relation to changes to the whole brain. Excluding the occipital lobes, changes in the whole brain significantly accounted for 65% of the variance observed in the intact projection zone, ($F(1, 6) = 9.28$, $p = 0.029$) but only 31% of the variance in the lesion projection zone ($F(1, 6) = 2.32$, $p = 0.189$). Although there was no significant difference between the two ROIs, because the whole-brain effects accounted for more of the variance in the intact projection zone, the data are suggestive that the reductions in cortical thickness of the lesion projection zone are due to decreased retinal input rather than aging.

2.3.2. Disease progression over time

What factors might determine the changes we observed in visual cortex? If the retinal lesions remain relatively stable over time, it is likely that cortical atrophy was a result of the duration of reduced input to cortex. However, if the retinal lesion progresses over time, we would be unable to dissociate the effects of disease progression and time on cortical atrophy. To monitor disease progression, measures of visual acuity and central retinal thickness were taken, coinciding with the MRI timepoints.

Visual acuity measures are shown in Figure 3A. Median acuity across the 7 participants was below the normal range in both treated and untreated eyes due to longstanding vision loss associated with bilateral dry AMD. Short-term assessments show visual acuity increased in the treated eye compared to baseline but not significantly (T2 vs. T1: $Z = -1.690$, $p = 0.091$). At long-term follow-up, acuity was still improved relative to baseline, but again not significantly (T3 vs. T1: $Z = -0.676$, $p = 0.499$). A similar pattern of results was observed for the untreated eye, with no significant changes in acuity between baseline and short-term (T2 vs. T1: $Z = -1.951$, $p = 0.051$), or baseline and long-term follow-up (T3 vs. T1: $Z = -0.169$, $p = 0.866$). As can be seen in Figure 3C, a decrease in visual acuity is evident in the untreated eye for 5 of 7 participants between the short- and long-term assessment (T2 vs. T3). Although the changes are not significant, the gradual decline in visual acuity could indicate changes in cortical input over time.

We also tracked any changes in retinal anatomy with treatment by measuring central retinal thickness as an indicator of resolved oedema (Figure 3D). Compared to

baseline, there was a significant decrease in central retinal thickness at the short-term assessment in the treated eye (T2 vs T1: $Z = -2.366$, $p = 0.018$), which remained significant at long-term follow-up (T3 vs T1: $Z = -2.366$, $p = 0.018$). For the untreated eye, although a decrease in central retinal thickness was observed in 5 of 7 participants, this was not significant, either between baseline and short-term (T2 vs T1: $Z = -0.254$, $p = 0.799$) or baseline and long-term follow-up (T3 vs T1: $Z = -0.507$, $p = 0.612$) with data remaining within the normal range.

Taken together, measures of visual function and retinal anatomy appear to indicate that although vision was subnormal in both eyes, it was largely stable over the period of our study. This suggests that treatment was successful in halting disease progression in the treated eye with central retinal thickness indicating resolution of the oedema. Nevertheless, a gradual decline in both eyes in some participants means we cannot assert that there is no change to the input to cortex over time.

Figure 3: Clinical assessments. A: Box plots showing visual acuity performance measured in ETDRS letter score for the treated eye (orange) and the untreated eye (cyan). Horizontal dashed line represents an ETDRS score of 84 letters, equivalent to 6/6 Snellen acuity, or 0.0 logMAR. D: Box plots showing changes in central retinal thickness for the treated eye (orange) and the untreated eye (cyan). Horizontal dashed lines represent a healthy central retinal thickness range for the Cirrus SD-OCT machine (Sabouri, Kazemnezhad, & Hafezi, 2016). *Horizontal lines represent the median, the upper and lower whiskers represent scores outside the middle 50%, whilst outliers are shown as points. Line graphs show individual changes in performance over time for each participant for the treated eye (**B / E**) and the untreated eye (**C / F**). Black arrows on plots **B** and **C** represent an ETDRS score of 84 letters, equivalent to 6/6 Snellen*

*acuity, or 0.0 logMAR whereas on plots **E** and **F** they represent a healthy central retinal thickness range for the Cirrus SD-OCT machine* (Sabouri et al., 2016). *All assessments were measured at three time points: T1 (baseline), T2 (short-term) and T3 (long-term assessment).*

2.4. Discussion

This study shows, for the first time, the time course of structural changes to visual cortex following the onset of acute unilateral vision loss due to nvAMD. We report that atrophy (shrinkage) of visual cortex, detectable in a small number of individuals followed longitudinally, is also retinotopic as it was detected in the representation of the central visual field, that is, the macular lesion projection zone. Atrophy was not detected over the initial treatment period of 3-4 months but developed over several years.

Our findings reinforce the evidence for retinotopic and atrophic changes in the brain following eye disease (Aguirre et al., 2016; Boucard et al., 2009; Hernowo et al., 2014; Malania et al., 2017; Neveu et al., 2008; Plank et al., 2011; Prins et al., 2016; Von Dem Hagen et al., 2005). Converging evidence suggests that when retinal disease occurs, changes to visual cortex emerge in retinotopic representations of the retinal lesion. For example, albinism appears to result in changes at or near the occipital pole reflecting foveal hypoplasia (Von Dem Hagen et al., 2005), and in an elegant study comparing individuals affected by glaucoma with peripheral field defects and macular degeneration with central visual defects, cortex was affected in regions corresponding to the representations of the affected visual fields (Boucard et al., 2009). Further research in central visual field defects arising from juvenile- and AMD also reveal atrophic changes in visual cortex and underlying white matter (Hernowo et al., 2014). The former appeared most pronounced in posterior visual cortical locations consistent with a retinotopic locus for the effect. However, these studies use cohorts of patients with bilateral vision loss. We find that even with significant unilateral loss, volume of the occipital cortex is reduced with a specific decrease in mean cortical thickness in the retinotopic representation of the retinal lesion.

In contrast to the majority of studies reporting cortical loss following retinal disease, one study has reported significant thickening of retinotopic representations of the intact retina, which was attributed to potential compensatory mechanisms (Burge et al., 2016). As with many other studies, the patients had bilateral vision loss thereby

increasing the need for compensatory mechanisms. However, the participants reported in this current study had predominantly unilateral vision loss, limiting the need for a compensatory mechanism, consistent with the lack of a significant change in representations of intact retina.

Our results also provide evidence for key elements that have not been addressed by previous investigations. Former studies have been cross-sectional, so whilst accumulating evidence of cortical loss has been relatively strong, there remained the possibility that cohorts of patients with visual deficits may also have comorbid brain properties differentiating them from control cohorts. Our longitudinal study demonstrates that atrophic changes can be observed within a group of patients followed over time.

We first asked whether changes occurred over a period of 3-4 months which we believe is shorter than that previously assessed. We detected no change at this early stage, offering some reassurance that changes in the status of visual cortex detectable with MRI are not rapid. Most cross-sectional studies tested patients who had established visual loss between 1-42 years duration (Boucard et al., 2009; Burge et al., 2016; Hernowo et al., 2014; Malania et al., 2017; Prins et al., 2016). It would appear therefore that atrophic changes in visual cortex due to retinal disease may emerge between 3- and 12-months post disease onset. Future longitudinal studies would benefit from assessing the anatomy of visual cortex during the first 24 months following visual loss to characterise better the time course of brain changes. Our long-term follow-up successfully detected retinotopic atrophy, which has featured in the literature. However, the fact that such changes were detectable in such a small sample indicates that following individual patients over time may be a valuable way of assessing the status of visual cortex following vision loss.

As mentioned above, previous literature has primarily addressed cortical changes following bilateral retinal loss. However, some studies have found structural changes following unilateral loss. Previous studies have reported that monocular enucleation performed early in development results in shrinkage of ocular dominance columns (Adams, Sincich, & Horton, 2007; Kelly, Desimone, Gallie, & Steeves, 2015; Kelly, McKetton, Schneider, Gallie, & Steeves, 2013) and reduced white matter connections (N. A. Wong et al., 2017). Moreover, early unilateral functional loss due to amblyopia has also been shown to result in structural changes to primary visual cortex (Mendola et al., 2005). Taken together, these studies suggest that changes to visual cortex can occur

as a result of both anatomical and functional unilateral loss occurring early in development. Importantly, we demonstrate that cortical changes can follow unilateral loss of input in adulthood when the visual system has reached maturity.

Finally, routine clinical assessments highlighted the effectiveness of anti-VEGF treatment for nvAMD. In all but one participant, vision was subnormal in both eyes but remained relatively stable over time, consistent with previous literature studying larger cohorts (Airody et al., 2015; Keane et al., 2008; J. H. Kim et al., 2016). Although visual acuity and central retinal thickness did not indicate significant changes in both eyes over time, we cannot rule out entirely the possible contribution of disease progression in either or both eye to the cortical atrophy we observe.

Significant thinning of visual cortex may ultimately limit the success of restorative treatments for eye disease. At present, such treatments are limited by the quality of information generated at the retina (Fine & Boynton, 2015; Fine, Cepko, & Landy, 2015), or indeed fed to the cortex directly (Dobelle, Quest, Antunes, Roberts, & Girvin, 1999; Pezaris & Reid, 2007). However, as the quality of visual information increases, the reliance on functional properties of visual cortex will come into play. For example, it has been proposed cortical plasticity would be required to process the limited visual inputs that can be restored (Fine & Boynton, 2015). However, it is not known whether atrophy can be reversed, or whether sufficient cortical plasticity can be achieved once functional input is restored.

Our current results cannot inform whether atrophy reflects degenerative processes in the cortex. Anterograde trans-synaptic degeneration has been reported within visual cortex in patients following retinal disease/damage (for a review, see (Dinkin, 2017)). Retrograde trans-synaptic degeneration has also been observed; when cortex is lesioned, retinal ganglion cell numbers reduce in regions projecting to the lesioned part of cortex (Beatty, Sadun, Smith, Vonsattel, & Richardson, 1982; Jindahra, Petrie, & Plant, 2009; Keller, Sánchez-Dalmau, & Villoslada, 2014; Mitchell, Oliveira, Tsiouris, & Dinkin, 2015; Yamashita et al., 2016). It may be valuable therefore to probe visual cortex for measures that can track degeneration, perhaps using magnetic resonance spectroscopy to assess neurochemical signatures of necrosis or apoptosis.

We conclude that longstanding unilateral loss of input to visual cortex results in significant atrophy. However, there is a window – at least within 3-4 months post-diagnosis – during which no detectable atrophy was present. This finding indicates that detrimental changes in visual cortex emerge relatively slowly.

Chapter 3

Does long-term visual deprivation result in atrophy or degeneration of visually deprived brain regions?

3.1. Introduction

Vision restoration techniques, including stem cell and gene therapies (Acland et al., 2001; Beltran et al., 2015; Boye, Boye, Lewin, & Hauswirth, 2013), antiangiogenics (D. M. Brown et al., 2006b; Rosenfeld et al., 2006) and visual prostheses (Humayun, de Juan, et al., 1999; Marc, Pfeiffer, & Jones, 2014; Weiland & Humayun, 2014) amongst others, have grown rapidly in recent years with the aim to restore retinal input in those with profound vision loss. However, the success of such techniques depends on the visual cortex of the brain remaining viable to process restored visual signals. Therefore, it is imperative to investigate and understand any potential alterations within visual cortex resulting from vision deprivation.

The vast majority of studies assessing cortical alterations associated with vision loss focus on central retinal disorders such as age-related macular degeneration (AMD), a progressive disease that affects more peripheral locations over time. In the developed world, AMD is the most common cause of visual impairment, affecting 12.2% of those aged 80 years and over (NICE, 2018). Significant atrophy (shrinkage) of the posterior visual pathway (the occipital cortex) has been reported in a number of studies including AMD cohorts (Aguirre et al., 2016; Boucard et al., 2009; Hanson et al., 2019; Hernowo et al., 2014; Malania et al., 2017; Plank et al., 2011; Prins et al., 2016), also reporting significant reductions in thickness in the cortical representation of the lesioned retina (Hanson et al., 2019).

Less research has focused on cortical changes associated with peripheral retinal disorders such as retinitis pigmentosa (RP). RP is a group of hereditary retinal diseases affecting 1 in 4000 worldwide (Hartong et al., 2006). Characterised by a progressive loss of photoreceptors, RP has been the main disease of focus in trials measuring the success of retinal prostheses such as the Argus II® (Ahuja et al., 2011; Castaldi et al., 2016; Castaldi, Cicchini, Falsini, Binda, & Morrone, 2019; da Cruz et al., 2016; Humayun et al., 2009; Luo, Davagnanam, & Dacruz, 2013; Luo, Zhong, & da Cruz,

2015; Rizzo et al., 2014) and gene therapy (Cehajic-Kapetanovic et al., 2020; Garafalo et al., 2020; Sudharsan & Beltran, 2019). Of the few studies that have looked at structural alterations to the visual cortex specifically in RP patients, results outline a significant decrease in volume of the occipital cortex (Rita Machado et al., 2017), suggesting cortical atrophy. Other reports outline a reduced cortical thickness in V1 (primary visual cortex) in RP patients (Castaldi et al., 2019; Cunningham, Shi, et al., 2015) whilst some report no difference in V1 compared to sighted controls (Ferreira et al., 2017). However, the mechanisms behind these structural changes for both central and peripheral retinal disease are not well understood.

Whilst the existing literature may provide conflicting evidence on whether structural alterations occur to the visual cortex following vision deprivation, it is also unclear whether alterations are dependent on the type of retinal disease and whether the adult brain is able to return to processing restored visual input despite structural alterations. The outcome of sight restoration procedures often varies for reasons that are not fully understood. For example, assessments of antiangiogenic treatments show declines in visual performance in the long-term, despite initial improvements (Airody et al., 2015). As the retinal disease advances in both AMD and RP, the visual field affected can also increase. Two possible mechanisms that could explain the continued decline in visual performance long-term are cortical demyelination (reduced myelination coating axons) or cortical degeneration (a shrinkage of the cortex due to cell death).

Evolved to expedite conduction of electrical signals along axons, myelin is essential for a healthy functioning nervous system. Within the cerebral white matter, myelinated fibres are abundant, carrying information from one brain area to another. However, myelin can also be found within cerebral cortex (grey matter), largely in the cortical input layers (layer IV) where these white matter tracts terminate (Shafee et al., 2015). Recent work has outlined a method to quantify myelination content within cortical grey matter using in vivo T1-weighted (T1w) and T2-weighted (T2w) MRI ratio, based on the hypothesis that cortical myelin content covaries with the intensity of both T1w and T2w images, but in the opposite direction (Glasser & Van Essen, 2011). Myelin is most dense in sensory input areas including primary visual cortex, with high myelin density in early visual areas, V1-V3 (Abdollahi et al., 2014; Sereno et al., 2013). Whereas studies have reported on changes in cortical thickness associated with long-term vision loss from AMD and RP, it is currently unknown how myelin density may

also change in these diseases, and what the impact of such changes may mean to future restoration techniques.

Proton magnetic resonance spectroscopy (^{1}H-MRS) is a non-invasive technique that allows detection and quantification of certain biochemical compounds (metabolites) in brain tissue. The resulting spectral peaks correspond with various metabolites, with the height of the peak reflecting the amount of the metabolite within the area of interest (Soares & Law, 2009). It is widely reported that levels of some metabolites may change in response to neurodegenerative disease (Kuzniecky, 2004; Lin, Shic, Enriquez, & Ross, 2003; Martin, 2007; Sijens, Mostert, Oudkerk, & De Keyser, 2006; Tedeschi et al., 1997) however, detecting changes associated with vision loss is a relatively new area of research.

N-Acetyl-Aspartate (NAA) is found at relatively high concentrations in the human central nervous system and is particularly localised within neurons and related to neuronal processes. A decrease in NAA is routinely considered an indicator of neuronal loss or dysfunction (Block et al., 2002; Gujar, Maheshwari, Bjo, & Sundgren, 2005) and has been observed in different brain regions in various neurodegenerative disorders (Kuzniecky, 2004; Sijens et al., 2006; Tedeschi et al., 1997) and neuro-ophthalmology (Ettl, Fischer-Klein, Chemelli, Daxer, & Felber, 1994). Choline (Cho), another metabolite, is considered a marker for cell turnover with increased Cho found in malignant tumours and in demyelination (Gujar et al., 2005). Glutamate (Glu), the most abundant excitatory neurotransmitter in the brain (Ramadan, Lin, & Stanwell, 2013), is an indicator of neuronal dysfunction and degeneration, with elevated levels often found in neurodegenerative disorders (Lin et al., 2003; Martin, 2007). Glu has also been shown to mediate neurotoxicity and excitotoxicity, with toxicity involved in oxidative stress and apoptosis (programmed cell death) (YueMei Zhang & Bhavnani, 2005). Creatine (Cr), which is known to play a role in cortical energy metabolism, is reported to be relatively stable and often used as a control reference (Gujar et al., 2005). However, reductions in Cr together with other major metabolites may also indicate tissue death or necrosis (unprogrammed cell death) (Gujar et al., 2005). γ-aminobutyric acid (GABA) is the principle inhibitory neurotransmitter involved in altering the excitatory/inhibitory balance mediating plasticity in the adult brain and as such, a potential indicator of cortical plasticity (Bavelier, Levi, Li, Dan, & Hensch, 2010; Hensch, 2005; Hensch & Fagiolini, 2005).

Adapting ^{1}H-MRS in vision loss research allows for direct evidence of brain plasticity and adaptive changes within the visual cortex. Whilst a number of studies have looked at chemical changes in early total blindness (Coullon, Emir, Fine, Watkins, & Bridge, 2015; Weaver, Richards, Saenz, Petropoulos, & Fine, 2013), very little research has focused on progressive central and peripheral retinal deficits such as AMD and RP respectively. One study assessing chemical differences using ^{1}H-MRS in AMD compared to glaucoma and sighted controls, reported no differences in the striate visual area (Boucard et al., 2007). The authors suggest that progressive retinal defects do not always induce measurable changes in metabolite concentration. In a cross-sectional study, in which two participants had RP, the only significant difference found was an increase in myo-Inositol (mIno), a glial marker, observed in the blind group compared to sighted controls. This study also reported no significant signs of atrophy in the occipital cortex (Bernabeu et al., 2009). The authors conclude this to be first evidence that plasticity mediated by glial cells is induced following vision deprivation. Notwithstanding, Boucard et al. and Bernabeu et al. do report mean differences in a number of metabolites between the patient groups and sighted controls, although these were not significant. This could suggest that underlying neurochemical changes may be associated with progressive retinal disease.

Whilst cortical atrophy has been reported in cases of central retinal disease, namely AMD, whether peripheral retinal disease results in cortical atrophy remains unclear. The effects of vision loss from AMD and RP on myelin density of the visual cortex is also unknown, particularly how this may differ with type of disease and the impact this may have. Nevertheless, ^{1}H-MRS has been shown to be useful in measuring metabolic alterations in the posterior visual pathway in early vision loss (Coullon et al., 2015; Weaver et al., 2013) however, research into vision loss due to progressive diseases such as AMD and RP remain very limited. The ability to confirm signs of cortical degeneration in retinal disease will have a crucial impact on restoration techniques and their success on a patient-by-patient case. However, if vision loss results in atrophy of the posterior visual pathway, this suggests a potential ability for the brain to return to processing visual information once input has been restored (Beyeler, Rokem, Boynton, & Fine, 2017; Fine & Boynton, 2015; Hensch, 2005). Therefore, understanding how the posterior visual pathway responds to different types of vision loss will ultimately aid our understanding of how this pathway might respond once/if vision is restored.

What has yet to be established from the current literature is whether cortical reductions represent a) atrophy: condensed cortex that remains plastic to restored visual input, b) demyelination: reductions in myelin density or c) degeneration: reduced cortical volume due to cell death. The aim of this study is to examine the effects of vision loss due to either central or peripheral retinal disease on the posterior visual pathway, with four main objectives: 1) use structural MRI to measure evidence of cortical atrophy via changes in cortical volume, mean cortical thickness and myelin density within visual cortex, 2) use MRS to measure neurochemical differences indicating cortical degeneration due to apoptosis and/or necrosis, 3) use MRS to investigate evidence of cortical plasticity with changes in GABA levels and 4) to investigate the relationship between structural and neurochemical measures within the visual cortex and how these may differ depending on the type of retinal disease.

3.2. Materials and Methods

3.2.1. Participants

Written informed consent was obtained from all participants. Ethical approval was granted by York Neuroimaging Centre Research, Ethics and Governance Committee and the NHS Research Ethics Committee (IRAS: 181823). This study followed the tenets of the Declaration of Helsinki.

Twenty-five participants were recruited to the SYNAPTIC study from York Teaching Hospital NHS Foundation Trust between November 2018 and September 2019. Inclusion criteria were bilateral vision loss with an overlapping scotoma resulting in allocation to either a central or peripheral vision loss group. Exclusion criteria included contraindications for completing the MRI procedures or receiving pupil dilation, enrolment on an interventional clinical trial and inability to comply with the study.

Eighteen participants were allocated to the central vision loss group. Three participants withdrew from the study before data collection and a fourth participant was unable to complete the magnetic resonance imaging (MRI) assessments and was excluded. This resulted in a final central vision loss cohort of fourteen participants (mean age = 78.07 years; age range = 63.07 – 90.10 years; 6 females; Table 1). Disease duration

outlined in Table 1 relates to bilateral onset, all participants had unilateral loss prior to this time. For further details on the clinical demographics of the full cohort, please refer to Chapter 4, section 2.1.

Seven participants were allocated to the peripheral vision loss group. One participant was excluded for not being able to complete the MRI assessments, a second participant was excluded due to MRI anomalies and a third participant withdrew from the study before data collection. This resulted in a final peripheral vision loss cohort of four participants (mean age = 47.03 years; age range = 26.03 – 66.11 years; 2 females; Table 1). Two participants (P15 and P16) fell within the age-range of the entire cohort whereas P17 and P18 were much younger (Table 1). Whilst the control group discussed below acted as controls for participants P15 and P16, an additional younger participant was recruited as a control for participants P17 and P18 (see below for further details).

Table 1: Demographics of participants enrolled in the SYNAPTIC study.

Subject	Gender	Age (y, m)	Bilateral Diagnosis	Group	Disease duration (y, m)
P01	Male	63, 7	nvAMD	Central	2, 3
P02	Female	69, 0	nvAMD	Central	5, 7
P03	Female	83, 7	nvAMD	Central	6, 5
P04	Female	75, 10	nvAMD	Central	5, 10
P05	Male	84, 4	nvAMD	Central	5, 4
P06	Male	74, 3	nvAMD	Central	13, 7
P07	Male	77, 5	nvAMD	Central	6, 1
P08	Female	90, 10	nvAMD	Central	13, 2
P09	Female	90, 4	nvAMD	Central	10, 3
P10	Male	75, 7	nvAMD	Central	7, 8
P11	Male	87, 11	nvAMD	Central	6, 6
P12	Male	76, 6	CSCR	Central	8, 4
P13	Male	73, 2	nvAMD	Central	11, 11
P14	Female	85, 1	nvAMD	Central	9, 1
P15	Female	63, 8	RP	Peripheral	20, 2
P16	Female	66, 11	RP	Peripheral	3, 10
P17	Male	26, 3	RP	Peripheral	7, 0
P18	Male	34, 3	RP	Peripheral	23, 1

*nvAMD: Neovascular Age-related macular degeneration; CSCR: Central Serous Chorioretinopathy; RP: Retinitis pigmentosa

Thirty-four healthy control participants were recruited from York Neuroimaging Centre between May 2018 and November 2019. All participants were age-range matched (mean age = 71.02 years; age range = 65.01 – 83.03 years; 14 females), had normal or corrected-to-normal vision and acted as a control group for the vision loss participants. All control participants completed the same structural MRI procedure with a subset of eleven participants also completing magnetic resonance spectroscopy (MRS) assessments (mean age = 70.5 years; age range 65.1 – 81.6 years; 5 females). One additional participant was recruited as control subject for the two younger peripheral loss participants, P17 and P18 (Male; age = 31 years) and completed the same structural MRI and MRS assessments.

Participants were excluded from the study if they had contraindications for completing the MRI procedures or receiving pupil dilation, if they were currently enrolled on an interventional clinical trial and if they were unable to comply with the study.

3.2.2. Design

In this cross-sectional study, all participants diagnosed with vision loss completed both MRI and MRS assessments on the same day. For the eleven control participants who also completed the MRS assessment, five participants completed this on the same day and six participants completed the MRS within 12 months of the structural MRI.

3.2.3. Procedures

Neuroimaging procedures took place on a 3 Tesla Siemens Magnetom Prisma scanner using a sixty-four-channel head receiver array. All participants were instructed to lie as still as possible during the scan. Foam padding was used around the head to minimise movement, with earplugs provided to protect against scanner noise. All statistical analysis was performed using SPSS (IBM Corp. Released 2017. IBM SPSS Statistics for Windows, Version 25.0. Armonk, NY: IBM Corp).

3.2.3.1. MRI. Two isotropic T1-weighted MPRAGE (TR = 2400ms, TE = 2.28ms, TI = 1010ms, Flip angle = 8°, Voxel size = 0.8 x 0.8 x 0.8mm, Matrix size =

256 x 256 x 167mm) and two isotropic T2-weighted SPACE (TR = 3200ms, TE = 563ms, Voxel size = 0.8 x 0.8 x 0.8mm, Matrix size = 256 x 256 x 167mm) anatomical volumes were acquired following guidelines from the Human Connectome Project (Glasser et al., 2013).

3.2.3.1.1. Analysis. Cortical reconstruction, volumetric segmentation and myelin quantification were performed using the Human Connectome Project analysis pipeline (version 6.0), incorporating the Freesurfer analysis suite (version 6.0). The three-stage structural analysis pipeline includes alignment of T1w and T2w images, bias field correction, volume segmentation, reconstruction of white and pial surfaces and surface registration (Glasser et al., 2013). Cortical myelin content is quantified by the ratio of T1w and T2w signal intensity, improving areal localisation by contrast to noise between heavily and lightly myelinated areas (Glasser & Van Essen, 2011).

Three structural characteristics of the cerebral cortex (grey matter) were assessed: cortical volume of the entire occipital cortex and mean cortical thickness and cortical myelination of the occipital pole and calcarine sulcus (Figure 1). The rationale for these assessments is the same as that outlined in Chapter 2. Mean grey matter volume was extracted from each parcellation within the occipital cortex ROI, from both the left and right hemispheres. An average across hemispheres was then calculated for each participant, creating the final entire occipital cortex ROI. A one-way ANOVA assessed changes in cortical volume between the controls and central loss group. Mean cortical thickness and myelination were extracted following this same procedure for two regions representing the central (occipital pole) and peripheral (calcarine sulcus) retina. Cortical thickness was defined as the shortest distance between the grey/white matter boundary and the grey/cerebrospinal fluid boundary at each vertex across the cortex in millimetres (mm), averaged over all vertices within each ROI. A one-way ANOVA compared mean cortical thickness within each ROI between the controls and central vision loss group. A separate one-way ANOVA compared mean cortical myelin within each ROI between the controls and central vision loss group. Due to the small group size, data from the peripheral vision loss group were not statistically analysed and will be discussed in relation to the sighted controls and central vision loss group.

3.2.3.2. MRS. For all participants, this scan session was the first scan acquired of the day in order to ensure homogeneity of the scan environment and to reduce

influence of any previous MRI scan on the gradient coils. For those participants completing the structural MRI and MRS on the same day, the MRS scan was completed first followed by the structural MRI session after a 60-minute interval. One localiser image was acquired (TR = 606ms, TE = 122ms, Voxel size = 0.5 x 0.5 x 6.0mm, Flip angle = 144º) to guide placement of the MRS voxel. Shimming and tuning were achieved with automated procedures along with variable power radio frequency pulses with optimised relaxation delays (VAPOR) water suppression followed by two MRS acquisitions (TR = 2010ms; TE = 135ms; 8 averages; spectral width = 2000Hz) using a multi-voxel CSI (chemical shift imaging) sLASER (semi-adiabatic localization by adiabatic selective refocusing) with MEGA (MEshcher-GArwood) spectral editing sequence (Deelchand et al., 2019; Öz & Tkáč, 2011). This sequence allowed for the quantification of GABA alongside the following metabolites of interest: NAA, Glu, Cho and Cr. For all participants, a large (8.0 x 8.0 x 1.5cm^2) multi-voxel grid was positioned in occipital cortex across both hemispheres, ensuring that the central four voxels of interest (VOIs) from the larger grid followed the angle of the calcarine sulcus, capturing as much of the calcarine sulcus and occipital pole as possible (Figure 2).

3.2.3.2.1. Analysis. Data were analysed using TARQUIN (Totally Automatic Robust Quantitation in NMR) version 4.3.10 (http://tarquin.sourceforge.net), a fully automated analysis software (Wilson, Reynolds, Kauppinen, Arvanitis, & Peet, 2011). Each MRS run was selected along with the localiser image in order to select the VOIs from the multi-voxel grid. One VOI was selected occupying the occipital pole (central retinal representations) and a second VOI occupying the calcarine sulcus (peripheral retinal representations) for both hemispheres. Upon inspection of the voxel placements, the VOI occupying the occipital pole included excess non-brain tissue, affecting the quality of the spectra across all participants (Figure 2A). Therefore, only data from the calcarine sulcus VOI were statistically analysed.

TARQUIN uses three main stages to process MRS data: pre-processing, including the removal of water, automatic phase adjustments and referencing; basis set simulation against built-in chemical shift and J-coupling values and non-linear least-squares fitting, modelling the data as a linear combination of modified simulated basis signals (Wilson et al., 2011). Basis sets encompass an example spectra of metabolites at their ppm in order to model the acquired data against to confirm which metabolites have been successfully acquired. The resulting spectra were extracted from the VOI from each

hemisphere for every participant with a hemisphere average calculated. Following the same rationale as that for the MRI analysis, an average of the two hemispheres was calculated here as there was no significant difference found between the hemispheres. A previous study used a relative quantification method to reduce systematic variation among participants and to avoid making assumptions about different metabolites remaining constant, calculating ratios of each metabolite of interest against Cr (Bernabeu et al., 2009). We implemented the same rationale here, calculating a ratio for the amplitude of each metabolite of interest to Creatine, resulting in four final rations NAA:Cr, GABA:Cr, Glu:Cr and PCh:Cr. A two-way mixed, repeated measures ANOVA compared the amplitude of each metabolite between the sighted controls and central vision loss group. Due to the small group size, data from the peripheral vision loss group were not statistically analysed and will be discussed in relation to the sighted controls and central vision loss group.

    3.2.3.3. MRI vs MRS. To explore whether the structural alterations we observe within the visual cortex could be explained by changes in neurochemistry, Pearson correlations were carried out on the outcome measures from the MRI and MRS procedures for all participants in central retinal disease group only. Due to the small sample size with peripheral retinal disease, correlational analyses were not carried out in this group. This enabled exploratory investigations into the relationship between the structure and neurochemical levels within the entire occipital cortex, particularly in the cortical representations of the lesioned and intact retina. Our predictions would be that 1) if long-term retinal disease results in neuronal loss/dysfunction, MRI reductions should correlate with decreased NAA:Cr, 2) if cortical degeneration is occurring, MRI reductions should correlate with increased Glu:Cr, 3) if cortical demyelination is occurring, MRI reductions should correlate with increased PCh:Cr and 4) signs of cortical plasticity should result in correlations between MRI outcome measures and reduced GABA:Cr.

Figure 1: *Structural MRI region of interest (ROI).* ***A:*** *Inflated medial surface of the left hemisphere showing the three ROIs. The entire visual cortex is represented by all coloured regions shown in blue including the cortical representations of the central visual field, the occipital pole, shown in red and the peripheral visual field, the calcarine sulcus, shown in green.* ***B:*** *Example cortical thickness map on an inflated medial surface of the left hemisphere. Cool colours represent cortical regions which are thinner than those of hotter colours, such as the visual cortex.* ***C:*** *Example myelin density map shown on an inflated medial surface of the left hemisphere. Hot colours represent cortical regions which have greater myelin density, such as the visual cortex.*

Figure 2: *MRS multi-voxel grid placement and example spectrum. **A:** Placement of the multi-voxel CSI grid in the occipital lobe, positioned parallel to the calcarine sulcus shown on a sagittal structural MRI image on the left-hand side and an axial MRI image on the right-hand side. The green box indicates the voxel of interest (VOI) over the calcarine sulcus from the left hemisphere. The equivalent VOI was also obtained from the right hemisphere with the final VOI an average of the two. The red box indicates the VOI placed over the occipital pole which was excluded from the analysis due to the inclusion of non-brain tissue. **B:** Example MRS spectrum showing the metabolites of interest, N-Acetyl-Aspartate (NAA), Creatine (Cr), Glutamate (Glu), γ-aminobutyric acid (GABA) and Phosphocholine (PCh).*

Table 2: *Description of the role for each ^{1}H-MRS metabolite of interest within the human brain, with the predicted change relative to the control group of each metabolite ratio stratified by type of retinal disease.*

Metabolite Ratio of Interest	Description	Predicted Change	
		Central retinal disease	Peripheral retinal disease
Glu:Cr	• Excitatory neurotransmitter and indicator of neuronal dysfunction and degeneration • Increased Glu found in neurodegenerative disorders, oxidative stress and apoptosis	↑	↑
NAA:Cr	• Localised within neurons and related to neuronal processing • Decreased NAA considered an indicator of neuronal loss or dysfunction	↓	↓
PCh:Cr	• Considered a marker for cell turnover. • Increased Cho found in malignant tumours and demyelination.	↑	↑
GABA:Cr	• Inhibitory neurotransmitter involved in altering the excitatory/inhibitory balance mediating cortical plasticity • Reduced GABA may indicate cortical plasticity	↓	↓

*Glu: Glutamate; NAA: N-Acetyl-Aspartate; PCh: Phosphocholine; GABA: γ-aminobutyric acid; Metabolite ratios are calculated against Creatine (Cr); ↑: Increased amplitude; ↓: Decreased amplitude.

3.3. Results

Data from the peripheral vision loss group have not been included in any statistical analysis due to the small group size therefore, the results from this group will only be discussed in relation to the two other cohorts (Table 3).

3.3.1. MRI. Our first objective was to establish evidence of atrophy (shrinkage) in the occipital cortex resulting from long-term central or peripheral vision loss (Figure 3). In the central vision loss group, despite a medium effect size, there was a non-significant reduction in cortical volume compared to sighted controls ($F(1,46) = 3.819$, $p = 0.057$, $\eta^2 = 0.078$).

Although the reduction in cortical volume did not reach significance, as expected with central vision loss, there was evidence of significant cortical atrophy via a reduction in cortical thickness in the retinotopic representation of the central retina, namely the occipital pole, where there was a large effect size ($F(1,46) = 13.086$, $p = 0.001$, $\eta^2 = 0.225$). Surprisingly, significant cortical atrophy was also observed with a reduction in cortical thickness in the retinotopic representation of the peripheral retina, namely the calcarine sulcus, also with a large effect size ($F(1,46) = 12.122$, $p = 0.001$, $\eta^2 = 0.212$; Table 3).

Examining the effects of vision loss on cortical myelin density, we found no significant difference between sighted controls and the central vision loss group in the retinotopic representation of the central retina, the occipital pole ($F(1,46) = 0.995$, $p = 0.324$, $\eta^2 = 0.022$) or the peripheral retina, the calcarine sulcus, ($F(1,46) = 0.653$, $p = 0.423$, $\eta^2 = 0.014$; Table 3).

Whilst no statistical analysis can be performed on the peripheral vision loss group, observational data suggest that cortical volume was reduced compared to sighted controls, possibly indicating evidence of cortical atrophy (Table 3). However, compared to the central vision loss group and sighted controls, mean cortical thickness appeared greater in the calcarine sulcus and occipital pole whilst myelin density levels also appeared greater in both the calcarine sulcus and occipital pole compared to sighted controls (Table 3).

3.3.2. MRS. Our second and third objectives were to establish signs of cortical degeneration and/or plasticity associated with long-term vision loss and whether this

differs depending on the type of retinal disease (Table 4; Figure 4). Data were removed from two outliers (one sighted control and one central vision loss participant) due to data falling more than 2 standard deviations before performing a two-way mixed, repeated measures ANOVA using the Greenhouse-Geisser correction. This analysis revealed the mean metabolite amplitude ratios were significantly different from each other across both groups (main effect of metabolite type) $(F(1.724, 34.483) = 139.072$, p $=$ $1.8476*10^{\wedge}-16$, $\eta^2 = 0.874$). However, despite slight reductions across all metabolite ratios, there was no significant difference between the sighted controls and central vision loss group, suggesting that cortical degeneration was not measurable in the group of participants tested here $(F(1.724, 34.483) = 0.041$, p $= 0.942$, $\eta^2 = 0.002$).

Observational data from the peripheral vision loss group showed greater mean amplitude ratios of Glu:Cr, NAA:Cr and GABA:Cr yet reduced PCh:Cr compared to sighted controls (Table 4). Based on our predictions, outlined in Table 2, the most interesting results are the greater mean amplitude ratio of Glu:Cr, as increased Glu is often associated with cortical degeneration via apoptosis although significance testing on a larger cohort is required to confirm this finding.

3.3.3. MRI vs MRS. Our fourth and final objective was to investigate the relationship between outcome measures obtained from the MRI and MRS procedures (Table 5; Figure 5). In the central vision loss group, we found that cortical thickness in the occipital pole significantly positively correlated with PCh:Cr $(R = 0.616$, p $= 0.025)$. One of our hypotheses was that if cortical demyelination is occurring, MRI reductions should correlate with increased PCh:Cr. However, whilst significant reductions in cortical thickness in the occipital pole was observed, we found no significant difference in myelin density or PCh:Cr in this cohort.

Table 3: *Mean and standard error of the mean (SEM) for structural measures of the cortex stratified by participant group.*

		Sighted Controls		Central Retinal Disease		Peripheral Retinal Disease	
		Mean	(SEM)	Mean	(SEM)	Mean	(SEM)
	Cortical Volume (mm3)	30,739	(4,695)	27,952	(3,863)	29,067	(1,240)
Mean Cortical Thickness	**Occipital Pole (mm)**	1.90	(.15)	1.74	(.11)	1.92	(.10)
	Calcarine Sulcus (mm)	1.85	(.13)	1.69	(.18)	1.92	(.13)
Cortical Myelin	**Occipital Pole (a.u)**	1.50	(.03)	1.51	(.03)	1.51	(.03)
	Calcarine Sulcus (a.u)	1.45	(.03)	1.44	(.03)	1.46	(.03)

Table 4: *Mean and standard error of the mean (SEM) for each MRS metabolite ratio stratified by participant group.*

Metabolite Ratio	Sighted Controls		Central Retinal Disease		Peripheral Retinal Disease	
	Mean	(SEM)	Mean	(SEM)	Mean	(SEM)
Glu:Cr	1.64	(.30)	1.58	(.62)	2.09	(.52)
NAA:Cr	1.34	(.43)	1.29	(.53)	1.42	(.55)
PCh:Cr	.18	(.08)	.15	(.11)	.13	(.11)
GABA:Cr	.57	(.16)	.56	(.27)	.73	(.28)

* Glu: Glutamate; NAA: N-Acetyl-Aspartate; PCh: Phosphocholine; GABA: γ-aminobutyric acid; Metabolite ratios are calculated against Creatine (Cr).

Figure 3: MRI results. From left to right, the boxplots show cortical volume of the entire occipital cortex, with mean cortical thickness and cortical myelin values for the two smaller ROIs: occipital pole (red boxes) and calcarine sulcus (green boxes). All boxplots show data for the three participant groups: age-matched sighted controls, central vision loss (CVL) and peripheral vision loss (PVL). The horizontal lines represent the median with the upper and lower whiskers representing scores outside the middle 50%. White stars represent the mean. Data for each individual participant is overlaid on the boxplots shown as black dots. Open black dots represent the young control and the two younger participants in the peripheral loss group. *p = 0.001.

Figure 4: *MRS results stratified by participant group. Boxplots show the amplitude ratio of each metabolite against Creatine for the control participants in grey, central vision loss group in orange and peripheral vision loss group in purple. The horizontal lines represent the median with the upper and lower whiskers representing scores outside the middle 50%. Red stars represent the mean. Data for each individual participant is overlaid on the boxplots shown as black dots. Open black dots represent the young control and the two younger participants in the peripheral loss group.*

Table 5: *Pearson correlations between structural (MRI) and neurochemical (MRS) outcome measures from the posterior visual pathway for the central retinal disease cohort.*

			MRS outcome measures			
			Glu:Cr	**PCh:Cr**	**NAA:Cr**	**GABA:Cr**
Cortical Volume			R = 0.454￼ p = 0.119	R = 0.310￼ p = 0.303	R = -0.044￼ p = 0.888	R = 0.336￼ p = 0.262
Cortical	**Thickness**	**Occipital Pole**	R = 0.517￼ p = 0.070	**R = 0.616***￼ **p = 0.025**	R = 0.200￼ p = 0.512	R = 0.318￼ p = 0.290
		Calcarine Sulcus	R = 0.329￼ p = 0.273	R = 0.242￼ p = 0.425	R = 0.182￼ p = 0.552	R = 0.156￼ p = 0.612
Cortical	**Myelin**	**Occipital Pole**	R = 0.304￼ p = 0.313	R = 0.444￼ p = 0.129	R = 0.316￼ p = 0.293	R = 0.340￼ p = 0.256
		Calcarine Sulcus	R = -0.018￼ p = 0.952	R = 0.210￼ p = 0.492	R = -0.069￼ p = 0.824	R = -0.043￼ p = 0.890

*Significant at 0.05, 2-tailed

Figure 5: MRS v MRI correlation showing a positive correlation between PCh:Cr and mean cortical thickness in the occipital pole with central retinal disease.

3.4. Discussion

This study shows that atrophy of the occipital cortex, due to a reduction in cortical volume, occurs following long-term bilateral vision loss. With central retinal disease, whilst we find significant atrophy in retinotopic representations of the lesioned retina, namely the occipital pole, surprisingly, we also find atrophy in the calcarine sulcus, the retinotopic representation of the intact retina. In the case of peripheral retinal disease, observational data reveal no evidence of atrophy in the retinotopic representations of the lesioned retina, namely the calcarine sulcus. Pilot MRS data reveal no significant evidence of degeneration with either central or peripheral retinal disease.

Previous research has reported evidence of cortical atrophy associated with central vision loss via reduced volume or thickness in retinotopic representations of the lesioned central retina (Aguirre et al., 2016; Boucard et al., 2009; Hanson et al., 2019; Hernowo et al., 2014; Plank et al., 2011; Prins et al., 2016). Our results show that, whilst not quite significant (p = 0.057), volume of the entire occipital cortex was reduced compared to controls, explaining 8% of the variation observed. Nevertheless, supporting previous research, we have shown significant atrophy in the retinotopic representation of the lesioned retina, the occipital pole, with a reduction in mean cortical thickness. Surprisingly, we also reveal evidence of significant atrophy in the calcarine sulcus, the retinotopic representation of the intact retina. These data could indicate that as the retinal disease advances to occupy more peripheral retinal locations, this loss of input is measurable in the cortex. This widespread reduction in cortical thickness likely contributed to the significant reductions in volume we found throughout the occipital lobes. However, it also leads to the possibility that other areas beyond primary visual cortex (calcarine sulcus) may be affected as well.

Although the effects of peripheral retinal disease, specifically RP, on the structure of the posterior visual pathway are limited, it is suggested that atrophy of the visual cortex occurs (Rita Machado et al., 2017). In this current study, observational data reveal that volume of the entire occipital cortex was reduced compared to sighted controls, indicating possible cortical atrophy. Whilst this finding was not significance tested due to the small cohort, it is in line with this previous finding. Unlike central retinal disease, previous RP reports have failed to address whether there is evidence of atrophy in the cortical representation of the lesioned peripheral retina, the calcarine sulcus (Castaldi et al., 2019; Cunningham, Shi, et al., 2015; Ferreira et al., 2017). Addressing this in the current study, we found no evidence of atrophy in the calcarine sulcus, with mean cortical thickness in this region within the range of sighted controls yet greater than the central vision loss group.

Despite the small number of participants with peripheral retinal disease in this current study, all were of similar age range, gender distribution and had similar disease durations to those reported in previous studies (Castaldi et al., 2019; Cunningham, Shi, et al., 2015; Ferreira et al., 2017; Rita Machado et al., 2017). Although the age range in the current study was varied, we do not believe that age had an impact on the measures

we obtained. Participants P17 and P18 were much younger than P15 and P16, yet their results, across all measures, were similar.

Another difference to consider between the current and previous studies is the advancement of the RP disease and its effect on visual acuity (VA) performance. Castaldi et al. reported VA ranging from hand movements to bare light perception (Castaldi et al., 2019), whereas the VA in the current cohort ranged from $1 - 90$ ETDRS letters (see Chapter 4, Table 1). This could also explain the reduced cortical thickness values reported in the Castaldi et al. study, which we did not find in our cohort. Research has shown that as RP advances, the central retina becomes affected (Hirakawa et al., 1999; Holopigian et al., 1996), in turn resulting in poor VA. This may indicate a degree of atrophy of the cortical representations of the central retina, the occipital pole, like those we observe in the central vision loss group in the current study (see Chapter 4, Table 1). Considering Castaldi et al. measured structural changes in primary visual cortex (V1) only, it is not possible to distinguish whether the reductions they observed are relating to the cortical representations of the lesioned or intact retina, as V1 includes both representations.

Until now, the effects of retinal disease due to AMD and RP on myelin density in the human visual cortex have been unknown. It is possible that the observed reductions in cortical volume and thickness associated with retinal disease may in part reflect changes in myelin density. Whilst we found reductions in both cortical volume and mean thickness with central retinal disease compared to sighted controls, this was not the case for cortical myelin. Myelin density was slightly greater in the occipital pole and lower in the calcarine sulcus (the cortical representations of the lesioned and intact retina respectively), but not significantly so. Interestingly, with peripheral retinal disease, we observed a reduction in volume of the entire occipital lobes, but this was not specific to mean cortical thickness in either the occipital pole or calcarine sulcus. Myelin density in these regions was also comparable to that in sighted controls.

There is an inverse relationship between cortical myelination and cortical thickness, such that lightly myelinated regions are found to be thicker whilst heavily myelinated regions tend to be thinner (excluding primary motor cortex and the frontal pole) (Glasser & Van Essen, 2011). Across all cohorts tested in this current study, we

did not find any correlation between cortical volume/thickness and myelin density. It has also been reported that in highly myelinated regions, distinguishing the deeper layers of cortex from white matter may be difficult, resulting in artificially thin estimates of cortical thickness (Glasser & Van Essen, 2011; Natu et al., 2019). As a consequence, myelin content is frequently underestimated in thin, heavily myelinated cortex (Glasser & Van Essen, 2011). This interaction could explain the apparent increase in relative amounts of myelin observed with central retinal disease, as a result of the reduced cortical thickness. However, considering there was no significant change in cortical thickness and myelin density with peripheral retinal disease, this may suggest a degree of preservation of retinal inputs to the cortex.

Whilst changes to cortical structure are currently associated with evidence of atrophy (shrinkage) due to retinal disease, the extent to which this may reflect cortical degeneration (cell death) or demyelination is unclear. Pilot data from this current study reveal no significant evidence of cortical degeneration, however, ^{1}H-MRS profiles obtained from the occipital cortex differed with disease type compared to sighted controls. Reductions in NAA are considered to indicate neuronal loss or dysfunction (Block et al., 2002; Gujar et al., 2005). In central retinal disease, we observed a slight reduction in NAA:Cr compared to sighted controls, whereas levels were slightly greater with peripheral retinal disease. Whilst these differences were not significant, they were in line with previous reports in both late (Bernabeu et al., 2009; Boucard et al., 2007) and early (Coullon et al., 2015; Weaver et al., 2013) blind subjects. The MRS voxel of interest was positioned occupying the calcarine sulcus which represents the intact retina in central retinal disease and the lesioned retina in peripheral retinal disease. Therefore, it is interesting to note this reduction in NAA:Cr in central retinal disease as it could also explain the reduction in cortical thickness observed in the calcarine sulcus.

Cortical atrophy resulting from long-term vision loss may also represent demyelination. Whilst we assessed changes myelin density changes using MRI, we also obtained levels of phosphocholine (PCh). A marker for cell turnover, increased Cho (and PCh) is found in malignant tumours and in demyelination (Gujar et al., 2005). Our results revealed, compared to sighted controls, PCh:Cr was slightly reduced in both central and peripheral retinal disease, although not significant. These data correspond with the MRI myelin density analysis outlined above which showed no significant

difference between central or peripheral retinal disease and sighted controls. Therefore, with central retinal disease, it would appear that the observed cortical atrophy is not being driven by demyelination. This is supported by the positive correlation between PCh and cortical thickness in the occipital pole.

Evidence of cortical degeneration can be assessed by measuring changes in Glu levels, as increased Glu indicates neuronal dysfunction (Lin et al., 2003; Martin, 2007) and cortical degeneration via apoptosis (YueMei Zhang & Bhavnani, 2005). This current study revealed that mean Glu:Cr levels appeared to be greater with peripheral retinal disease whilst lower in central retinal disease compared to sighted controls. As previously mentioned, placement of the MRS voxel favoured assessments of the calcarine sulcus, the representation of the lesioned retina in peripheral retinal disease and not the occipital pole, the representation of the lesioned retina in central retinal disease. Future studies would benefit from obtaining MRS from multiple voxels in the brain to ensure efficient coverage of brain regions relevant to different disease types. However, the difference in Glu:Cr levels may reflect the different underlying mechanism of the retinal disease. Peripheral retinal disease due to RP results from degeneration of the photoreceptor layer in the retina whereas central retinal disease due to nvAMD, results from neovascularisation affecting the retinal pigment epithelium. Consequently, anterograde degeneration may occur at a faster rate in RP, in which no treatment exists compared with the preventative treatment which exists for nvAMD.

Non-significant differences in Glu levels have been previously reported in studies with late (Bernabeu et al., 2009) and early (Weaver et al., 2013) blind subjects however, one early blind study did reveal significantly greater Glu/Gln in early blind subjects (Coullon et al., 2015). However, the latter study was unable to break down the two neurochemicals thus distinguishing the effect of retinal disease on Glu alone is difficult to infer from this study as changes in one could mask changes in the other. The advantage of this current study is the utilisation of a ^{1}H-MRS acquisition which allowed for the quantification of these two compounds independently.

The final assessment using ^{1}H-MRS in this current study investigated changes in GABA levels to probe signs of cortical plasticity in retinal disease. Involved in altering the excitatory/inhibitory balance mediating plasticity of the adult brain, research

suggests that a reduction in GABAergic inhibition leads to a reawakening of plasticity in the visual cortex (Bavelier et al., 2010; Hensch, 2005; Hensch & Fagiolini, 2005). While the differences in GABA:Cr levels in this current study were not significantly different to sighted controls, results do suggest a reduction in GABA:Cr with central retinal disease with increased GABA:Cr found with peripheral retinal disease. Considering the placement of the MRS voxel, this result may reflect that the loss of projections from the central visual field may awaken plasticity in neighbouring peripheral representations, although further research is required to support this theory.

In conclusion, we report significant evidence of cortical atrophy via a reduction in volume of the entire occipital cortex with central retinal disease. Significant atrophy is also found in both the retinotopic representation of the lesioned and intact retina with central retinal disease, namely the occipital pole and calcarine sulcus respectively. We report no significant evidence of either cortical degeneration or demyelination in the central retinal disease cohort compared to sighted controls. Observational data from a small cohort with peripheral retinal disease reveal no evidence of cortical atrophy, although cortical volume of the entire occipital lobe was reduced, no cortical degeneration or demyelination.Whilst pilot ^{1}H-MRS results indicate a trend towards evidence of cortical degeneration via apoptosis, this may indicate that the reduced cortical volume could be a result of cortical degeneration rather than cortical atrophy due to the lack of reduced mean thickness observed. However, testing this hypothesis on a larger cohort is required.

Ultimately, preservation of the visual cortex is essential in the success of vision restorative techniques which restore visual input. Whilst we are showing significant evidence of cortical atrophy with central retinal disease, the potential plasticity of visual cortex should be considered a double-edged sword. If plasticity is representing reorganisation of the visual cortex to perform new functions, this would be detrimental to restorative techniques. However, if reorganisation has not occurred, plasticity provides hope that restorative techniques may be successful. Moreover, these data only represent changes to the calcarine sulcus, the cortical representation of the intact retina in central retinal disease, thus we do not know what neurochemical changes are taking place in the representation of the lesioned retina, the occipital pole. Considering peripheral retinal disease, the potential cortical degeneration would suggest that

restorative techniques may not be successful. Whilst these ^{1}H-MRS pilot data are interesting, further research is required with much larger cohorts to establish significance in these changes. It is also worth considering that the lack of significance between both patient cohorts and sighted controls could simply indicate that although patients may have the same diagnosed retinal disease, the effects could be different for each patient, thus one could exhibit signs of cortical atrophy whilst another cortical degeneration. Consequently, treatment regimens should be tailored to the individual patient rather than based on disease alone.

Chapter 4

What is the relationship between the anterior and posterior visual pathway in long-term central retinal disease?

4.1. Introduction

The prevalence of vision loss due to retinal disease is on the rise. As a result, current research is focusing on treatment techniques to prevent disease progression in the eye and to restore visual input. Nevertheless, it is important to ensure we fully understand the relationship between changes occurring in the anterior and posterior visual pathways to possibly help determine biomarkers of disease, neuroprotection and future restorative treatment technologies.

Age-related macular degeneration (AMD) is one of the progressive retinal diseases of focus in this thesis. AMD is the leading cause of vision loss in the developed world (Lim et al., 2012) with two sub-types: "dry" geographic atrophy (GA) and "wet" neovascular AMD (nvAMD). In GA, there is a slow progressive atrophy of the retinal pigment epithelium and photoreceptors, whereas in nvAMD, choroidal neovascularisation (CNV) occurs along with an accumulation of either subretinal or intraretinal fluid and haemorrhage resulting in fibrous scarring (Lim et al., 2012). Classification of this leakage either falls under Type 2 CNV, in which the lesion penetrates the retinal pigment epithelium layer (RPE) and lies in front, or Type 1 CNV, whereby the lesion lies under the RPE (Lim et al., 2012) (Figure 1). Patients with nvAMD will often experience metamorphopsia (distortion of straight lines), a scotoma obscuring their central vision or both (Lim et al., 2012). Typically affecting individuals over the age of 50 years, it is estimated that 40,000 people develop nvAMD in the UK every year (NICE, 2018). In both cases, AMD affects the central macula of the retina and progresses to occupy more peripheral retinal locations over time.

Clinical assessments of the anterior visual pathway monitor disease progression through functional and structural measures of the retina. In the management of central retinal disease such as AMD, functional measures such as best corrected visual acuity (BCVA), measured using the Early Treatment Diabetic Retinopathy Study (ETDRS)

vision chart (ETDRS, 1985), has been established as the most important outcome measure in clinical research (Ou et al., 2017). Early clinical trials including MARINA, ANCHOR and later HORIZON, investigated the use of anti-vascular endothelial growth factor (anti-VEGF) treatment for nvAMD, revealing significant increases in the number of ETDRS letters read following treatment, which is maintained over time (D. M. Brown et al., 2006b; Rofagha et al., 2013; Rosenfeld et al., 2006). Nevertheless, whilst these results suggest that some vision loss is recoverable, BCVA performance often varies considerably between session (Patel, Chen, Rubin, & Tufail, 2008). Moreover, more recent reports suggest that BCVA performance begins to decline again after ~5 years of treatment (Airody et al., 2015).

Alongside BCVA assessments in central retinal disease, retinal sensitivity can be measured with microperimetry using, for example, the Nidek MP (Nidek Technologies, Padova, Italy) and Macular Integrity Assessment (MAIA, CentreVue, Padova, Italy) microperimeters. The most common outcome measure is mean sensitivity (MS), a mean of the light sensitivity across all stimulus locations, which has been shown to decrease with disease severity in AMD (Dinc et al., 2008; Vujosevic et al., 2011). However, reduced light sensitivity measured using microperimetry has been reported even with good visual acuity (for a review, see (Cassels et al., 2017)), therefore, microperimetry is often used in addition to other measures of visual function as it gives complimentary information.

Structural assessments of the retina have become a vital part of routine care, allowing clinicians to evaluate retinal and subretinal structures affected by disease. High resolution images acquired using spectral domain optical coherence tomography (SD-OCT) can quantify total thickness changes across the retinal layers along with changes in peripapillary RNFL thickness (pRNFL) of the optic nerve head. In central retinal disease, retinal thickness is widely used to measure the magnitude of the macular oedema particularly in nvAMD. Studies have shown by measuring the central retinal thickness, that treatment with anti-VEGF reduces the size of the oedema over the initial treatment phase (~4 months) with monthly anti-VEGF injections (Airody et al., 2015; Flinn, 2017; Hanson et al., 2019). However, assessing changes to specific retinal layers such as the ganglion cell layer (GCL) may be more informative as the inner retina will be less contaminated by subretinal fluid associated with nvAMD. Reports suggest that

thinning of the GCL occur in nvAMD compared with sighted controls (Beck, Munk, Ebneter, Wolf, & Zinkernagel, 2016; Martinez-de-la-Casa et al., 2012; Zucchiatti et al., 2015). Trajectories of the retinal nerve fibre bundles from the optic nerve head have revealed that foveal fibres occupy a large portion of the temporal quadrant (Fitzgibbon & Taylor, 1996; Jansonius et al., 2009). Two studies have reported significantly thinner optic nerve head thickness, particularly in the superior, inferior, and temporal quadrants in both nvAMD (Martinez-de-la-Casa et al., 2012) and dry-AMD (E. K. Lee & Yu, 2015).

Assessments of the posterior visual pathway, primarily measured using neuroimaging techniques such as magnetic resonance imaging (MRI), have provided an abundance of information on cortical changes associated with central retinal disease, including age-related macular degeneration (AMD). Structural MRI has revealed significant atrophy (shrinkage) of the visual cortex with reductions in volume of the entire visual cortex and specific significant reductions in cortical thickness in cortical representation of the lesioned retina, the occipital pole (Aguirre et al., 2016; Boucard et al., 2009; Hanson et al., 2019; Hernowo et al., 2014; Malania et al., 2017; Plank et al., 2011; Prins et al., 2016). In Chapter 3 of this thesis, we also report significant atrophy in volume of the entire occipital cortex, cortical thickness of the occipital pole and the calcarine sulcus, cortical representations of the central and peripheral retina respectively.

Whilst some of these neuroimaging studies have reported on potential relationships between changes to the posterior and anterior visual pathways (Malania et al., 2017), it is not known whether changes in one eye alone could predict alterations further down the visual stream. Consequently, to better understand the relationship between clinical and neuroimaging data and to potentially identify biomarkers of disease progression, this study aimed to observe the relationship between changes to the anterior (the eye) and posterior (the brain) visual pathways in patients with long-term central retinal disease.

Retinal Layers

Abbr.	Name
ILM	Internal Limiting Membrane
RNFL	Retinal Nerve Fiber Layer
GCL	Ganglion Cell Layer
IPL	Inner Plexiform Layer
INL	Inner Nuclear Layer
OPL	Outer Plexiform Layer
ONL	Outer Nuclear Layer
ELM	External Limiting Membrane
PR1/2	Photoreceptor Layers
RPE	Retinal Pigment Epithelium
BM	Bruch's Membrane
CC	Choriocapillaris
CS	Choroidal Stroma

Figure 1: *Layers of the human retina measurable using the Heidelberg Optical Coherence Tomography (OCT), and the cells contained within them. Know Your Retinal Layers (Heidelberg, 2016).*

4.2. Materials and Methods

4.2.1. Participants

Written informed consent was obtained from all participants. Ethical approval was granted by York Neuroimaging Centre Research, Ethics and Governance Committee and the NHS Research Ethics Committee (IRAS: 181823). This study followed the tenets of the Declaration of Helsinki.

Twenty-five participants were recruited to this SYNAPTIC study from York Teaching Hospital NHS Foundation Trust between November 2018 and September 2019. Inclusion criteria were bilateral vision loss with an overlapping scotoma, resulting in allocation to either a central or peripheral vision loss group. Exclusion criteria included contraindications for completing the MRI procedures or receiving pupil dilation, enrolment on an interventional clinical trial and inability to comply with the study.

Following some withdrawals outlined in Chapter 3, section 3.2.1, a final cohort of eighteen participants completed the clinical assessment element of the SYNAPTIC study; fourteen participants were diagnosed with central retinal disease (Table 1) and four patients were diagnosed with peripheral retinal disease (discussed in Chapter 5). Disease duration for all central retinal disease participants is outlined in Table 1 and refers to the time at which the disease became bilateral. All participants had unilateral retinal disease prior to this timepoint and as a result, the effect of unilateral retinal disease on the following outcomes measures is unknown. Nevertheless, we would expect the most significant effect of retinal disease on the following outcomes measures to occur following bilateral vision loss. Participant P03 was diagnosed with bilateral nvAMD but also had a cataract in the left eye. Whilst visual acuity was recorded for this eye as hand movements only (HM), it was not possible to complete all other clinical assessments as P03 was unable to detect any stimuli or maintain fixation and as a result, this eye was excluded from these analyses.

4.2.2. Design

In this cross-sectional design, routine clinical assessments, detailed below, took place no more than two weeks prior to the neuroimaging assessments of the posterior visual pathway detailed in Chapter 3, section 3.2.3.

Table 1: *Demographics of participants recruited to the SYNAPTIC study diagnosed with central retinal disease.*

Subject	Gender	Age (y, m)	Bilateral Diagnosis	Worse Eye OD / OS	BCVA	Better Eye OD / OS	BCVA	Disease Duration (y, m)
P01	Male	63, 7	nvAMD	OS	20	OD	29	2, 3
P02	Female	69, 0	nvAMD	OD	HM	OS	34	5, 7
P03	Female	83, 7	nvAMD	OS	HM	OD	29	6, 5
P04	Female	75, 10	nvAMD	OD	65	OS	68	5, 10
P05	Male	84, 4	nvAMD	OS	52	OD	67	5, 4
P06	Male	74, 3	nvAMD	OD	46	OS	75	13, 7
P07	Male	77, 5	nvAMD	OD	68	OD	71	6, 1
P08	Female	90, 10	nvAMD	OS	24	OD	31	13, 2
P09	Female	90, 4	nvAMD	OS	HM	OD	48	10, 3
P10	Male	75, 7	nvAMD	OD	85	OS	85	7, 8
P11	Male	87, 11	nvAMD	OS	50	OD	71	6, 6
P12	Male	76, 6	CSCR	OS	3	OD	42	8, 4
P13	Male	73, 2	nvAMD	OS	37	OD	48	11, 11
P14	Female	85, 1	nvAMD	OD	25	OS	68	9, 1

*nvAMD: Neovascular age-related macular degeneration; CSCR: Central Serous Chorioretinopathy; OD: Oculus Dexter (right eye); OS: Oculus Sinister (left eye); BCVA: Best Corrected Visual Acuity; HM: Hand movements

4.2.3. Procedures

All clinical assessments were completed at York Teaching Hospital NHS Foundation Trust during the participants' routine clinical visits.

4.2.3.1. Structural assessments. All participants completed an additional structural assessment of the eye using the Heidelberg Spectralis spectral-domain optical coherence tomography (SD-OCT; Heidelberg Engineering, Heidelberg, Germany). Autofluorescence and infrared images of the central macula and optic nerve head were acquired through dilated pupils for each eye.

4.2.3.1.1. Macular Thickness. Foveal volumetric scans acquired 25 frames in an area of 30 x 30 degrees at 1536 x 1536 pixels (Figure 2). Infrared images of the macula enabled segmentation of the retinal layers using the built-in Heidelberg Eye Explorer software, version 1.9.17.0. Thickness measures were calculated for the ganglion cell layer (GCL) with total macular thickness calculated to include all retinal layers between the internal limiting membrane (ILM) and Bruch's membrane (BM) shown in Figure 1. The central 1mm and 3mm diameter ETDRS locations were used to represent the central macula (0 - 5 degrees eccentricity), with the 6mm diameter ETDRS location representing the peripheral macula, from 5 - 10 degrees eccentricity (Figure 3).

4.2.3.1.2. Optic Nerve Head Thickness. Peripapillary RNFL (pRNFL) thickness was acquired using a 3.5mm diameter disk (768 A-scans) centred over the optic disk head (Figure 4) allowing for classification of seven quadrants of the optic nerve head: Temporal, Inferior Temporal, Superior Temporal, Nasal, Inferior Nasal, Superior Nasal and all quadrants, Global. Built-in software analysed all quadrants identifying those which fell within and outside of (below) normal thickness limits for the age range of each participant (Figure 5). Previous research has shown that fibres from the central macula occupy a large portion of the temporal quadrant (Fitzgibbon & Taylor, 1996; Jansonius et al., 2009), therefore, it would be expected that reduced thickness in the temporal quadrants, relating to the central retina, may be found in this patient group. It is important to note that the three nasal quadrants represent projections from the far peripheral retina, including retinal locations beyond that classified as the peripheral macula in Section 4.2.3.1.1. above.

4.2.3.1.3. Lesion Size. Autofluorescence images of the central macular region were used to measure the size of the structural lesion in each eye for all participants (Figure 6). The border of the affected retina was traced using built-in software, with the resulting value showing the area of the affected region in mm^2.

4.2.3.2. Functional Assessments. All participants completed a best corrected visual acuity and retinal sensitivity assessments during their routine clinical visit.

4.2.3.2.1. Best Corrected Visual Acuity. Standard clinical visual acuity was measured in an illuminated room at 4 meters, with the participant's spectacle correction in each eye using an ETDRS (Early Treatment Diabetic Retinopathy Study) letter chart

(ETDRS, 1985). If participants were able to read four or more of the five letters on the first line of the chart they were asked to continue reading down the chart until they could read fewer than three letters on a single line. At this point, the total number of letters read correctly was recorded and an additional 30 letters were added to the total. If participants were unable to read 4 letters correctly on the first line, they were brought to 1 meter and asked to continue reading down the chart until they could read fewer than three letters on a single line. Thirty letters were not added to the final ETDRS score in this circumstance. Participants P02, P03 and P09 were not able to read any ETDRS letters in one eye and could only detect hand movements (HM). For analysis purposes, the ETDRS letter score for that eye was set to 0 letters.

4.2.3.2.2. Retinal Sensitivity. Microperimetry examinations, completed in twenty-seven eyes from fourteen participants in the central vision loss group, were carried out using the AMD-20 examination (Nidek MP1, Nidek Technologies, Padova, Italy). Examinations took place in a darkened room testing each eye independently through a dilated pupil whilst the fellow eye was patched. Participants were instructed to place their chin on the chin rest and look directly down the camera lens. Once the macula was in view, participants were asked to maintain their gaze for the duration of the examination. Stimuli would appear at different retinal locations and at varying intensities and the participant pressed a button when they could detect the stimuli. The range of intensities was $0 - 20$ decibels (dB), with 0 representing the brightest light, corresponding to the lowest visual sensitivity. An eccentricity grid covering the central 20 degrees of visual angle was centred over the fovea for each eye for each participant (Figure 7). The total number of stimuli presented which fell within the eccentricity border were calculated. The intensity of all stimuli which were responded to were added up and divided by the total number of stimuli presented to give an average retinal sensitivity (RS) value. Any points falling on or outside of the outer eccentricity border were not included to keep the area measured consistent across individuals. This was carried out for each eye. Data were excluded for one eye from participant P03 due to the participant having a cataract. Participants P07, P12 and P18 were not able to identify any stimulus presented during the microperimetry assessment for one eye, whereas P10 could not complete the assessment in either eye. As a result, the RS for these 5 eyes was set to 0dB.

4.2.3.3. Bilateral Disease Duration. Disease duration was calculated as the time at which each patient was diagnosed with bilateral retinal disease in years (Table 1). Prior to this, all patients were diagnosed with unilateral retinal disease. Whilst we are not able to measure the effects of unilateral loss on the entire visual pathway, knowing when patients were diagnosed with bilateral retinal disease provides the point in time when a significant loss of bilateral visual input occurred.

4.2.3.4. Analysis. Best corrected visual acuity was used to determine the better and worse seeing eye for each participant (Table 1). Apart from disease duration, outcome measures for all other clinical assessments were separated in relation to the worse and better seeing eye.

The first stage of the analysis used one-sample t-tests to establish whether values from the worse or better seeing eye were significantly different from normal. This was carried out on assessments where a normal value existed, including retinal structure, optic nerve head structure and BCVA. Normative mean thickness values assessing retinal structure were extracted from a different study using the same model of SD-OCT machine (Nieves-Moreno et al., 2017). The normative means were extracted from a group of age-range matched control subjects, ranging between 69-87 years. Normative optic nerve head thickness values were taken from the OCT output of this study whilst normal BCVA represented an ETDRS letter score of 84 letters, equivalent to 6/6 Snellen acuity or 0.0 logMAR. Paired-samples t-tests then established whether the worse and better seeing eye were significantly different from each other for all clinical measures.

The second stage of the analysis addressed four research questions investigating the relationship between changes to the anterior and posterior visual pathway. These questions included 1) Does retinal structure predict cortical structure?, 2) Does retinal structure predict visual function?, 3) Does cortical structure predict visual function?, and 4) Does bilateral disease duration predict retinal structure, visual function or cortical structure? Pearson correlations were carried out between the clinical output measures listed above relating to changes to the anterior visual pathway and output measures outlined in Chapter 3 relating to changes to the posterior visual pathway.

Figure 2: *Infrared SD-OCT retinal image of the right eye.* ***A:*** *Infrared image of the central macular region showing the 25 slices (horizontal green lines) used to segment the layers of the macula.* ***B:*** *Cross-section of slice 14 of the central macular region from A (bold green horizontal line) showing the different retinal layers. The central dip represents the foveal location with the optic nerve head on the right-hand side of the images.*

Figure 3: *Macula thickness by ETDRS location. **A:** Macula thickness map in which cool (blue/purple) colours indicate thinner areas, and warm (green/yellow/red) regions indicate thicker areas. The overlaid grid represents the 1mm (centre ring), 3mm (inner ring) and 6mm (outer ring) diameter ETDRS locations. **B:** Cross-section through the retina showing that the total macula thickness measure includes the retinal layers from the internal limiting membrane (ILM) to Bruch's membrane (BM), marked by the red borders.*

Figure 4: *SD-OCT-generated RNFL map of the optic nerve head.* ***A:*** *Segmentation of the optic disk was acquired using a 3533µm diameter disk centred over the optic disk, shown in green.* ***B:*** *Cross-section of the unfolded optic nerve head showing the segmented layers highlighting the retinal nerve fibre layer (RNFL) by the horizontal cyan line, automatically segmented using the SD-OCT software.*

Figure 5: Peripapillary RNFL classification. A: Seven quadrants of the optic nerve head, NS: Nasal Superior; N: Nasal; NI: Nasal Inferior; TI: Temporal Inferior; T: Temporal; TS: Temporal Superior; G: Global. Colours indicate quadrants in which values fall within normal limits (green), borderline (yellow) and below normal limits (red) with numbers shown in green inside the brackets representing normative values for those segments. B: Graph illustrating optic nerve head thickness in microns (μm) of the seven quadrants. Coloured areas denote the limits defined in A with the black line representing the thickness values of the participant. The green vertical line corresponds to the green vertical line in Figure 4B.

Figure 6: SD-OCT autofluorescence images of the twenty-seven eyes diagnosed with central retinal disease. Left eyes are presented on the left-hand side with right eyes on the right-hand side. Dark regions to the far left in all left eyes and far right in all right eyes denote the optic nerve head. Dark and mottled areas within the centre of all images reflect damage to the central macula, extending to more peripheral retinal locations in some patients. In all images, the area of the lesion (in mm^2) has been measured using built-in software, represented by the yellow line.

Figure 7: *Colour fundus image of the right eye of a participant in the central vision loss group. Overlaid is the retinal sensitivity performance measured using an AMD-20 examination on the Nidek MP1 microperimeter. Coloured box/number pairs represent the different intensities of the presented stimuli. Higher numbers represent a dimmer stimulus, i.e. greater retinal sensitivity, with numbers ranging from 0-20 dB. Filled squares indicates a response was made to the stimulus. If no response was made, the box remained empty. The black eccentricity grid maps the central 20-degree diameter visual angle. All responses which fall within the eccentricity grid were used to calculate the retinal sensitivity for each eye. Those falling on or outside the eccentricity grid were excluded.*

4.3. Results

4.3.1. Structural Assessments

4.3.1.1. Macular Thickness. Macular thickness for the total macula (averaged across the 1mm, 3mm and 6mm diameter ETDRS locations), central macula (1mm and 3mm diameter ETDRS locations) and peripheral macula (6mm diameter ETDRS location) for each participant is shown in Figure 8. Data from three individuals (P01, P08 and P09) were shown to be excessively greater compared to the remaining cohort when considering total macular thickness in the worse seeing eye. Upon closer inspection of the OCT images, the increased macular thickness appears to be driven by active oedemas in these participants (Figure 8). Whilst we expect that regular anti-VEGF treatment being received by all patients in this cohort would reduce any active oedema, the presence of such has contaminated the total thickness measure. Therefore, data from these three participants were removed. The following *t*-tests were then conducted to analyse whether total macular thickness significantly differed from a normative mean thickness in the following three macular locations.

Total macular thickness was measured as the average of the three retinal locations, 1mm, 3mm and 6mm diameter ETDRS locations (0 – 10 degrees eccentricity). Total macular thickness was greater in the worse compared to the better seeing eye, although this was not significant ($t(9) = 1.027$, p = .331; Table 2). Compared against the normative mean of 317.5µm, only the better seeing eye was significantly thinner (Worse: $t(9) = -2.017$, p = .074; Better: $t(10) = -3.417$, p = .007, 2-tailed; Figure 9A).

Central macular thickness was measured as the average of the 1mm and 3mm diameter ETDRS locations (0 – 5 degrees eccentricity). Central macular thickness was greater in the worse compared to the better seeing eye, although this was not significant ($t(9) = 1.310$, p = .223; Table 2). Compared against the normative mean of 320.6µm, only the better seeing eye was significantly thinner (Worse: $t(9) = -1.162$, p = .275; Better: $t(10) = -3.005$, p = .013, 2-tailed; Figure 9B).

Finally, peripheral macular thickness was measured as the 6mm diameter ETDRS location (5 - 10 degrees eccentricity). Whilst thickness in the worse seeing eye was slightly thinner than in the better seeing eye, this was not significant ($t(9) = -.355$,

p = .731; Table 2). However, both eyes were significantly thinner than the normative mean of 313.8µm (Worse: $t(9)$ = -5.051, p = .001; Better: $t(10)$ = -5.189, p = .000408, 2-tailed; Figure 9C).

4.3.1.2. Ganglion Cell Layer (GCL) Thickness. Highlighted above, data from three participants was removed from the macular thickness analysis due to active oedemas contaminating the thickness measures. Oedemas tend to affect the outer retinal layers more so than the inner retinal layer. Therefore, the GCL should be less contaminated by the active oedema in the three participants identified above. Data were assessed for these three participants to ensure that the automatic segmentation of the GCL was not affected by the active oedema (Figure 10). Examining the automatic segmentations revealed that GCL thickness estimations were affected for patient P01 only (Figure 10). As a result, patient P01 was removed from the subsequent analyses of GCL thickness whilst data from patients P08 and P09 were retained.

Total macula GCL thickness was measured as the average of the three macular locations, 1mm, 3mm and 6mm diameter ETDRS. Total GCL thickness was greater in the worse compared to the better seeing eye, although this was not significant ($t(11)$ = .689, p = .505; Table 2). Compared against the normative mean of 36.8µm, both the worse ($t(11)$ = -5.257, p = .000269, 2-tailed) and better ($t(12)$ = -4.977, p = .000321, 2-tailed) seeing eye were significantly thinner (Figure 11A).

Central macula GCL thickness was measured as the average of the 1mm and 3mm diameter ETDRS locations (0 – 5 degrees eccentricity). Central macula GCL thickness was greater in the worse compared to the better seeing eye, although this was not significant ($t(11)$ = .780, p = .452; Table 2). Compared against the normative mean of 40.2µm, both the worse ($t(11)$ = -4.895, p = .000475, 2-tailed) and better ($t(12)$ = -5.409, p = .000158, 2-tailed) seeing eye were significantly thinner (Figure 11B).

Finally, peripheral macula GCL thickness was measured as the 6mm diameter ETDRS location (5 - 10 degrees eccentricity). With very similar values between the worse and better seeing eyes, they were not significantly different ($t(11)$ = .038, p = .970; Table 2). Compared against the normative mean of 32.5µm, both the worse ($t(11)$ = -5.262, p = .000268, 2-tailed) and better ($t(12)$ = -3.728, p = .003, 2-tailed) seeing eyes were significantly thinner (Figure 11C).

4.3.1.3. Optic Nerve Head Thickness. Assessing the raw values revealed increased thickness measures for participant P01 across all quadrants of the optic nerve head. Data from P01 were therefore removed from the following analyses as an outlier.

Mean global optic nerve head thickness was calculated as the average across six quadrants shown in Figure 12. Thickness values were not significantly reduced in the worse compared to the better seeing eye, ($t(11) = -.481$, p = .640; Table 2), however both eyes were significantly thinner than the normative mean of 95.0μm (Worse: $t(11) = -3.229$, p = .008; Better: $t(12) = -2.357$, p = .036).

Next, we wanted to see if thickness in the temporal quadrants differed from normal, as these quadrants represent projections from the central retina (Figure 12). Mean thickness was not significantly different between eyes for the Superior Temporal ($t(11) = .824$, p = .428). Temporal ($t(11) = -1.173$, p = .266) and Inferior Temporal quadrants ($t(11) = -1.187$, p = .260; Table 2),). Compared against the normative mean values in each quadrant, both eyes were significantly thinner for the Inferior Temporal quadrant (NM = 135.0μm; Worse: $t(11) = -5.531$, p = .000178; Better: $t(12) = -3.716$, p = .003). However, there was no significant difference between either eye and the normaltive mean in the Temporal quadrant (NM = 72.0μm; Worse: $t(11) = -1.337$, p = .208; Better: $t(12) = -1.005$, p = .335), nor the Superior Temporal quadrant (NM = 130.0μm; Worse: $t(11) = -1.183$, p = .262; Better: $t(12) = -1.814$, p = .095).

Finally, we assessed changes in thickness across the nasal quadrants, which represent projections from the far peripheral retina, beyond the 10 degrees visual angle captured in the total macula and GCL thickness outlined above. This was done to investigate whether loss in peripheral retinal projections might explain the significant atrophy of the cortical representation of the peripheral retina, the calcarine sulcus, we reported in Chapter 3 (Figure 12). There was no significant difference in mean thickness between eye in the Nasal($t(11) = 1.004$, p = .337)Superior Nasal ($t(11) = -.310$, p = .762) and Inferior Nasal quadrants ($t(11) = -.230$, p = .822; Table 2).Compared against the normative mean (NM) values in each quadrant, thickness values were not significantly different for either eye in the Inferior Nasal quadrant (NM = 103.0μm; Worse: $t(11) = -.757$, p = .465; Better: $t(12) = -.252$, p = .805), the Nasal quadrant (NM = 72.0μm; Worse: $t(11) = -1.772$, p = .104; Better: $t(12) = -1.675$, p = .120), nor the Superior Nasal

quadrant (NM = 102.0µm; Worse: $t(11)$ = -1.475, p = .168; Better: $t(12)$ = -1.409, p = .184).

4.3.1.4. Lesion Size. Including all participants, whilst lesion size appeared greater in the worse seeing eye compared to the better seeing eye, this was not significant($t(12)$ = .823, p = .426).

4.3.2. Functional Assessments

Raw data from the functional assessments were investigated for outliers as with the previous analyses. No outliers were identified and as a result, the BCVA analysis contained data from both eyes for all fourteen participants. As outlined in Section 4.2.3.1., the exception in analysing retinal sensitivity, was that data from the worse seeing eye for participant P03 was not obtained due to concurrent cataract restricting this measurement. Therefore, thirteen data points are included from the worse seeing eye with fourteen data points from the better seeing eye.

4.3.2.1. Best Corrected Visual Acuity. Best corrected visual acuity (BCVA) determined the better and worse seeing eye for the analyses reported in this chapter. Statistical analysis revealed that both eyes were significantly different from each other ($t(13)$ = -4.810, p = .000340; Figure 13A) and were significantly reduced from normal (Worse: $t(13)$ = -6.670, p = .000015, 2-tailed; Better: $t(13)$ = -5.628, p = .000082, 2-tailed).

4.3.2.2. Retinal Sensitivity. Retinal sensitivity measured using microperimetry, is assessed in dB ranging from 0-20dB where the higher the number, the dimmer the stimulus, corresponding to greater sensitivity. Figure 13B shows that whilst retinal sensitivity was consistently reduced across the cohort for both the worse and better seeing eyes, there was no significant difference between the two eyes ($t(13)$ = .025, p = .981).

4.3.3. Summary of structural and functional retinal assessments.

To summarise this first stage of the results, these data show that even with regular anti-VEGF treatment for central retinal disease, active oedema persists in some individuals,

contaminating thickness of the macula (Figure 8). When data from such individuals are removed, retinal structure appears to be significantly impacted by the central retinal disease. This is evidenced by significant reductions in mean macular thickness, including all retinal layers, GCL thickness and optic nerve head thickness in regions containing projections from the central retina. Assessing visual function in all individuals reveals that both BCVA and retinal sensitivity are reduced in all participants, with BCVA significantly impaired in both eyes compared to normal. Moreover, the worse and better seeing eye were only significantly different from one another in terms of BCVA, with no significant difference found between the two eyes across all other measures.

Table 2: *Mean and standard error of the mean (SEM) for the worse and better seeing eye across all assessments of the anterior visual pathway. Bold values indicate those which are significantly different from the normative mean.*

	Normative Mean	Worse Seeing Eye		Better Seeing Eye	
		Mean	**(SEM)**	**Mean**	**(SEM)**
Macular thickness (µm):					
Total macula	317.6	**298.3**	(9.5)	285.2	(9.4)
Central macula	320.6	**305.6**	(12.9)	285.4	(11.7)
Peripheral macula	313.8	**283.6**	(6.0)	**284.8**	(5.6)
GCL Thickness (µm):					
Total macula	36.8	**26.2**	(2.0)	**24.3**	(2.5)
Central macula	40.2	**26.4**	(2.8)	**23.6**	(3.1)
Peripheral macula	32.5	**25.6**	(1.3)	**25.6**	(1.9)
Optic Nerve Head Thickness (µm):					
Global	95	**82.8**	(3.8)	**86.2**	(3.8)
Inferior Temporal	135	**99.5**	(6.4)	**111.8**	(6.2)
Temporal	72	60.8	(8.4)	68.5	(3.4)
Superior Temporal	130	122.3	(6.6)	117.0	(7.2)
Inferior Nasal	103	97.2	(7.7)	100.9	(8.2)
Nasal	72	66.8	(3.0)	63.9	(4.8)
Superior Nasal	102	90.5	(7.8)	94.0	(5.7)
Lesion Size (mm^2)	-	22.8	(4.3)	19.8	(2.7)
BCVA (# of ETDRS letters)	84	**33.9**	(7.5)	**54.7**	(5.2)
Retinal Sensitivity (dB)	-	5.2	(1.6)	5.2	(1.4)

*BCVA: Best Corrected Visual Acuity; ETDRS: Early Treatment Diabetic Retinopathy Study

Figure 8: *Macular thickness variation for all eyes diagnosed with central retinal disease. Left eyes are presented on the left-hand side with right eyes on the right-hand side. Increased macular thickness is associated with the presence of active oedema which is a factor of nvAMD. Active oedemas appear as black bubbles within the retinal layers, indicted by the red arrows, result in increasing macular thickness evident in patients P01, P08 and P09. N: Nasal, I: Inferior, T: Temporal.*

A. Total Macula

B. Central Macula

C. Peripheral Macula

Macula Thickness (μm)

Seeing Eye

Figure 9: *Macular thickness for the worse and better seeing eye by ETDRS location.* *A:* *Total macular thickness, averaged across the 1mm, 3mm and 6mm diameter ETDRS locations.* *B:* *Central macular thickness calculated as an average of the 1mm and 3mm diameter ETDRS locations.* *C:* *Peripheral macular thickness representing the 6mm diameter ETDRS location. For all box plots, horizontal lines represent the median with upper and lower whiskers representing scores outside the middle 50%. Red crosses indicate the mean thickness value. Dots represent data from each participant. Horizontal dashed lines represent the normative mean taken from age-range matched sighted controls (Nieves-Moreno et al., 2017). NS = Non-significant. *Significant at .001, 2-tailed.*

Figure 10: *Automatic segmentation of the macula ganglion cell layer (GCL). Left eyes are presented on the left-hand side with right eyes on the right-hand side. The top panel outlined in red, shows the automatic segmentation of the GCL for patient P04 who does not exhibit macula oedema. This is shown as a comparison against the three patients (P01, P08 and P09) who do exhibit macula oedemas, shown as black 'bubble-like' areas within the retinal layers. GCL segmentation is denoted by the cyan and purple horizontal lines following the contour of the retina. The large oedema in patient P01 has resulted in this segmentation not capturing the GCL particularly over the central macula, in both eyes. However, compared with patients P08 and P09, whilst they also show macula oedemas, the automatic segmentation has been able to follow the contour of the retina to provide an accurate thickness of the GCL. As a result, patient P01 was removed from subsequent analysis due to inaccurate retinal segmentation whilst data from patients P08 and P09 remained.*

A. Total Macula

B. Central Macula

C. Peripheral Macula

Ganglion Cell Layer (GCL) Thickness (μm)

Worse Better

Worse Better

Worse Better

Seeing Eye

Figure 11: *Macula ganglion cell layer (GCL) thickness for the worse and better seeing eye by ETDRS location.* ***A:*** *Total macula GCL thickness, averaged across the 1mm, 3mm and 6mm diameter ETDRS locations.* ***B:*** *Central macula GCL thickness calculated as an average of the 1mm and 3mm diameter ETDRS locations.* ***C:*** *Peripheral macula GCL thickness representing the 6mm diameter ETDRS location. For all box plots, horizontal lines represent the median with upper and lower whiskers representing scores outside the middle 50%. Red crosses indicate the mean thickness value. Dots represent data from each participant. Horizontal dashed lines represent the normative mean taken from age-range matched sighted controls (Nieves-Moreno et al., 2017). *Significant at .001, 2-tailed.*

Figure 12: *Peripapillary retinal nerve fibre layer (pRNFL) thickness of the optic nerve head stratified by quadrant for the central vision loss group. Schematics above the line graph denote the quadrant of interest for each data set. The dashed line represents thickness values from each quadrant for the worse seeing eye with the dotted line representing the better seeing eye. An average of the two eyes is shown by the full orange line, with error bars representing the standard error of the mean. The black line represents normative mean values built into the Heidelberg SD-OCT machine. Global thickness is calculated as the average of all nasal and temporal quadrants. *Significant at .001, 2-tailed.*

Figure 13: *Visual function results stratified by the worse or better seeing eye. **A:** Best corrected visual acuity results measured by the number of ETDRS letters read by each eye. **B:** Retinal sensitivity measures using the Nidek MP-1 microperimeter. For all box plots, horizontal lines represent the median with upper and lower whiskers representing scores outside the middle 50%. Red crosses indicate the mean value. Dots represent data from each participant. The dashed black horizontal line in A represents an ETDRS letter score of 84 letters, equivalent to 6/6 Snellen acuity or 0.0 logMAR. *Significant at .001, 2-tailed.*

4.3.4. Anterior vs Posterior Visual Pathway

Evidence of significant atrophy to the visual cortex with central retinal disease has been previously reported in this cohort of patients in Chapter 3, Section 3.3 of this thesis. This Chapter revealed significant reductions in cortical volume of the entire occipital cortex, with significant reductions in thickness in the occipital pole and calcarine sulcus, the cortical representations of the central and peripheral retina respectively. Here, I report on whether changes to the anterior visual pathway may be related to the significant atrophy of the posterior visual pathway via a series of Pearson correlations addressing three specific research questions.

4.3.4.1. Does retinal structure predict cortical structure? To address this first question, three sets of Pearson correlations were conducted. The first set of correlations assessed whether changes to total macular and GCL thickness, global optic nerve head thickness and lesion size were significant predictors of reduced volume of the entire occipital cortex. The second set of correlations assessed whether changes to the central macula, including central macula across all retinal layers and central GCL thickness, projections from the central retina to the optic nerve head and lesion size were significant predictors of reduced cortical thickness in the occipital pole. This cortical region represents the lesioned retina in central retinal disease. The third and final set of correlations assessed whether changes to the peripheral macula, including peripheral macular thickness across all retinal layers and the GCL layer, projections from the far peripheral retina to the optic nerve head and lesion size were significant predictors of reduced cortical thickness in the calcarine sulcus. This cortical region represents the peripheral retina. Unfortunately, across all three sets of correlations, there was no significant relationship between any variable (Table 3). Therefore, in this cohort, there is no significant evidence that changes to the structure of the retina predict changes to the structure of the cortex.

4.3.4.2. Does retinal structure predict visual function? To address this second question, three sets of Pearson correlations were conducted (Table 4). Set one assessed whether structure of the central macula, including central macular thickness of all retinal layers and thickness of the GCL predicted visual function of the central macula, BCVA. Results indicated a trending relationship between central macular thickness and BCVA

performance in the better seeing eye, suggesting the possibility that reduced central macular thickness in the better seeing eye, including all retinal layers, may be related to reduced BCVA (Table 4; Figure 14). It also suggests this may be a neural effect (i.e. fewer retinal cells = fewer cortical cells) rather than an inflammation effect (thicker retina = thinner cortex).

Set two assessed whether structure of the total macula, including total macular thickness of all retinal layers and thickness of the GCL predicted visual function measured using retinal sensitivity. Changes to the total macula was used in this correlation since retinal sensitivity covered the central 20-degree diameter visual angle, capturing both the central and peripheral macula. Here, results revealed no significant relationship between any variable (Table 4).

The third and final set of correlations assessed whether lesion size in the worse and better seeing eye could predict visual function from BCVA and retinal sensitivity. Whilst lesion size was not significantly correlated with BCVA in either eye, it was significantly correlated with retinal sensitivity in the worse seeing eye (Figure 15). This indicates that lesion size is a significant predictor of visual function, such that the greater the retinal lesion the poorer the visual performance.

4.3.4.3. Does cortical structure predict visual function? To address this final question, two sets of Pearson correlations were conducted (Table 5). The first set of correlations assessed whether changes in cortical thickness of the occipital pole, the cortical representation of the central macula, can predict visual function measured from BCVA and retinal sensitivity. Results show that cortical thickness in the occipital pole was not significantly correlated with retinal sensitivity in either the better or worse seeing eye. However, cortical thickness was significantly correlated with BCVA in the worse seeing eye with results indicating a trend towards a significant relationship with the better seeing eye (Figure 16). To the best of my knowledge, this study is the first to report that reduced cortical thickness in the occipital pole significantly predicts reduced visual acuity in the worse seeing eye.

The second set of correlations assessed whether changes in cortical thickness of the calcarine sulcus, the cortical representation of the peripheral macula, can predict visual function measured using BCVA and retinal sensitivity. Due to previous evidence

of significant cortical atrophy of the calcarine sulcus in this cohort (reported in Chapter 3), it could well be that BCVA relies on intact structure throughout the visual cortex, not just the occipital pole. However, our results showed no significant correlation. Correlating cortical thickness in the calcarine sulcus with retinal sensitivity also revealed no significant relationship.

4.3.4.4. Does bilateral disease duration predict retinal structure, visual function, or cortical structure? To address this final question, three sets of Pearson correlations were carried out (Table 6). The first set assessed whether bilateral disease duration can predict retinal structure, including total macular thickness, GCL thickness and global optic nerve head thickness. The second set assessed whether bilateral disease duration can predict visual function, including BCVA and retinal sensitivity. The third and final set assessed whether bilateral disease duration can predict cortical structure, including cortical volume and mean thickness of the occipital pole and calcarine sulcus. Across all correlations, the only significant relationship found was between bilateral disease duration and total macula GCL thickness in the better seeing eye (Figure 17). This indicates that the longer the disease duration, the thinner the GCL. This result supports previous literature showing that retinal remodelling occurs in nvAMD and that inner retinal layers become affected as nvAMD progresses (Beck et al., 2016; Martinez-de-la-Casa et al., 2012; Zucchiatti et al., 2015).

4.3.5. Summary of the anterior vs posterior visual pathway.

To summarise this second stage of the results, this data reveal that retinal structure can predict visual function, such that the larger the lesion size, the worse the visual function, measured using both BCVA and retinal sensitivity. There is also a trending relationship suggesting that reduced macular thickness across all retinal layers from the better seeing eye, may predict BCVA in both eyes, although this did not reach significance. Excitingly, this data also revealed that cortical structure can predict visual function, specifically, reduced cortical thickness in the occipital pole significantly predicts reduced BCVA in the worse seeing eye, with a trending relationship with BCVA in the better seeing eye. This indicates that BCVA does not rely only on efficient functioning of the macula but also on maintained structure of the visual cortex, specifically the occipital pole. The final relationship found that bilateral disease duration significantly

predicts retinal structure, such that greater disease duration is significantly correlated with reduced GCL thickness in the better seeing eye only.

Table 3: Pearson correlation and significance values assessing whether retinal structure predicts cortical structure.

	Worse Seeing Eye		Better Seeing Eye	
	R	**(p)**	**R**	**(p)**
Volume				
Total macular thickness (N = 11)	.467	(.174)	.241	(.475)
Total macula GCL thickness (N = 13)	.324	(.304)	.003	(.992)
Global ONH thickness (N = 13)	.148	(.647)	.450	(.123)
Lesion size (N = 14)	.157	(.593)	-.376	(.185)
Mean Thickness – Occipital Pole				
Central macular thickness (N = 11)	.036	(.922)	.400	(.223)
Central macula GCL thickness (N = 13)	-.134	(.677)	.274	(.364)
Av. Temporal ONH thickness (N = 13)	.049	(.880)	-.135	(.660)
Lesion size (N = 14)	-.135	(.646)	-.322	(.261)
Mean Thickness – Calcarine Sulcus				
Peripheral macular thickness (N = 11)	-.126	(.729)	.426	(.192)
Peripheral macula GCL thickness (N = 13)	.119	(.712)	.005	(.988)
Av. Nasal ONH thickness (N = 13)	-.165	(.609)	.202	(.509)
Lesion size (N = 14)	.003	(.991)	-.452	(.104)

*GCL: Ganglion Cell Layer; ONH: Optic Nerve Head

Table 4: *Pearson correlation and significance values assessing whether retinal structure predicts visual function.*

		BCVA		RS	
		WE	**BE**	**WE**	**BE**
Central macular thickness (N = 11)	**WE**	R = .056 p = .878	-	-	-
	BE	-	R = .543 p = .084	-	-
Central macula GCL thickness (N = 13)	**WE**	R = -.005 p = .988	-	-	-
	BE	-	R = .286 p = .343	-	-
Total macular thickness (N = 11)	**WE**	-	-	R = .023 p = .950	-
	BE	-	-	-	R = .101 p = .769
Total macula GCL thickness (N = 13)	**WE**	-	-	R = .010 p = .975	-
	BE	-	-	-	R = .226 p = .459
Lesion Size (N = 14)	**WE**	R = -.387 p = .172	-	**R = -.638*** **p = .014**	**-**
	BE	-	R = .375 p = .186	-	R = .437 p = .119

*BCVA: Best Corrected Visual Acuity; RS: Retinal Sensitivity; WE: Worse seeing eye; BE: Better seeing eye; GCL: Ganglion Cell Layer

Figure 14: *Scatterplot showing the trending relationship between central macular thickness, including all retinal layers, and visual function measured using BCVA for the better seeing eye. Dots represent data from each individual participant with the dotted line representing the line of best fit. Pearson R and significance values indicate the trending relationship between these variables.*

Figure 15: *Scatterplot showing the significant correlation between lesion size and visual function measured using retinal sensitivity, for the worse seeing eye. Dots represent data from each individual participant with the dotted line representing the line of best fit. Pearson R and significance values indicate the significant relationship between these variables.*

Table 5: Pearson correlation and significance values assessing whether cortical structure predicts visual function.

	BCVA		RS	
	WE	**BE**	**WE**	**BE**
Mean Thickness – Occipital Pole (N = 14)	**R = .576***	R = .513	R = .275	R = .065
	p = .031	p = .061	p = .341	p = .825
Mean Thickness – Calcarine Sulcus (N = 14)	R = .332	R = .142	R = -.093	R = -.196
	p = .246	p = .629	p = .752	p = .501

*Significant at .005, 2-tailed; BCVA: Best Corrected Visual Acuity; RS: Retinal Sensitivity; WE: Worse seeing eye; BE: Better seeing eye

Figure 16: *Scatterplot showing the relationship between cortical thickness in the occipital pole and visual function measured using BCVA. BCVA for the worse seeing eye is plotted in dark grey and the better seeing eye plotted in light grey. Dots represent data from each individual participant with the dotted line representing the line of best fit. Pearson R and significance values indicate the significant relationship between BCVA from the worse seeing eye and the trending relationship with BCVA from the better seeing eye.*

Table 6: *Pearson correlation and significance values assessing whether bilateral disease duration predicts retinal structure, visual function, or cortical structure.*

		Bilateral Disease Duration	
Retinal Structure:			
Total macular thickness (N = 11)	W	R = -.148	p = .683
	B	R = -.344	p = .300
Total macula GCL Thickness (N = 13)	W	R = -.140	p = .665
	B	**R = -.804****	**p = .001**
Global ONH Thickness (N = 13)	W	R = .367	p = .240
	B	R = .003	p = .992
Lesion size (N = 14)	W	R = .426	p = .147
	B	R = .223	p = .443
Visual Function (N = 14):			
BCVA	W	R = -.083	p = .777
	B	R = .073	p = .805
Retinal Sensitivity	W	R = -.149	p = .611
	B	R = -.127	p = .666
Cortical Structure (N = 14):			
Cortical Volume		R = -.168	p = .566
Mean Cortical Thickness – Occipital Pole		R = .223	p = .444
Mean Cortical Thickness – Calcarine Sulcus		R = -.027	p = .927

*BCVA: Best Corrected Visual Acuity; WE: Worse seeing eye; BE: Better seeing eye; GCL: Ganglion Cell Layer; ONH: Optic Nerve Head

Figure 17: *Scatterplot showing the significant correlation between bilateral disease duration and total macula GCL thickness of the better seeing eye, indicating that bilateral disease duration can predict retinal structure. Dots represent data from the better seeing eye from each individual participant with the dotted line representing the line of best fit. Pearson R and significance values indicate the significant relationship.*

4.4. Discussion

This study has shown that with central retinal disease, there are significant changes to the structure of the retina, evidenced by reduced macular thickness across all retinal layers, with a specific thinning of the ganglion cell layer (GCL) and thinning of projections from central retina to the optic nerve head. Central retinal disease is also associated with reduced visual function, with a significant reduction in best corrected visual acuity (BCVA) in both the worse and better seeing eye. In the cohort tested here, results indicate significant relationships between the anterior and posterior visual pathway such that retinal structure and cortical structure predict visual function and bilateral disease duration predicts retinal structure.

In line with previous research, this data reveals significant reductions in macular thickness across all retinal layers. In addition to these previous reports we show that whilst thickness values were not significantly different between the worse or better seeing eye, total macular thickness averaged across the 1-6mm diameter ETDRS locations and central macular thickness, averaged across the 1 and 3mm diameter ETDRS locations were significantly reduced in the better seeing eye only. However, peripheral macular thickness of the 6mm diameter ETDRS location was significantly reduced in both eyes.

Nevertheless, in nvAMD, neovascularisation occurs due to subretinal or intraretinal fluid (Lim et al., 2012) which contaminates macular thickness. In this cohort, macular thickness is quite varied as the disease manifests differently in each patient, with some patients exhibiting active oedemas (Figure 8). This in turn could mask changes occurring to specific layers of the retina which may reflect thinning due to degeneration. Therefore, assessing changes to other retinal layers which are less contaminated by oedema, may provide more sensitive measures of retinal changes than macular thickness alone. This study assessed changes to the GCL and revealed significant thinning to the GCL in both eyes at all macula ETDRS locations, supporting previous research (Beck et al., 2016; Zucchiatti et al., 2015). This suggests that degeneration of the GCL may be occurring due to apoptosis, following reduced input from the photoreceptors. It may well be that GCL could be a more sensitive biomarker of disease progression than total macular thickness.

Morphological studies have investigated the trajectories of the retinal nerve fibre bundles from the optic nerve head demonstrating that foveal fibres from the central macula occupy a large portion of the temporal quadrant (Fitzgibbon & Taylor, 1996; Jansonius et al., 2009). Consequently, we should expect to find that central retinal disease due to nvAMD is associated with reduced pRNFL thickness particularly in temporal quadrants compared the nasal quadrants. Whilst thickness values did not differ significantly between eyes, compared to normative data there was a significant reduction in global pRNFL thickness, with specific thinning in the Inferior Temporal quadrant, consistent with previous research (Malania et al., 2017). This suggests that changes to the structure of the central macula may lead to changes in thickness of projections to the optic nerve head, indicating a progressive loss of neurons in both outer and inner retinal layers.

As expected with this central retinal disease cohort, this study showed that visual function was also impaired in both the worse and better seeing eyes. In line with previous research, retinal sensitivity measured using microperimetry was reduced in both eyes (Cassels et al., 2017; Dinc et al., 2008; Vujosevic et al., 2011). BCVA was also significantly reduced from normal in both eyes, consistent with previous research (Airody et al., 2015; D. M. Brown et al., 2006a; Hanson et al., 2019; Rosenfeld et al., 2006), with the worse seeing eye significantly impaired compared to the better seeing eye. This is consistent with previous research suggesting that despite an initial increase in BCVA following anti-VEGF treatment for nvAMD, long-term visual function continues to decline (Airody et al., 2015).

The second stage of the results assessed the relationship between changes to the anterior and posterior visual pathway. Progression of central retinal disease due to nvAMD moves from the photoreceptor layer to more inner retinal layers including the GCL, which in turn projects to the visual cortex via the optic radiations. Investigating the relationship between the two visual pathways may address whether neuronal loss in one pathway can lead to neuronal loss in the other. Conversely, we may find that the loss of visual input to the anterior visual pathway alone may be sufficient to lead to cortical atrophy in the posterior visual pathway.

Assessing the anterior visual pathway first, this data reveal that retinal structure significantly predicts visual function, such that the larger the lesion size, the worse the visual function, measured using retinal sensitivity. There is also a trending relationship suggesting that reduced macular thickness across all retinal layers from the better seeing eye, may predict BCVA in the better seeing eye, although this did not reach significance. Finally, this data revealed that bilateral disease duration significantly predicts retinal structure, such that greater disease duration is significantly correlated with reduced GCL thickness in the better seeing eye only. This supports previous literature showing that retinal remodelling occurs in nvAMD and that inner retinal layers, such as the GCL, become affected as nvAMD progresses (Beck et al., 2016; Martinez-de-la-Casa et al., 2012; Zucchiatti et al., 2015).

Whilst we report no significant relationships between structural changes to anterior and posterior visual pathway, we did reveal that structure of the posterior visual pathway significantly correlated with visual function. Excitingly, this data revealed that reduced cortical thickness in the occipital pole significantly predicts reduced BCVA in the worse seeing eye, with a trending relationship with BCVA in the better seeing eye. Existing knowledge suggests that maintained structure of the central macula is essential to see in fine detail including BCVA (Lim et al., 2012). Importantly, however, the current study suggests that BCVA also relies on maintained structure of the visual cortex, specifically the occipital pole. Reduced BCVA may in fact be due to both retinal and cortical loss. To the best of our knowledge, this is the first study to report that BCVA is significantly predicted by cortical thickness in the occipital pole.

In conclusion, this study demonstrates that in central retinal disease, visual function is significantly impaired as measured by retinal sensitivity and BCVA. There are also significant changes in retinal structure, with reduced macular thickness and macula GCL thickness. This is also reflected by a reduction in pRNFL thickness in the inferior temporal quadrant, implying reduced projections from the macula to the optic nerve head. Such structural changes may suggest that retinal degeneration may be occurring with long-term reduced input from the photoreceptors. Monitoring GCL thickness changes specifically in individuals without active oedemas may therefore be a more sensitive biomarker of disease progression.

We have shown significant relationships between different measures of the anterior visual pathway, such that bilateral disease duration predicts GCL thickness in the better seeing eye and large lesion size predicts visual function. Furthermore, the advantage of this study has been to address the relationship between changes to the anterior and posterior visual pathway in central retinal disease. Here we have shown, for the first time, that cortical structure predicts BCVA. What this study does not address is the order of these changes, for example, do reductions in retinal thickness result in impaired BCVA which then results in atrophy of the visual cortex or is impaired BCVA alone sufficient to cause atrophy of the cortex, and together these result in reduced thickness of the retina?

Together, this information is important in future research into patient selection for vision restoration techniques. The ability to measure the impact of long-term vision loss on the extent of cortical atrophy and/or degeneration of the posterior visual pathway is vital as the success of such restorative devices relies on the posterior visual pathway remaining viable to process restored visual input.

<u>Chapter 5</u>

What is the relationship between the anterior and posterior visual pathway in long-term peripheral retinal disease?

5.1. Introduction

Following on from Chapter 4, which focused on the relationship between the anterior and posterior visual pathway in central retinal disease, this chapter will focus on those relationships in a peripheral retinal disease known as retinitis pigmentosa (RP). RP is a form of hereditary retinal disease resulting from degeneration of rod and cone photoreceptors. Rod photoreceptors mediate achromatic vision in dim light (e.g., starlight or moonlight) whereas cone photoreceptors are important for colour vision and fine acuity in bright light (e.g., daylight) (Hartong et al., 2006). Rod and cone photoreceptor nuclei are found in the outer nuclear layer of the retina which is attenuated with RP (Hartong et al., 2006). Although the inner nuclear layer, ganglion cell layer and retinal nerve fibre layer remain well preserved (Figure 1), degeneration of these layers is often seen as the disease advances (Hartong et al., 2006). While some patients develop symptoms in childhood, others remain asymptomatic until mid-adulthood (Hartong et al., 2006). Typically, patients exhibit difficulties with dark adaptation and night blindness due to loss of rods, with a loss of the mid-peripheral visual field. As RP advances, far peripheral vision will be lost with the eventual development of tunnel vision, finally losing central vision (Hartong et al., 2006).

As outlined in Chapter 4, visual function is often assessed via best corrected visual acuity (BCVA), using the Early Treatment Diabetic Retinopathy Study (ETDRS) vision chart (ETDRS, 1985). In contrast to central retinal disease, monitoring central visual function in peripheral retinal disease may not be as informative in diseases such as retinitis pigmentosa (RP), as often performance can remain normal whilst there is a small area of central macula preserved (Hartong et al., 2006). Assessments of the visual field such as the Humphrey Field Analysers (HFA) are therefore routinely used alongside BCVA in the management of peripheral retinal disease. These assessments have revealed that some patients exhibit midperipheral scotomas and some show

asymmetrical visual field loss with preservation of the central visual field (S. Grover et al., 1997; Sandeep Grover et al., 1998). However, there are also reports that progressive loss of visual function over an average 5-year period is associated with significant deterioration of the central 10-degree visual field (Hirakawa et al., 1999; Holopigian et al., 1996). This highlights the importance of assessing the whole visual field, even in retinal diseases primarily affecting peripheral visual field loss.

Structural assessments of the retina are in line with those discussed in Chapter 4. High resolution images acquired using spectral domain optical coherence tomography (SD-OCT) can quantify total thickness changes across the retinal layers along with changes in peripapillary RNFL thickness (pRNFL) of the optic nerve head. In RP, reduced central retinal thickness (Hood et al., 2009; Rita Machado et al., 2017; Vámos et al., 2011), thought to potentially indicate cell loss, has been significantly correlated with reduced visual acuity (Y. J. Kim et al., 2013; Sandberg, Brockhurst, Gaudio, & Berson, 2005) however, increased central retinal thickness can also be present due to oedema (Sandberg et al., 2005). OCT has also enabled researchers to identify whether reductions are occurring to other layers of the retina which may be driving total retinal thickness reductions. Some reports have revealed a reduction in the ganglion cell layer (GCL) in RP (Humayun, Prince, et al., 1999; Santos et al., 1997; Stone, Barlow, Milam, Juan, & Milam, 1992; Vámos et al., 2011), indicating transneuronal degeneration whereas others have reported thickening (Hood et al., 2009; Yoon & Yu, 2018). Current reports on changes to peripapillary RNFL (pRNFL) thickness in RP are also contradictory, with reports of pRNFL thickening (Anastasakis et al., 2012; Hood et al., 2009), pRNFL thinning (Anastasakis et al., 2012; Oishi et al., 2009; Walia et al., 2007) and pRNFL thickness within normal limits (Rita Machado et al., 2017). Therefore, there is some debate as to whether degeneration of multiple retinal layers and/or pRNFL thickness may be occurring with RP.

The effects of RP on the posterior visual pathway are currently under-researched and remain unclear. Whilst previous reports are limited, there is evidence of atrophy of the visual cortex with reductions in cortical volume (Rita Machado et al., 2017). However, there are mixed results in terms of atrophy in the form of reduced cortical thickness, with some reporting thinner primary visual cortex (Castaldi et al., 2019) whilst other report no or minor changes (Cunningham, Weiland, et al., 2015; Ferreira et

al., 2017). Please see Chapter 3, section 3.1 for a more extensive review of MRI assessments of the posterior visual pathway in retinal disease.

Whilst some of these neuroimaging studies have also reported on structural changes to the anterior visual pathway (Ferreira et al., 2017; Rita Machado et al., 2017), they have not established whether changes to the anterior and posterior pathways are correlated. For example, are changes to one eye alone driving potential changes further along the visual pathway? Consequently, to increase our understanding of the relationship between clinical and neuroimaging data, to potentially identify biomarkers of disease progression, this study aimed to observe the relationship between changes to the anterior (the eye) and posterior (the brain) visual pathways in patients with long-term peripheral retinal disease. The objective of this study was to compare the worse and better seeing eye across several clinical assessments of the anterior visual pathway with data from the central retinal disease group discussed in Chapter 4. This data will also be compared with outcome measures showing potential atrophy of the posterior visual pathway outlined in Chapter 3, to see if there are any indications that changes to the anterior visual pathway may drive changes to the posterior visual pathway.

Figure 1: *Layers of the human retina measurable using the Heidelberg Optical Coherence Tomography (OCT), and the cells contained within them. Know Your Retinal Layers (Heidelberg, 2016).*

5.2. Materials and Methods

5.2.1. Participants

Written informed consent was obtained from all participants. Ethical approval was granted by York Neuroimaging Centre Research, Ethics and Governance Committee and the NHS Research Ethics Committee (IRAS: 181823). This study followed the tenets of the Declaration of Helsinki.

Details relating to recruitment numbers and dates, inclusion and exclusion criteria are outline in Chapter 4, Section 4.2. Of the final cohort of eighteen participants, fourteen of whom are discussed in Chapter 4, four patients were diagnosed and allocated into the peripheral retinal disease group (Table 1).

Table 1: *Demographics of participants recruited to the SYNAPTIC study diagnosed with peripheral retinal disease.*

Subject	Gender	Age (y, m)	Diagnosis	Worse Eye		Better Eye		Disease duration (y. m)
				OD / OS	BCVA	OD / OS	BCVA	
P15	Female	63, 8	RP	OD	45	OS	58	20, 2
P16	Female	66, 11	RP	OD	90	OS	90	3, 10
P17	Male	26, 3	RP	OD	1	OS	63	7, 4
P18	Male	34, 3	RP	OD	60	OS	71	23, 1

*RP: Retinitis pigmentosa; OD: Oculus Dexter; OS: Oculus Sinister; BCVA: Best Corrected Visual Acuity.

5.2.2. Design

In this cross-sectional design, routine clinical assessments (outlined in Chapter 4, Section 4.2.3), took place no more than two weeks prior to the neuroimaging assessments of the posterior visual pathway detailed in Chapter 3, Section 3.2.3.

5.2.3. Procedures

All clinical assessments were completed at York Teaching Hospital NHS Foundation Trust during the participants' routine clinical visit. Whilst this cohort completed the

same structural assessments outlined in Chapter 4, Section 4.2.3, the functional assessments differed slightly. Best corrected visual acuity (BCVA) was conducted under the same procedure described in Chapter 4, Section 4.2.3.1.1. However, this cohort did not complete microperimetry, which focuses on central retinal sensitivity. Instead, information was taken from a Humphrey Visual Field assessment completed within 12-months of joining the SYNAPTIC study, providing a broader, more standardised measure of visual field sensitivity (see below).

5.2.3.1. Visual Field Sensitivity. Visual field examinations had been completed by all four participants in the peripheral vision loss group within 12 months of joining the SYNAPTIC study. As it is known this disease progresses slowly, no new assessment was conducted, with data extracted from these existing assessments. Examinations had been carried out using the Swedish Interactive Threshold Algorithm (SITA) standard of the Humphrey Field Analyser (HFA) II (Carl Zeiss, Meditec, Dublin, CA, USA). Two participants (P15 and P17) had an existing examination using the central 10-2 threshold test (Figure 2A) whilst participants P16 and P18 had an existing examination using the central 24-2 threshold test (Figure 2B). Output measures from the examinations included mean deviation (MD) and pattern standard deviation (PSD) which were taken for both eyes for all participants. MD demonstrates the difference between the patient and age-range matched normative values built into the HFA machine at tested points on the retina with one overall value. Negative values indicate visual field loss whilst positive values indicate above average visual fields. PSD records focal loss only resulting from the pathology in question whilst accounting for general reductions in vision caused by cataract, uncorrected refractive error and age-related reduced sensitivity. A high PSD indicates irregular vision and is a useful measure of disease progression. Retinal sensitivity (RS) of the central 10-degree radius visual field was also calculated using the visual sensitivity results from the HFA output from the central part of the 10-2 and 24-2 threshold examinations (Figure 2). For both examinations, central retinal sensitivity was calculated from all values within the red hexagon on the numeric sensitivity map, denoting the central 10-degree visual angle. This was calculated for both eyes and allowed for a more direct (but approximate) comparison in visual field function between participants in the peripheral vision loss group, despite the different examinations completed. This method also allowed a more direct comparison between function of the

central retina between participants diagnosed with central (Chapter 4) and peripheral retinal disease.

5.2.3.2. Lesion Size. Autofluorescence images of the central macular region were used to measure the size of the structural lesion in each eye for all participants (Figure 3). In this cohort, there were signs of retinal disease affecting both the peripheral and central retina, particularly for participant P17 (Figure 3). As a result, the lesion size for P17 was deemed to affect the entire retina captured with spectral domain optical coherence tomography (SD-OCT) and given a value of 60, the size of the whole screen minus the optic nerve head. For the remaining peripheral vision loss participants, scotoma size reflects the entire captured area ($60mm^2$) minus the unaffected area shown in Figure 3. The border of the affected retina was traced using built-in software, with the resulting value showing the size of the affected area in mm^2.

5.2.3.3. Bilateral Disease Duration. Disease duration was calculated as the time at which each patient was diagnosed with bilateral peripheral retinal disease in years (Table 1).

5.2.3.4. Analysis. Due to the small sample size diagnosed with peripheral retinal disease, no statistical analyses were carried out on these data. Instead, individual data were visually compared with normative data between the worse and better seeing eye following a similar rationale as that outlined in Chapter 4. This was determined by best corrected visual acuity for each participant (Table 1). Apart from disease duration, outcomes for all other clinical assessments were separated in relation to the worse and better seeing eye. This was to investigate the relationship between each eye and the indication towards volumetric atrophy of the entire occipital cortex outlined in Chapter 3. Lesion size was not assessed in relation to other measurements of the anterior visual pathway as they each captured changes within the central macula whereas the lesion size refers to the extent of damage within the peripheral retina.

A **P15**

B **P16**

P17

P18

Figure 2: *Results from the Humphrey Field Analyser II. Visual field sensitivity maps from* **A:** *the central 10-2 examination for participants P15 (top row) and P17 (bottom row) and* **B:** *the 24-2 examination for participants P16 (top row) and P18 (bottom row). Images on the left-hand side for each patient indicate the threshold of stimulus intensity detected in dB. The brightest intensity corresponds to 0dB, with normal sensitivity values around 30dB. The grey scale map on the right-hand side is a visual representation of the numeric map, with darker areas indicating poorer sensitivity to the stimulus. The red hexagons denote the central 10-degree radius visual field used to compare central retinal sensitivity across the peripheral vision loss participants.*

Figure 3: SD-OCT autofluorescence images of the eight eyes diagnosed with peripheral vision loss. Left eyes are presented on the left-hand side with right eyes on the right-hand side. In all images, the extent of the retina affected by the disease falls outside of the yellow line, with the area inside the yellow line representing unaffected retina. The size of the lesion is therefore calculated as the total area of the window, minus the representation of the unaffected retina. The lesion for P17 was calculated as the full extent of the window, occupying both central and peripheral retinal locations.

5.3. Results

The following data will be compared between the worse and better seeing eye and published normative data. For those assessments which were carried out by the central retinal disease cohort, outlined in Chapter 4, data will be compared in terms of eye and disease type.

5.3.1. Structural Assessments

5.3.1.1. Macular Thickness. Macular thickness was assessed covering three categories; total macula thickness, calculated as an average of the 1mm, 3mm and 6mm diameter ETDRS locations, central macula thickness, calculated as an average of the 1mm and 3mm diameter ETDRS locations, and peripheral macula thickness, the 6mm diameter ETDRS location. Mean total macula thickness was slightly less in the worse (292.9µm) compared to the better seeing eye (298.2µm). Compared against the normative mean of 317.5µm, two patients had thickness values above whilst two had thickness values below. Compared with the central retinal disease cohort, mean total macula thickness was comparable in both eyes (Table 2; Figure 4A).

Mean central macula thickness was also less for the worse (301.1µm) compared to the better seeing eye (312.2µm), with two patients falling below the normative mean of 320.6µm. Compared against the central retinal disease cohort, central macula thickness was comparable in the worse seeing eye whilst slightly thicker in the better seeing eye (Table 2; Figure 4B).

Finally, mean peripheral macula thickness was slightly greater for the worse (276.5µm) compared to better seeing eye (270.3µm) however, three out of four patients fell below the normative mean of 313.6µm. Compared to the central retinal disease cohort, mean peripheral macula thickness was reduced in both eyes (Table 2; Figure 4C).

5.3.1.2. Ganglion Cell Layer (GCL) Thickness. GCL thickness was assessed covering three categories; total macula GCL thickness, calculated as an average of the 1mm, 3mm and 6mm diameter ETDRS locations, central macula GCL thickness, calculated as an average of the 1mm and 3mm diameter ETDRS locations, and peripheral macula GCL thickness, the 6mm diameter ETDRS location. Mean total

macula GCL thickness was slightly reduced in the worse (23.0µm) compared to the better seeing eye (25.4µm). Compared against the normative mean of 36.8µm, all patients fell below this value for the worse seeing eye whilst three out of four patients fell below for the better seeing eye. Compared to the central retinal disease cohort, mean total macula GCL thickness was comparable for both eyes (Table 2; Figure 5A).

Mean central macula GCL thickness was also reduced for the worse (23.7µm) compared to the better seeing eye (26.8µm). Compared against the normative mean of 40.2µm, all patients fell below this value for the worse seeing eye whilst three out of four patients fell below for the better seeing eye. Compared against the central retinal disease cohort, mean central macula GCL thickness was comparable in both eyes (Table 2; Figure 5B).

Finally, mean peripheral macula GCL thickness was slightly reduced for the worse (21.7µm) compared to better seeing eye (22.6µm). As with the other ETDRS locations, compared against the normative mean of 32.5µm, all patients fell below this value for the worse seeing eye whilst three out of four patients fell below for the better seeing eye. Compared to the central retinal disease cohort, mean peripheral macula GCL thickness was reduced for both eyes (Table 2; Figure 5C).

5.3.1.3. Optic Nerve Head Thickness. Global optic nerve head thickness was calculated as the average of the following six quadrants: superior nasal, nasal, inferior nasal, superior temporal, temporal and inferior temporal. Results show that global thickness was greater for the worse (114.8µm) compared to better seeing eye (97.3µm), with both eyes thicker than the normative mean of 95.0µm. On average, global optic nerve head thickness was slightly greater in both eyes when compared against the central retinal disease cohort (Table 2; Figure 6).

Next, the three nasal quadrants were assessed which represent projections from the peripheral retina affected in RP. Mean thickness for the Inferior Nasal quadrant was greater in the worse (101.8µm) compared to the better seeing eye (75.8µm), with both eyes falling below the normative mean of 103.0µm. Mean thickness for the Nasal quadrant was also greater in the worse (67.3µm) compared to the better seeing eye (59.5µm), with both eyes falling below the normative mean of 72.0µm. Mean thickness for the Superior Nasal quadrant was reduced in the worse (76.3µm) compared to the

better seeing eye (86.5µm), again with both eyes falling below the normative mean of 102.0µm. As expected, mean thickness of each Nasal quadrant appears to be reduced in this cohort when compared against the central retinal disease cohort (Table 2; Figure 6).

Finally, the three temporal quadrants were assessed which represent projections from the central retina. Mean thickness for the Inferior Temporal quadrant was greater in the worse (165.3µm) compared to the better seeing eye (123.0µm), with only the worse seeing eye greater than the normative mean of 135.0µm. Mean thickness for the Temporal quadrant was greater in the worse (156.5µm) compared to the better seeing eye (110.3µm), with both eyes greater than the normative mean of 72.0µm. Mean thickness for the Superior Temporal quadrant was reduced in the worse (129.0µm) compared to the better seeing eye (153.3µm), with only the better seeing eye falling above the normative mean of 130.0µm. Again, as expected, mean thickness of each Temporal quadrant appears greater in this cohort when compared with the central retinal disease cohort (Table 2; Figure 6).

5.3.1.4. Lesion Size. Lesion size appears comparable between the two eyes, measuring 39.0 and 36.5mm^2 for the worse and better seeing eyes, respectively. Compared against the central retinal disease cohort, whilst the lesion size was greater it must be noted that they capture different parts of the retina; lesion size for the central cohort mainly captures the central retina whereas for the peripheral cohort, the lesion occupies primarily the peripheral retina although the central retina may also be affected by disease (Table 2; Figure 3).

5.3.2. Functional Assessments

5.3.2.1. Best Corrected Visual Acuity. Best corrected visual acuity (BCVA) was reduced from normal (84 ETDRS letters) in both the worse (49) and better seeing eyes (70.5), revealing a degree of central retinal deficit. Compared to the central retinal disease cohort, BCVA was slightly better in both eyes (Table 2; Figure 7).

5.3.2.2. Visual Field Sensitivity. Visual field sensitivity was measured using the Humphrey Visual Field Analyser and gave two output measures, mean deviation (MD) and pattern standard deviation (PSD). MD is an indicator of global visual field loss, with normal values ranging between 0 - -2dB; negative values indicating greater visual field loss (poorer vision). PSD is an indicator of localised visual field loss with larger values

indicating irregular vision. As expected, results show that visual function is consistent across the worse and better seeing eye, both in terms of MD (Worse Eye: Mean = -28.5dB, SEM = 3.1dB; Better Eye: Mean = -28.8dB, SEM =2.7dB) and PSD (Worse Eye: Mean = 7.2dB, SEM = 2.2dB; Better Eye: Mean = 7.1dB, SEM = 2.0dB). This shows that all participants had extensive global visual field deficits, with large negative MD values (Figure 8).

Additionally, retinal sensitivity (RS) of the central 10-degree radius visual field was calculated using data from the Humphrey examination, to allow a more direct comparison between retinal sensitivity obtained from the central retinal disease cohort described in Chapter 4. Here, results reveal that all participants diagnosed with peripheral retinal disease also had central retinal defects, with a marginal difference between the worse (9.7dB) and better seeing eyes (9.4dB). Compared against the central retinal disease cohort, retinal sensitivity was greater for both the worse and better seeing eye (Table 2; Figure 9).

5.3.3. Summary of structural and functional retinal assessments.

To summarise this first stage of the results, this small pilot dataset shows that macular thickness, including all retinal layers, is reduced in some patients but not all. Specifically assessing thickness of the macula GCL, all patients have reduced thickness in the worse seeing eye compared to the normative mean, whilst three out of four patients show reductions in the better seeing eye compared to the normative mean. Optic nerve head thickness across the nasal quadrants also appears to be reduced compared to both the normative mean and central retinal disease cohort, suggesting the possibility that projections from the peripheral retina are reduced. However, testing this hypothesis on a larger RP cohort is required to make a definitive conclusion.

Whilst functional assessments of the anterior visual pathway confirm visual field loss in both eyes (PSD and MD outcomes) they also reveal reduced BCVA in both eyes in three out of four patients compared against normal. Retinal sensitivity is also reduced, albeit slightly greater than the central retinal disease cohort in both eyes. These data suggest that even in RP, a peripheral retinal disease, some patients may also have central retinal deficits.

Table 2: *Mean and standard error of the mean (SEM) for the worse and better seeing eye across all assessments of the anterior visual pathway.*

	Normative Mean	Peripheral Retinal Disease				Central Retinal Disease			
		Worse Seeing Eye		Better Seeing Eye		Worse Seeing Eye		Better Seeing Eye	
		Mean	**(SEM)**	**Mean**	**(SEM)**	**Mean**	**(SEM)**	**Mean**	**(SEM)**
Macular thickness (µm):									
Total macula	317.6	292.9	(22.6)	298.2	(27.8)	298.3	(9.5)	285.2	(9.4)
Central macula	320.6	301.1	(24.0)	312.2	(30.9)	305.6	(12.9)	285.4	(11.7)
Peripheral macula	313.8	276.5	(25.0)	270.3	(27.7)	283.6	(6.0)	284.8	(5.6)
GCL Thickness (µm):									
Total macula	36.8	23.0	(4.3)	25.4	(6.5)	26.2	(2.0)	24.3	(2.5)
Central macula	40.2	23.7	(5.7)	26.8	(7.8)	26.4	(2.8)	23.6	(3.1)
Peripheral macula	32.5	21.7	(3.2)	22.6	(4.4)	25.6	(1.3)	25.6	(1.9)
Optic Nerve Head Thickness (µm):									
Global	95	114.8	(12.8)	97.3	(10.4)	82.8	(3.8)	86.2	(3.8)

Inferior Temporal	135	165.3	(12.3)	123.0	(11.7)	99.5	(6.4)	111.8	(6.2)
Temporal	72	156.5	(14.0)	110.3	(12.4)	60.8	(8.4)	68.5	(3.4)
Superior Temporal	130	129.0	(15.4)	153.3	(15.2)	122.3	(6.6)	117.0	(7.2)
Inferior Nasal	103	101.8	(12.0)	75.8	(11.2)	97.2	(7.7)	100.9	(8.2)
Nasal	72	67.3	(14.5)	59.5	(11.8)	66.8	(3.0)	63.9	(4.8)
Superior Nasal	102	76.3	(14.7)	86.5	(11.9)	90.5	(7.8)	94.0	(5.7)
Lesion Size (mm^2)	-	39.0	(7.5)	36.5	(9.2)	22.8	(4.3)	19.8	(2.7)
BCVA (# of ETDRS letters)	84	49	(18.5)	70.5	(7.0)	33.9	(7.5)	54.7	(5.2)
Retinal Sensitivity (dB)	-	9.7	(4.0)	9.4	(4.0)	5.2	(1.6)	5.2	(1.4)

BCVA: Best Corrected Visual Acuity; ETDRS: Early Treatment Diabetic Retinopathy Study

A. Total Macula

B. Central Macula

C. Peripheral Macula

Figure 4: *Macula thickness stratified by disease type for the better and worse seeing eye by ETDRS location. A:* *Total macula thickness, averaged across the 1mm, 3m and 6mm diameter ETDRS locations. B:* *Central macula thickness calculated as an average of the 1mm and 3mm diameter ETDRS locations. C:* *Peripheral macula thickness representing the 6mm diameter ETDRS location. CVL = Central vision loss. PVL = Peripheral vision loss. ND = Normative data from age-range matched sighted controls* (Nieves-Moreno et al., 2017). *Dark grey boxplots represent data for the worse seeing eye with light grey boxplots representing data for the better seeing eye. For all box plots, horizontal lines represent the median with upper and lower whiskers representing scores outside the middle 50%. Red crosses denote the mean value. Overlaid dots represent data from each participant.*

A. Total Macula   **B. Central Macula**   **C. Peripheral Macula**

Figure 5: *Ganglion cell layer (GCL) thickness stratified by disease type for the better and wrose seeing eye by ETDRS location.* ***A:*** *Total macula GCL thickness, averaged across the 1mm, 3m and 6mm diameter ETDRS locations*. ***B:*** *Central macula GCL thickness calculated as an average of the 1mm and 3mm diameter ETDRS locations.* ***C:*** *Peripheral macula GCL thickness representing the 6mm diameter ETDRS location. CVL = Central vision loss. PVL = Peripheral vision loss. ND = Normative data from age-range matched sighted controls* (Nieves-Moreno et al., 2017). *Dark grey boxplots represent data for the worse seeing eye with light grey boxplots representing data for the better seeing eye. For all box plots, horizontal lines represent the median with upper and lower whiskers representing scores outside the middle 50%. Red crosses denote the mean value. Overlaid dots represent data from each participant.*

Figure 6: *Peripapillary retinal nerve fibre layer (pRNFL) thickness of the optic nerve head stratified by quadrant and disease type. Schematics above the line graph denote the quadrant of interest for each data set. The dashed lines represent thickness values from each quadrant for the worse seeing eye with the dotted lines representing the better seeing eye. The full line represents the average across the two eyes, with error bars representing the standard error of the mean. The orange lines represent data from the central retinal disease cohort whilst the purple lines represent data from the peripheral retinal disease cohort. Global thickness is calculated as the average of all nasal and temporal quadrants.*

Figure 7: *Best correct visual acuity for the worse and better seeing eye stratified by disease type. Dark grey boxes represent data for the worse eye, with light grey boxes representing the better eye. CVL = Central vision loss PVL = Peripheral vision loss. For all box plots, horizontal lines represent the median with upper and lower whiskers representing scores outside the middle 50%. Red crosses denote the mean value. Overlaid dots represent data from each participant. The dashed horizontal line represents an ETDRS letter score of 84 letters, equivalent to 6/6 Snellen acuity or 0.0 logMAR*

Figure 8: *Visual Field Sensitivity obtained from the Humphrey Visual Field Analyser. Pattern standard deviation (PSD), in which larger numbers indicate irregular localised deficits, is plotted on the left-hand side. Mean deviation (MD), in which more negative values indicate greater visual field loss, is plotted on the right-hand side. Dashed lines indicate the range in which values are considered to represent normal vision (0 - -2dB). Dark grey boxes represent data for the worse eye, with light grey boxes representing the better eye. For all box plots, horizontal lines represent the median with upper and lower whiskers representing scores outside the middle 50%. Overlaid dots represent data from each participant.*

Figure 9: *Retinal sensitivity of the 10-degree radius central retina. CVL = Central vision loss. PVL = Peripheral vision loss. Smaller values represent reduced sensitivity. Dark grey boxes represent data for the worse eye, with light grey boxes representing the better eye. For all box plots, horizontal lines represent the median with upper and lower whiskers representing scores outside the middle 50%. Red crosses denote the mean value. Overlaid dots represent data from each participant.*

5.3.4. Anterior vs Posterior Visual Pathway

Chapter 3, Section 3.3. revealed lower mean cortical volume of the entire occipital cortex in participants with peripheral retinal disease compared to sighted controls. Whilst this difference could not be assessed statistically due to the small sample size, we want to see whether changes to the anterior visual pathway may be related to the observed differences in volume of the posterior visual pathway. No statistics have been carried out on this small data set; therefore, the following scatterplots will be discussed in relation to the following questions:

5.3.4.1. Does retinal structure predict cortical structure? Of the four participants, one individual appears to have lower total macula thickness with lower cortical volume whereas the other three individuals have greater total macula thickness with greater cortical volume (Figure 10A). Although this data requires a larger sample size to calculate significance, it may suggest that cortical volume is positively related to total macula thickness.
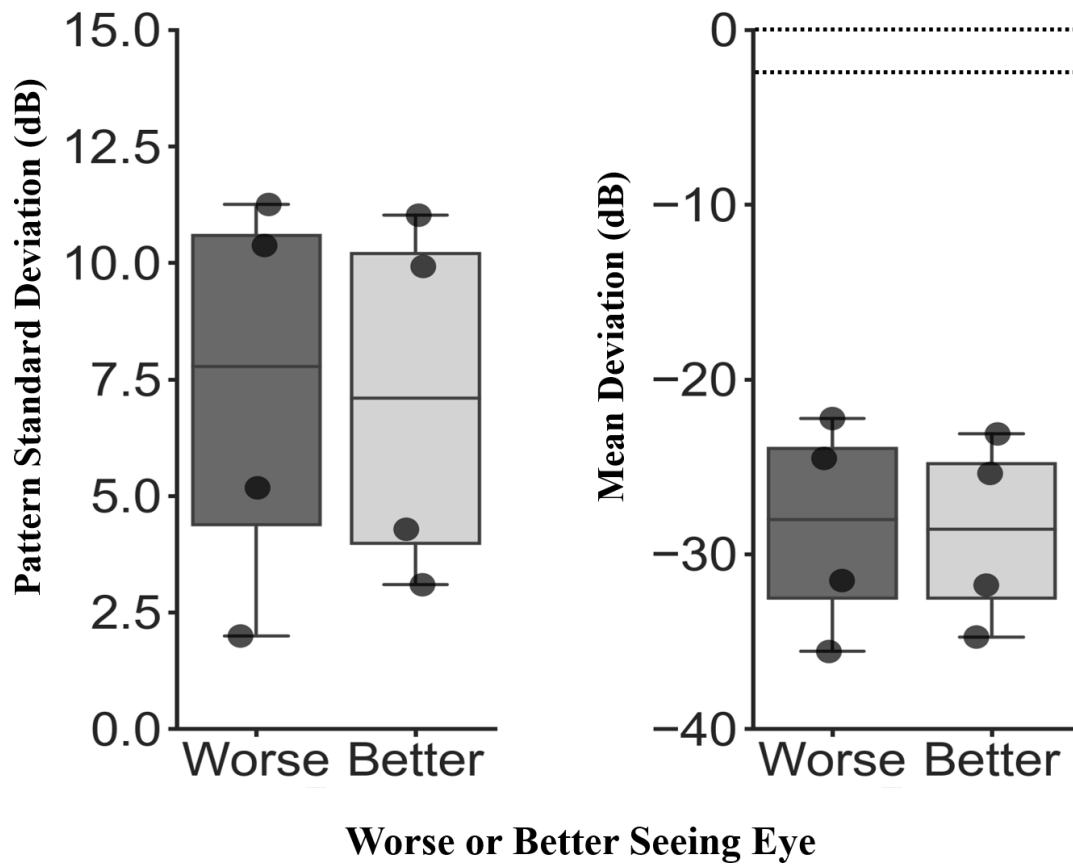
The relationship between macula ganglion cell layer (GCL) thickness and cortical volume appears to be similar across three participants in this cohort whilst one participant has greater GCL thickness values for both the better and worse seeing eye compared to the other three (Figure 10B). As such, we cannot state whether a correlation exists between these two measures based on the sample size.

Similarly to GCL thickness, the relationship between thickness of the peripapillary retinal nerve fibre layer (pRNFL) of the optic nerve head and cortical volume appears to be comparable between three participants, with one individual showing slightly greater pRNFL thickness with greater cortical volume (Figure 10C). However, a larger sample size is required to evaluate whether this data reflect a positive trending relationship.

5.3.4.2. Does retinal structure predict visual function? Figure 11 shows the relationship between retinal structure and BCVA performance. Central macula thickness does not appear to correlate with BCVA performance for either the worse or better seeing eye (Figure 11A). However, central macula GCL thickness may correlate with BCVA performance, such that lower BCVA is associated with reduced GCL thickness. However, this is based on one participant in this cohort showing greater BCVA and

thicker GCL, therefore a larger sample size is required to establish significance (Figure 11B). pRNFL thickness averaged across the three temporal quadrants appears to be comparable between participants, although there are differences with the better seeing eye for two participants having thinner pRNFL (Figure 11C).

Figures 12 - 14 show the relationship between retinal structure and visual field sensitivity. Central macula thickness does not appear to be correlated with pattern standard deviation, mean deviation or retinal sensitivity as measures from both eyes are comparable across the cohort (Figure 12). Interestingly, whilst central macula GCL thickness is similar for three participants, one participant shows thicker GCL with slightly greater visual field sensitivity. Although more data is required to confirm, this may suggest that reduced GCL thickness is associated with reduced (poorer) retinal sensitivity (Figure 13C). However, when considering visual field sensitivity measuring PSD and MD, there is no clear pattern in this small cohort. Finally, the relationship between pRNFL thickness averaged across the temporal quadrants and visual field sensitivity was assessed (Figure 14). However, there appears to be no strong relationship between either PSD, MD or retinal sensitivity measures from either eye.

5.3.4.3. Does cortical structure predict visual function? Here, we report on potential relationships between cortical volume and visual function, measured using BCVA and visual field sensitivity. The data reveal a possible negative relationship with BCVA, such that greater BCVA is associated with reduced cortical volume, more so for the worse seeing eye (Figure 15A). However, this does appear to be driven by one participant, so further data would be required to make a definitive conclusion. There also appears to be no relationship between cortical volume and visual field sensitivity measuring PSD (Figure 15B), MD (Figure 16A) or retinal sensitivity. Yet, there is one patient who has reduced retinal sensitivity and reduced cortical volume, so again, further testing would be required to make a definitive conclusion (Figure 16B).

5.3.4.4. Does bilateral disease duration predict retinal structure, visual function, or cortical structure? Figure 17 shows the relationship between disease duration and retinal structure. It appears that the two particpants with longer disease duration exhibited reduced total macula thickness and GCL thickness yet comparable global pRNFL thickness. Next, disease duration was assessed against visual function. It

appears there is no relationship between BCVA performance (Figure 18A), PSD (Figure 18B), MD (Figure 19A) or retinal sensitivity (Figure 19B). Finally, the relationship between disease duration and cortical structure is shown in Figure 20. It appears that longer disease duration may be associated with reduced cortical volume of the entire occipital cortex however, there is no clear relationship with cortical thickness in the occipital pole or calcarine sulcus. Of the two patients with the longer disease duration, one has reduced cortical thickness and the other has greater cortical thickness in both cortical locations.

5.3.5. Summary of the anterior vs posterior visual pathway.

To summarise this second stage of the results, data suggest that retinal structure may predict cortical structure as reduced total macula thickness appears related to reduced cortical volume in one participant. The second assessment suggests that retinal structure may predict visual function, with reduced central macula GCL thickness related with reduced BCVA.The third assessment suggests that cortical structure may predict visual function with a possible negative relationship between reduced cortical volume and greater BCVA.. Finally, bilateral disease duration may predict cortical structure, such that longer disease duration may be associated with reduced cortical volume of the entire occipital cortex. It is important to note here that these suggested relationships would need testing in a larger sample size for a definitive conclusion.

Figure 10: *Scatterplots showing the relationship between retinal structure and cortical structure.* ***A:*** *Total macula thickness plotted against cortical volume for the entire occipital cortex.* ***B:*** *Total macula ganglion cell layer (GCL) thickness plotted against cortical volume.* ***C:*** *Global peripapillary retinal nerve fibre layer (pRNFL) thickness plotted against cortical volume. For all plots, dark grey dots represent data from the worse seeing eye with light grey dots representing the better seeing eye. Dotted lines denote the line of best fit with the black horizontal line representing the normative mean.*

Figure 11: *Scatterplots showing the relationship between retinal structure and visual function measured using BCVA.* ***A:*** *Central macula thickness is plotted in* ***A****, central macula GCL thickness in* ***B*** *and pRNFL thickness averaged across the temporal quadrants in* ***C****. For all plots, dark grey dots represent data from the worse seeing eye with the light grey dots representing the better seeing eye. Dashed lines represent the line of best fit with horizontal black lines denoting the normative mean.*

Figure 12: *Scatterplots showing the relationship between central macula thickness and visual function measuring visual field sensitivity.* ***A:*** *Central macula thickness plotted against visual field sensitivity measuring pattern standard deviation.* ***B:*** *Central macula thickness plotted against visual field sensitivity measuring mean deviation.* ***C:*** *Central macula thickness plotted against retinal sensitivity. In all plots, dark grey dots represent data from the worse seeing eye with the better seeing eye shown in the light grey dots. Dashed lines represent the lines of best fit.*

Figure 13: Scatterplots showing the relationship between macula GCL thickness and visual function measuring visual field sensitivity. A: Central macula GCL thickness plotted against visual field sensitivity measuring pattern standard deviation. B: Central macula GCL thickness plotted against visual field sensitivity measuring mean deviation. C: Central macula GCL thickness plotted against retinal sensitivity. In all plots, dark grey dots represent data from the worse seeing eye with the better seeing eye shown in the light grey dots. Dashed lines represent the lines of best fit.

***Figure 14:** Scatterplots showing the relationship between pRNFL thickness and visual function measuring visual field sensitivity. **A:** Temporal pRNFL thickness averaged across the three temporal quadrants is plotted against visual field sensitivity measuring pattern standard deviation. **B:** Temporal pRNFL thickness plotted against visual field sensitivity measuring mean deviation. **C:** Temporal pRNFL thickness plotted against retinal sensitivity. In all plots, dark grey dots represent data from the worse seeing eye with the better seeing eye shown in the light grey dots. Dashed lines represent the lines of best fit.*

A

B

Figure 15: *Scatterplots showing the relationship between cortical structure and visual function measuring BCVA and PSD.* *A:* *Cortical volume of the entire occipital cortex is plotted against BCVA, shown as the number of ETDRS letters.* *B:* *Cortical volume plotted against visual field sensitivity measuring PSD, in which larger values indicate poorer vision. For both plots, dark grey dots relate to data from the worse seeing eye with the light grey dots relating to the better seeing eye. Dashed lines represent the lines of best fit.*

A

B

*Figure 16: Scatterplots showing the relationship between cortical structure and visual function measuring mean deviation (**A**) and retinal sensitivity (**B**). In A, more negative values indicate greater visual field defect whilst in B, smaller values indicate poorer vision. For both plots, dark grey dots related to data from the worse seeing eye with the light grey dots relating to the better seeing eye. Dashed lines represent the lines of best fit.*

Figure 17: *Scatterplot showing the relationship between bilateral disease duration and retinal structure. Disease duration is plotted against total macula thickness in **A**, total macula GCL thickness in **B** and global pRNFL thickness in **C**. For all plots, dark grey dots related to data from the worse seeing eye with the light grey dots relating to the better seeing eye. Dashed lines represent the lines of best fit.*

Figure 18: *Scatterplot showing the relationship between bilateral disease duration and visual function. measuring BCVA (**A**) and pattern standard deviation (**B**). For both plots, dark grey dots related to data from the worse seeing eye with the light grey dots relating to the better seeing eye. Dashed lines represent the lines of best fit.*

Figure 19: *Scatterplot showing the relationship between bilateral disease duration and visual function. measuring mean deviation (**A**) and retinal sensitivity (**B**). For both plots, dark grey dots related to data from the worse seeing eye with the light grey dots relating to the better seeing eye. Dashed lines represent the lines of best fit.*

Figure 20: *Scatterplot showing the relationship between bilateral disease duration and cortical structure. A: Disease duration plotted against cortical volume of the entire occipital cortex. B: Disease duration plotted against mean cortical thickness of the occipital pole (red) and calcarine sulcus (green). Dots represent data from each individual participant with dashed lines representing the line of best fit.*

5.4. Discussion

This study has reported on structural and function changes to the anterior visual pathway in four individuals diagnosed with peripheral retinal disease due to retinitis pigmentosa (RP). Data reveal reductions to total macula thickness and specifically ganglion cell layer (GCL) thickness, whilst reduced thickness across the nasal quadrants of the optic nerve head suggest a possible reduction in the number of projections from the peripheral retina to the optic nerve head. Functional assessments confirm visual field loss in both eyes, whilst reduced BCVA and retinal sensitivity suggest that these RP patients also exhibit central retinal deficits. Assessing relationships between the anterior and posterior visual pathway, these pilot data suggest that retinal structure may predict cortical structure and visual function, cortical structure may predict visual function and bilateral disease duration may predict cortical structure. Whilst statistical analysis on the data reported here is not possible, future investigations into these associations is required to identify their significance as new biomarkers of disease progression in RP.

Consistent with previous work (Hood et al., 2009; Y. J. Kim et al., 2013; Rita Machado et al., 2017; Sandberg et al., 2005; Vámos et al., 2011), our data suggest that macula thickness is reduced in RP. Interestingly, macula thickness values fall in line with a cohort diagnosed with central retinal disease (described in Chapter 4), whilst falling below a normative mean of age-range matched sighted controls (Nieves-Moreno et al., 2018). It has been reported that such reductions in macula thickness in RP are driven by transneuronal degeneration of the ganglion cell (GCL) and inner plexiform layer (Vámos et al., 2011). Whilst we do not have data relating to changes to the inner plexiform layer, we are able to show that on average, central GCL thickness is reduced compared against the normative mean and against the central retinal disease cohort. This is in contrast to a recent report showing thickening of the GCL in less advanced RP, with GCL thickness matching sighted controls with advanced disease (Yoon & Yu, 2018). However, this report assessed the GCIPL (ganglion cell and inner plexiform layer) and the authors suggest that such increases could have actually reflected thickening of the IPL caused by neural and/or glial remodelling rather than thickening of the GCL.

Reduced GCL thickness has major implications to recent technologies aimed at restoring visual input including retinal prosthesis, as even epiretinal prostheses, which do not rely on an intact outer retina, do rely on transmitting signals via intact GCL and RNFL. If significant GCL thinning does occur in RP, this could indicate transneuronal

degeneration of the retina following damage to the photoreceptor layer. As such, assessing changes in GCL thickness may therefore be a useful biomarker of disease progression in potential patients for such retinal prosthetic devices.

Considering the current contradictory reports on changes to peripapillary RNFL (pRNFL) thickness in RP, our data show that pRNFL thickness is reduced across the three nasal quadrants. Whilst this confirms some previous reports (Anastasakis et al., 2012; Oishi et al., 2009; Walia et al., 2007), it also contradicts others showing no changes (Rita Machado et al., 2017) and even thickening (Anastasakis et al., 2012; Hood et al., 2009). Nevertheless, compared against a cohort of patients with central retinal disease (see Chapter 4), our data reveal that pRNFL thickness is reduced across the nasal quadrants whilst thicker across the temporal quadrants. Reduced nasal pRNFL thickness may suggest a reduction in the number of projections from the peripheral retina to the optic nerve head, which would be somewhat expected in a peripheral retinal disease and based on previous morphological research (Fitzgibbon & Taylor, 1996; Jansonius et al., 2009). Notwithstanding, evaluating statistical significance in the reductions observed in the current study is not possible and so we can only state these results are suggestive of reduced nasal pRNFL thickness.

As expected, functional assessments of the anterior visual pathway revealed impairment in visual field sensitivity, indicating that all participants had global and localised visual field deficits (S. Grover et al., 1997; Sandeep Grover et al., 1998). However, previous reports have also suggested that deficits often occur to more central retinal locations with RP over time (Hartong et al., 2006). Our data also suggest this is the case, as coupled with a reduced BCVA, we report reduced sensitivity of the central 10-degree visual field (Hirakawa et al., 1999; Holopigian et al., 1996). Whilst these data are comparable with sensitivity of the central 10-degree in a cohort of central retinal disease patients, it worth noting that different assessments were used to obtain this data, Humphrey visual field analyser and Nidek MP-1 microperimetry, respectively. Despite this, it is important to note that even with a predominantly peripheral affecting disease, the central retina has become affected.

Correlating changes to the anterior visual pathway with changes to the posterior visual pathway addressed four possibilities. Firstly, our data suggest that retinal structure may be predictive of cortical structure. We find that reduced total macula thickness is associated with reduced cortical volume of the entire occipital cortex in one of the four

participants. Secondly, our data suggest that retinal structure may also predict visual function, such that reduced central macula GCL thickness is positively related with reduced BCVA. Interestingly, our data did not indicate that reduced central macula thickness relates to reduced BCVA or visual field sensitivity, contrasting previous reports (Y. J. Kim et al., 2013; Sandberg et al., 2005). Thirdly, this data suggest that cortical structure may predict visual function in RP, albeit reduced cortical volume appears negatively related with and greater BCVA, contrasting previous reports which found a positive correlation with the extent of visual field loss (Rita Machado et al., 2017). Finally, bilateral disease duration appears to predict cortical structure, such that longer disease duration may be associated with reduced cortical volume of the entire occipital cortex. It is important to note here that all the above suggested relationships would need testing in a larger sample size for a definitive conclusion.

The main difference between the current study and previous reports cited with RP patients is the sample size. This current study included four RP patients, as such should be considered pilot data for further investigation. It is also important to note that each patient included in this current study exhibited different values across all clinical assessments. This highlights that RP is not a uniform retinal disease, but a collection of diseases that stem from different genotypes and present with different phenotypes (Hartong et al., 2006). Not only will the same retinal disease manifests differently across individuals but the patient sample in this current study were also of varying age and had the disease for different lengths of time. Whilst changes in macula and GCL thickness may be potential biomarkers of disease progression, it is important to note that such assessments are required on a patient-by-patient basis when evaluating the most efficient form of treatment.

In conclusion, reduced retinal and GCL thickness appear to be possible predictors of atrophy of the posterior visual pathway in RP. Further research should assess the benefit of these measures as biomarkers of disease progression in larger RP cohorts. This is particularly important when considering retinal prostheses, as transneuronal degeneration of the GCL not only means that the retina has undergone irreversible changes, but this is fed back to the visual cortex of the brain.

Chapter 6

Vision restoration via the Argus® II retinal prosthesis: How is the structure and function of primary visual cortex affected?

6.1. Introduction

The Argus® II epiretinal prosthesis system (Second Sight Medical Products, Sylmar, CA) was developed to provide electrical stimulation of the retina to induce visual perception in patients with retinal pathologies (Ahuja et al., 2011; Humayun et al., 2009). Since obtaining a CE Mark in 2011 and Food and Drug Administration (FDA) approval in 2013, the Argus® II system has been used as a commercial treatment option for retinitis pigmentosa (RP). Several clinical trials have reported benefits in patients' performance with the device ON, including improvements in object location (da Cruz et al., 2016; Luo et al., 2015), spatial-motor tasks (Ahuja et al., 2011), motion detection (Dorn et al., 2013), visual acuity (da Cruz et al., 2016), word identification (da Cruz et al., 2013) and significantly improved vision-related quality of life (Duncan et al., 2017). Considering the positive outcomes following implantation of the Argus® II in RP patients, it is important to assess whether the same level of response can be seen in other retinal pathologies.

Age-related macular degeneration (AMD) is currently the leading cause of vision impairment in the developed world, affecting 12.2% of those aged 80 years or over in the UK (NICE, 2018), with an estimated 288 million people affected by the year 2040 (W. L. Wong et al., 2014). A progressive form of blindness, AMD primarily affects the central retina which is responsible for high resolution vision such as reading, driving, face and object recognition. Of the two forms of AMD, neovascular AMD (nvAMD) is less common, but more advanced and treatable, whereas dry-AMD is the early and most common form, but currently untreatable.

Structural and functional alterations to primary visual cortex following long-term vision deprivation from AMD have been discussed in the literature. Some reports reveal significant cortical atrophy, as evidenced by reductions in cortical thickness and volume, particularly in regions of the visual cortex retinotopically representing the lesioned retina (Aguirre et al., 2016; Boucard et al., 2009; Hanson et al., 2019; Hernowo et al., 2014;

Malania et al., 2017; Plank et al., 2011). Conversely, others have reported cortical atrophy in retinotopic representations of the intact retina but not the lesioned retina in AMD (Prins et al., 2016), whilst some have shown significant thickening in cortical representations of the intact retina, believed to be a compensatory phenomenon (Burge et al., 2016).

Functionally, there is evidence both for (Baker et al., 2008, 2005; Dilks et al., 2009, 2014) and against (Baseler, Gouws, et al., 2011; Smirnakis et al., 2005; Sunness et al., 2004) cortical reorganisation, debating whether the cortical representation of the lesioned retina, or lesion projection zone (LPZ), takes on new functions to process visual information from the intact peripheral retina. Some studies have shown stimulus-synchronised responses in the LPZ, but only when patients perform a one-back task and not under passive viewing, and suggest that this is evidence of existing feedback from extrastriate visual areas due to task demands, rather than cortical reorganisation per se (Masuda et al., 2008, 2010).

Critically, the success of a retinal prosthesis depends on the brain remaining viable, modality specific (i.e. responsive to visual input), and topographically stable to process visual information accurately when such signals are restored; however, the capacity of the adult human visual system to process restored visual input is uncertain. Whilst some research has shown only limited activity in primary visual cortex (V1) following vision restoration after 40 years of deprivation (Fine et al., 2003) others have revealed enhanced activity in V1 and the lateral geniculate nucleus (LGN) 17 months post-implantation of the Argus® II retinal prosthesis (Castaldi et al., 2016). Cross-modal plasticity (Noppeney, Friston, Ashburner, Frackowiak, & Price, 2005) can also occur following late-onset blindness (Sabbah et al., 2017), which may provide an obstacle if visual inputs are restored. Nevertheless, reports of gradual suppression of cross-modal plasticity in V1 have been suggested following implantation of the Argus® II retinal prosthesis (Cunningham, Shi, et al., 2015).

Although these studies have reported on changes in brain macrostructure and visual responsiveness following retinal disease and restoration, very little is known about the neuronal changes that underpin them. Enhanced plasticity early in life (the 'critical period') depends on the balance between excitation and inhibition (Hensch, 2005). Animal models of congenital blindness have reported that reorganisation is driven by changes to the excitatory and inhibitory pathways that underlie development

on the occipital cortex, such that visual deprivation results in increased excitatory cholinergic pathways (Coullon et al., 2015; Zheng et al., 2014) with an attenuation of inhibitory GABAergic pathways (Benevento, Bakkum, & Cohen, 1995; Fosse, Heggelund, & Fonnum, 1989).

Magnetic resonance spectroscopy (MRS) is a non-invasive method to measure metabolic changes in the human brain that can signal changes in cell physiology. Detectable via MRS, γ-aminobutyric acid (GABA) is a neurotransmitter involved in altering the excitatory/inhibitory balance mediating adult plasticity (Hensch & Fagiolini, 2005). Research has shown that ocular dominance plasticity is triggered in response to reduced resting GABAergic inhibition, modulating the critical period (Lunghi, Emir, Morrone, & Bridge, 2015). Therefore, measuring GABA levels in visual cortex could be a sensitive indicator of plasticity following vision deprivation. Whilst studies have reported metabolic alterations following early blindness (Weaver et al., 2013), congenital blindness (Coullon et al., 2015) and glaucoma (Boucard et al., 2007), to the best of our knowledge, there is no evidence of metabolic changes before and after vision restoration. Changes in GABA concentrations, an indicator of cortical plasticity, will be of particular interest.

The aim of this pilot study is to report on quantitative measures of brain structure and function in participants with dry-AMD before and after implantation with a retinal prosthesis. Our first objective is to investigate how restoration of visual inputs affect brain structure, hypothesising that visual areas may become thicker following successful restoration. Our second objective will address the effects of restoration to brain function. Following the theory outlined by Masuda et al. (Masuda et al., 2008) we would hypothesise that both active and passive conditions would result in activity in the cortical representation of the lesioned retina. Our third objective is to assess whether GABA levels in the brain before implantation can predict the success of retinal prosthesis restoring sight, hypothesising that reduced GABA within the visual cortex may indicate a reawakening of plasticity.

Figure 1: *Argus® II retinal prosthesis system. External elements of the device include a transmitter coil, camera mounted onto the glasses and a video processing unit. Internal elements of the device include a 60-electrode array, receiver coil and electronics.*

6.2. Materials and Methods

6.2.1. Participants

Written informed consent was obtained from all participants in the study. This study followed the tenets of the Declaration of Helsinki with experimental protocols approved by the York Neuroimaging Centre, Research, Ethics and Governance Committee and the NHS Research Ethics Committee (IRAS: 171426, REC: 15/YH/0092, http://www.isrctn.com/ISRCTN52484108).

Recruitment was organised by Manchester Royal Eye Hospital in accordance with eligibility criteria outlined for the first UK clinical trial for the use of a retinal prosthesis in patients with long-term vision loss due to dry-AMD (IRAS: 157253, ClinicalTrials.gov Identifier: NCT02227498). All five participants were given the option of also taking part in the current study; three participants from the cohort consented (P02, P03 and P04; all female; mean age = 74 years; age range = 69-78 years).

All participants underwent surgical implantation of the Argus® II epiretinal prosthesis (Second Sight Medical Products, Sylmar, California, USA). The external components of the device include a video camera mounted on glasses with a transmitter coil and a video processing unit (VPU) whilst the internal elements include a 60-electrode epiretinal array and receiver coil (Figure 1). The array is surgically inserted

into the eye to stimulate the inner retina, mainly the ganglion and possibly the bipolar cells. The signal is transmitted via the normal visual pathway to the visual cortex in the brain (Humayun et al., 2003).

Magnetic resonance imaging (MRI) took place in all participants 5-19 days before implantation with post-implantation assessments taking place ~13-months following device activation in participant P02 only. Of the remaining two participants, one was deceased, and one withdrew for non-study related reasons (Table 1). Therefore, the results shown will be in relation to participant P02 with whom pre- and post-surgery data exists. Post-implantation MRI adhered to published safety guidelines, with the device turned OFF (Weiland, Faraji, Greenberg, Humayun, & Shellock, 2012).

Fourteen sighted, age-range matched control participants (7 females, mean age = 70.07 years, age range = 62.03 – 83.03 years) were scanned under the same structural MRI protocol. One participant from this control group also completed the same MRS procedure (Female, age = 64.07 years).

6.2.2. Design

In this longitudinal study, structural MRI, functional MRI and magnetic resonance spectroscopy (MRS) were acquired at a baseline assessment taking place prior to implant surgery of the Argus® II retinal device. Post-surgery assessments took place ~13-months later and included structural and functional MRI. MRS was not completed as the device has not been safety tested under these imaging parameters.

Table 1: Participant demographics.

Subject	Age, Sex	Diagnosis	Date of implantation	Date of device activation	Implanted eye	Date of pre-surgery MRI	Date of post-surgery MRI	Total time with device
P02	78, F	AMD	07/10/2015	27/10/2015	Left	02/10/2015	11/11/2016	12m, 15d
P03	69, F	AMD	03/11/2015	25/11/2015	Right	29/10/2015	Withdrew	
P04	75, F	AMD	24/11/2015	11/12/2015	Right	05/11/2015	Deceased	

6.2.3. Procedures

All neuroimaging procedures were acquired using an eight-channel phased-array head coil tuned to 127.4 MHz, on a GE Healthcare 3 Tesla Signa HD Excite scanner. Participants were instructed to lie as still as possible during the scans. Foam padding was used around the head to minimise movement, with earplugs provided to protect against scanner noise.

6.2.3.1. MRI. Structural MRI protocols were based on guidelines for the Human Connectome Project acquisition, adapted for a GE 3T scanner (Glasser & Van Essen, 2011). Scans included one T1-weighted anatomical volume (TR, 7.78ms; TE, 2.98ms; TI, 600ms; voxel size, 1 x 1 x 1mm^3; flip angle, 90^0; 256 x 256 x 176 matrix; FOV, 256mm) and one T2-weighted anatomical volume (TR, 2500ms; TE, 84.93ms; voxel size, 1 x 1 x 1mm^3; flip angle, 10^0; 256 x 256 x 176 matrix; FOV, 256mm) were acquired.

6.2.3.1.1. Analysis. Cortical reconstruction, volumetric segmentation and myelin quantification were performed using the Human Connectome Project analysis pipeline (version 6.0), incorporating the Freesurfer analysis suite (version 6.0). The three-stage structural analysis pipeline includes alignment of T1w and T2w images, bias field correction, volume segmentation, reconstruction of white and pial surfaces and surface registration (Glasser et al., 2013). Three structural characteristics of the cerebral cortex (grey matter) were assessed: 1) cortical volume of the entire occipital cortex; 2) mean cortical thickness and 3) cortical myelination of the occipital pole and calcarine sulcus (Figure2). The rationale for these assessments is the same as that outlined in Chapter 2.

6.2.3.2. fMRI. Before scanning commenced, the right eye in patient P02 was patched to test the left eye which would receive the retinal implant. Functional MRI (fMRI) was acquired using the following parameters: TR, 3000ms; TE, 29ms; voxel size, 2 x 2 x 2mm^3; flip angle, 90^0; 96 x 96 matrix; 37 axial slices; FOV, 192mm. In order to determine the region of cortex representing the intact and damaged retina, a flickering radial checkerboard stimulus, alternating between a central (6° radius visual angle) and peripheral annulus (6° - 15° radius visual angle) was presented for 12 seconds each at 6Hz for 8 cycles (Figure 3). The main functional experiment consisted a one-back task performed under active and passive viewing conditions. For the active condition, an initial blank screen was followed by 12 blocks of stimuli in which 12 images (6 x faces,

6 x scrambled faces) were presented for 8 seconds followed by a 2 second blank screen (Figure 3). Participants were instructed to complete a one-back task, pressing a response button when they thought an image had been presented consecutively. During the passive condition, participants were asked to observe the stimuli being presented without making any judgement. There were four runs altogether – two active and two passive. To determine the position and size of the stimuli to be presented during the main functional experiment, all participants completed a psychophysics test outside of the scanner until the they could see the whole image and distinguish between the gender and stimulus type (faces or scrambled faces; Figure 3).

6.2.3.2.1. Analysis. Localiser data were analysed using FEAT (FMRI Expert Analysis Tool; (Woolrich, Ripley, Brady, & Smith, 2001)). At the first level, a high-pass filter cut-off with a period of 48s was used to correct for low-frequency drift, followed by MCFLIRT (Motion Corrected FMRIB's Linear Image Registration Tool) motion processing, spatial smoothing with a Gaussian kernel of 4mm full-width half maximum (FWHM) and FILM (FMRIB's Improved Linear Model) pre-whitening. Finally, a fixed-effects analysis with cluster correction ($Z > 2.3$, $p < 0.05$) was performed. Data from the functional scans were also analysed using the above FEAT parameters, along with co-registration to the individuals own high-resolution structural T1 image. For each condition (active and passive), contrasts were set up to compare each stimulus type (faces vs scrambled faces). The two active runs and the two passive runs were combined in a higher-level analysis and retained in the high-resolution space. This resulted in two final datasets: one active and one passive. The number of voxels within significant clusters of activation relating to each stimulus type, both under active and passive conditions (Figure 8), were extracted and compared pre- and post-surgery for patient P02 (Figure 9).

6.2.3.3. MRS. Proton magnetic resonance spectroscopy (^{1}H-MRS) was acquired using a single voxel, J-edited, MEGA-PRESS (MEshcher-GArwood Point RESolved Spectroscopy) sequence (R. a E. Edden, Intrapiromkul, Zhu, Cheng, & Barker, 2012) with the following parameters: TR, 1800ms; TE, 68ms; voxel size, 34.04 x 28.78 x 24.08mm; volume, 23.59ml. The first acquisition took place with the voxel of interest (VOI) positioned in the occipital lobe of the right hemisphere whilst for the second acquisition the VOI was positioned in a control region within the frontal lobe right hemisphere (Figure 4).

6.2.3.3.1. Analysis. To assess whether inhibitory neurotransmitter levels in the brain before implantation could predict successful restoration of sight after implantation, GABA concentrations from two VOIs were assessed using Matlab version 8.5 and Gannet, the batch-processing tool for quantitative analysis of GABA-edited MRS (version 2.0) (R. A. E. Edden, Puts, Harris, Barker, & Evans, 2014). J-difference editing involves the subtraction of two experiments (obtained during a single acquisition) which treat the GABA spin system differently. The ON experiment applies frequency-selective editing pulses to GABA spins at 1.9ppm (parts per million) to refocus evolution of their coupling to 3ppm, the spins of interest. In the OFF experiment, no frequency-selective editing pulses are applied, so the coupling evolves for the duration of the TE. In both cases, the overlying creatine (Cr) signals remain the same whereas there is a different shape of the 3ppm multiplet. Therefore, subtraction of two experiments removes the Cr leaving a measurable GABA signal. The five-stage analysis pipeline processes time-domain MRS data into a frequency-domain GABA-edited spectrum, generates a mask of the MRS voxel in T1-image space, uses nonlinear least-squares fitting to integrate the edited GABA peak at 3ppm, derives grey matter and CSF voxel fractions finally calculating tissue-corrected GABA levels.

A Region of Interest

B Cortical Thickness Map   **C Cortical Myelin Map**

*Figure 2: Structural MRI regions of interest (ROIs). **A**: Inflated medial surface of the left hemisphere showing the three ROIs. The entire visual cortex is represented by all coloured regions shown in blue including the cortical representations of the central visual field, the occipital pole, shown in red and the peripheral visual field, the calcarine sulcus, shown in green. **B**: Example cortical thickness map on an inflated medial surface of the left hemisphere. Cool colours represent cortical regions which are thinner than those of hotter colours, such as the visual cortex. **C**: Example myelin density map shown on an inflated medial surface of the left hemisphere. Hot colours represent cortical regions which have greater myelin density, such as the visual cortex.*

Figure 3: *fMRI paradigm.* ***A:*** *Functional localiser checkerboard stimulus for the central visual field on the left-hand side and the peripheral visual field on the right-hand side.* ***B:*** *Size and position of the stimulus for the main functional experiment was determined via psychophysics prior to scanning.* ***C:*** *Main functional experiment paradigm in which, following an initial blank screen, test blocks alternated between faces and scrambled faces, ending with another blank screen.*

Figure 4: *MRS voxel of interest (VOI) position.* ***A:*** *VOI placement for patient P02 showing the VOI in the occipital cortex in the image on the left-hand side with the control VOI shown in the image on the right-hand side.* ***B:*** *VOI placements for the control participant. In both subjects, the VOI was placed in the right hemisphere of the brain.*

6.3. Results

Statistical analysis has not been performed for any of the measures noted below. As only one participant, P02, completed both pre- and post-implantation assessments, data will be discussed in relation to a control where available.

6.3.1. MRI. The first objective was to investigate how restoration of visual inputs affects brain structure. Results reveal that long-term vision loss due to AMD in patient P02 resulted in atrophy (shrinkage) of the occipital cortex. Volume of the entire occipital cortex was greatly reduced in P02 compared to age-matched sighted controls, by 22.21% (controls = 37,847mm^3). However, there was a 1.11% increase in cortical volume for P02 post-surgery, increasing from 29,441.5mm^3 to 29.772.5mm^3 (Figure 5). Mean cortical thickness in both ROIs was also greatly reduced in P02 compared to controls, by 14.76% in the calcarine sulcus (controls = 2.50mm) and 44.19% in the occipital pole

(controls = 3.52mm). However, post-surgery measurements revealed a 1.85% increase in mean cortical thickness in the calcarine sulcus, increasing from 2.13mm to 2.17mm, and a 5.16% increase in the occipital pole, increasing from 1.97mm to 2.07mm (Figure 6A). Similarly, myelin density was also greatly reduced in P02 compared to the controls, by 0.54% in the calcarine sulcus (controls = 1.46a.u) and 1.74% in the occipital pole (1.53a.u). Again, there were post-surgery increases of 0.5% in the calcarine sulcus, increasing from 1.45a.u to 1.46a.u and 0.6% in the occipital pole, increasing from 1.50a.u to 1.51a.u (Figure 6B). It is important to note here, that despite the increases in cortical volume, thickness and myelin density observed in the patient post-surgery, due to the scan resolution of 1x1x1mm, such increases are likely representative of general fluctuations in the MRI scanner.

6.3.2. fMRI. The second objective was to investigate how restoration of visual inputs affects brain function. The localiser scan was used to establish cortical representations from the central (intact) and peripheral (damaged) retina and how these may change in response to vision restoration. Data showed that pre-surgery, the significantly active cluster of activity relating to the central retinal projections contained 640 active voxels whereas 351 voxels were active in relation to stimulation of the peripheral retina. However, post-surgery, there were no clusters of activity in relation to either stimulus type (Figure 7).

Pre-surgery data from the main functional task revealed there were two clusters of significant activation in response to the face stimuli and one active cluster in response to scrambled face stimuli, under both active and passive conditions (Figure 8). Overall, there were more active voxels within the two clusters responding to face stimuli under the active condition (Figure 9). There were also more active voxels within these clusters in the left hemisphere (Active: cluster 1 = 264 voxels, cluster 2 = 1571 voxels; Passive: cluster 1 = 154 voxels, cluster 2 = 1356 voxels) compared to the right hemisphere (Active: cluster 1 = 311 voxels, cluster 2 = 703 voxels; Passive: cluster 1 = 119 voxels, cluster 2 = 756 voxels). However, with the scrambled face stimuli, there were more active voxels in the significant cluster under passive conditions for both the left (Active = 254 voxels; Passive = 634 voxels) and right hemispheres (Active = 0 voxels; Passive = 42 voxels; Figure 9).

Post-surgery, there was no significant cluster of activity under the active condition for either stimulus type (Figure 8). However, under passive conditions, there

was one significant cluster of activity in response to the face stimuli, activating 41 voxels within the left hemisphere (Figures 8 and 9). Despite the reduction in cortical activity post-surgery, it is worth noting that during the active condition patient P02 completed a one-back task with performance at 100%. The lack of post-surgery activation could possibly be due to distortions created by the implanted device affecting the analysis (Figure 10). However, it is unclear to what extent the observed distortion affects the occipital lobe in this patient. Another possible explanation could be that the device itself was implanted obscuring the remaining functional retina which subsequently impacted functional cortical responses. To confirm this, a detailed examination of the placement of the device would be required.

6.3.3. MRS. Our third objective was to assess whether pre-surgery levels of GABA, considered an indicator of plasticity, could predict the success of retinal prosthesis restoring sight. Pre-surgery corrected GABA concentration in the voxel of interest located in the occipital cortex was 1.54% higher in patient P02 (5.35a.u) compared to the control participant C03 (5.27a.u) and 65.4% higher in the control voxel (P02 = 13.88a.u, C03 = 4.80a.u; Figure 11). However, it is important to note that the placement of the control VOI in the patient did not match the control participant (see Figure 4). This change in location would have resulted in a different ratio of tissue, CSF and non-brain matter which likely have contributed to the large difference in the GABA concentration measured.

Figure 5: *Bar graph showing the cortical volume of the entire occipital cortex. The left-hand plot shows the cortical volume for patient P02 pre- and post-surgery with each subsequent bar representing an individual control participant. The plot on the right-hand side shows the cortical volume for patient P02 against an average of all control participants.*

Figure 6: *Structural MRI by region of interest.* ***A:*** *Bar graph showing mean cortical thickness with cortical myelin density shown in* ***B.*** *Plots on the left-hand side show values for each ROI for patient P02 pre- and post-surgery with each subsequent bar representing an individual control participant. The plot on the right-hand side shows values for patient P02 against an average of all control participants. Values for the calcarine sulcus are represented by the green bars, with those for the occipital pole represented by the red bars. The horizontal dashed line specifies the break between patient P02 and the control participants.*

Figure 7: *Functional localiser results.* *A:* *Cortical activation to stimulation of the central visual field.* *B:* *Cortical activation of the peripheral visual field. Left-hand plots represent pre-surgery activation with post-surgery activation shown on the right-hand plots. Hot colours represent regions responding significantly to the stimulus.*

Figure 8: *Clusters of significant cortical activation during the fMRI procedure. Data on the left-hand side show significantly active clusters of cortical activity during "Active" runs, with the "Passive" runs shown on the right-hand side. From top to bottom, rows 1-3 relate to fMRI performed pre-surgery, with the final row beneath the dashed line relating to the fMRI performed post-surgery in patient P02. Rows 1 and 2 depict significant clusters (shown within the red circles) in relation to "Face" stimuli, whilst row 3 depicts the significant cluster activated in response to "Scrambled Face" stimuli. Data beneath the dashed line show no cortical activity under "Active" conditions for either stimulus type whilst there is a small cluster of activity under "Passive" conditions to "Face" stimuli.*

Figure 9: *Bar chart showing the number of voxels within the significant clusters of activity per stimulus type, pre- and post-surgery. Data are shown for the two stimulus types, "Faces" and "Scrambled Faces" (Scram). Black bars represent data under "Active" conditions for the left hemisphere (full black) and the right hemisphere (black dash). Grey bars represent data under the "Passive" conditions for the left hemisphere (full grey) and right hemisphere (grey dash).*

Figure 10: *MRI artefacts from the Argus® II retinal prosthesis. Blue dashed circles highlight artefacts in the structural images on the left-hand side, a functional image in the middle and the proton density image on the right-hand side.*

Figure 11: *Bar chart showing corrected GABA ^{1}H-MRS results comparing two voxels of interest, one located in the occipital cortex and a control voxel. Black bars represent corrected GABA concentrations for patient P02 whilst grey bars represent the control participant C03*

6.4. Discussion

This feasibility study is the first to report on quantitative measures of brain structure, function and neurochemistry in a participant with dry-AMD before and after implantation with the Argus® II retinal prosthesis. Our results indicate that 13-months after implantation, there is a retinotopically specific increase of visual cortex structure, more so in the occipital pole, the representation of the lesioned retina. These structural changes were observed despite a decrease in stimulus-driven functional responses post-surgery. Pre-surgery GABA levels were comparable to a sighted control participant thus reflecting a potential indicator of successful restoration.

Pre-implantation, our findings revealed substantial cortical atrophy resulting from long-term central vision loss. This atrophy was so great that the occipital pole, the cortical representation of the lesioned central retina was even thinner than the calcarine sulcus, the naturally thin cortical representation of the intact peripheral retina. Surprisingly, post-implantation data revealed an increase in cortical thickness in both of these cortical representations, although such increases may in fact represent fluctuations in the MRI scanner rather than physical cortical increase. Despite this, these regions remained substantially atrophied compared to sighted controls. Supporting previous research, these data highlight the profound effects long-term retinal disease has on the structure of visual cortex (Boucard et al., 2009; Hanson et al., 2019; Hernowo et al., 2014; Malania et al., 2017). This is in stark contrast to the reported increase in cortical thickness in the occipital lobe of congenitally and early blind patients compared to sighted controls (Anurova, Renier, De Volder, Carlson, & Rauschecker, 2015; Bridge, Cowey, Ragge, & Watkins, 2009; Jiang et al., 2009; Park et al., 2009; Voss & Zatorre, 2012).

Previous research has shown that in AMD patients, stimulus-driven activity is observed in the occipital pole, the cortical representation of the lesioned retina, when performing a task compared with passive viewing conditions (Masuda et al., 2008, 2010). The authors suggested this was evidence of feedback from extrastriate visual areas rather than evidence of reorganisation. Following this theory, we hypothesized that restoration of visual inputs due to the Argus® II would yield stimulus-driven activity in the occipital pole under both active (task) and passive conditions. Unfortunately, our data reveal that post-surgery, fMRI responses were diminished to all visual stimulation, regardless of condition (active vs passive task) or stimulus type (faces vs scrambled faces).

These diminished post-surgery functional responses could not be explained by a complete reduction in vision over time. During the active conditions, the patient performed a one-bask to task in which performance remained at ceiling level both pre- and post-surgery. Consequently, could the diminished functional activity be related to the device itself? Although the Argus® II device has been reported as safe for MRI under certain conditions (Weiland et al., 2012), previous research has shown the presence of artefacts from the device (Cunningham, Shi, et al., 2015). Considering so few studies have been able to assess the potential for device-related artefacts distorting MRI

outcomes, further investigation would be required to establish the possibility of distortion effects on our data. A further explanation to be explored would surround the placement of the retinal device on the retina as this may have obscured functioning retina which subsequently affected the cortical responses measured here.

Of course, the success of vision restoration techniques relies on the adult visual system being able to process re-established visual input. Whilst some researchers have reported on both structural (Boucard et al., 2009; Hanson et al., 2019; Hernowo et al., 2014; Malania et al., 2017) and functional (Baker et al., 2005; Dilks et al., 2009; Masuda et al., 2008) changes to the cortex resulting from long-term vision loss, we do not fully understand the impact these changes have on vision restoration techniques. Previous research has suggested a reduction in GABAergic inhibition can reawaken plasticity (Bavelier et al., 2010; Hensch, 2005; Hensch & Fagiolini, 2005). Therefore, we wanted to assess the feasibility of measuring pre-surgery GABA levels within the occipital cortex as a potential indicator of restoration success. However, our results revealed that compared to an age-matched sighted control participant, patient P02 exhibited comparable GABA levels in the occipital cortex pre-surgery. Although it would be useful to measure GABA levels post-surgery and following use of the device, this was not possible due to the fact the Argus® II device has not been safety tested under this type of acquisition.

A number of contributing factors should be taken into account when assessing the success of the Argus® II device in restoring vision. One important factor is the amount of time using the device. Anecdotal evidence from patient P02 reveals difficulties getting used to wearing the device. Patient P02 felt the cable of the device "got in the way", causing problems in her normal day-to-day activities so she resorted to not using the device whilst out of her home. This resulted in the device only being used when at home watching TV. Patient P02 also discussed needing several further surgeries after the device was implanted due to complications with the initial surgery. It is currently unclear the extent these complications had in relation to the patients' intact vision, and whether it resulted in a further reduction of visual input to cortex. However, we do know that these additional surgeries reduced the amount of time P02 was able to adjust to using the device before the 13-month post-surgery assessments took place.

We conclude that obtaining structural, functional and neurochemical levels within the visual cortex before and after implantation with the Argus® II retinal

prosthesis is feasible in a patient with long-term vision loss due to dry-AMD. Whilst our results show a very modest increase in cortical thickness of the occipital cortex 13-months post-surgery, substantial atrophy remained compared to sighted controls. Unfortunately, stimulus-driven responses were diminished post-surgery in this patient. It may well be that our ability to restore vision in this patient is limited by the fact that the visual cortex, specifically the occipital pole, was severely degraded pre-surgery due to long-term retinal disease. Surgical complications reducing the amount of time allowed to use the device may have also impacted potential improvements.

<center>**Chapter 7**</center>

<center>**Conducting research in the NHS; Feasibility and participant feedback on the SYNAPTIC study**</center>

7.1. Introduction

The SYNAPTIC study, results of which have been outlined in Chapters 3 and 4, set out to examine the effects of long-term vision loss on the anterior and posterior visual pathway. Participants diagnosed with bilateral vision loss resulting from either central or peripheral retinal damage, or both, underwent clinical assessments of the anterior visual pathway which were compared with neuroimaging assessments of the posterior visual pathway. The aim of this study was to investigate associated changes to the posterior visual pathway following damage to the anterior visual pathway, determining if such changes 1) represent cortical reduction via a) atrophy: condensed cortex which remains plastic to restored visual input or b) degeneration: reduced cortical volume due to cell death and 2) are influenced by changes in the anterior visual pathway.

The primary objective was to measure how the posterior visual pathway changes as a result of diminished visual input following long-term vision loss. The secondary objective was to measure changes to the anterior visual pathway following long-term vision loss and the relationship between changes in the brain and the retina. The third objective was to measure visual behaviour and its relationship with the anterior and posterior visual pathways.

In this chapter, I will outline my experience of the application process for undertaking the SYNAPTIC study with York Teaching Hospital NHS Foundation Trust. I will cover the timeline of events leading up to the study opening, the recruitment window and reasons why participants decided not to take part in the study. The chapter will end with a summary of feedback from a subset of participants relating to their experience whilst taking part in the SYNAPTIC study and how this information could be used when designing future research studies.

7.2. Applying for NHS ethical approval

Once the basic outline of the study has been decided, the application process can begin. All steps within this process are highlighted in Figure 1. There are a number of different teams and systems involved in applying to complete a basic science project within the NHS, including the local Research and Development (R&D) team at the NHS Trust, University and Trust sponsors, the Health Research Authority (HRA), the Clinical Research Network (CRN) and the Integrated Research Application System (IRAS). All information below is taken from my experience in gaining ethical approval to conduct the SYNAPTIC study.

The first stage involved creating a set of study documents which outline the whole study; rationale, aims, objectives, participant groups, information sheets, consent forms, list of procedures and a complete protocol. Liaising with the R&D team at York Teaching Hospital NHS Foundation Trust (York Teaching Hospital) was extremely useful at this stage as they have template documents which can be used if this is your first application. This step of the process took 4 months to complete for SYNAPTIC. All study documents were then forwarded for assessment by the R&D team at York Teaching Hospital for clarity of information. Upon receiving feedback from R&D, study documents were edited with the final versions considered suitable to submit along with the IRAS application at the end of October 2017.

Once the application has been received at IRAS, it is initially reviewed by the HRA who decides whether or not the application requires a face-to-face meeting. In this instance, HRA decided that SYNAPTIC would benefit from a face-to-face meeting which was scheduled for early February 2018. During the meeting, key members of the research team discussed the study and all supporting documents with a panel of 10-12 lay and expert members. The panel ensure that all information in the supporting documents will be clearly understood by potential participants. Following this meeting, the panel suggested minor edits to some SYNAPTIC documents to increase clarity. These amendments were considered satisfactory and HRA approval was granted in April 2018.

As soon as the NHS grants ethical approval, additional ethical approval from the York Neuroimaging Centre at the University of York was required in order to complete the neuroimaging aspect involved in the SYNAPTIC study. Copies of all study

documents and approval notifications were submitted to the York Neuroimaging Centre Research and Ethics Committee with approval granted on the 23rd May 2018.

The final stage in the application process is to obtain approval from the R&D team at York Teaching Hospital confirming capacity and capability for the site to conduct this project. Once this is approved the study is activated with a green light, indicating recruitment can commence. For SYNAPTIC, this was issued on the 29th May 2018.

7.3. Recruitment

Following study activation (green light issued), there is a 75-day window to recruit the first participant to the study. For SYNAPTIC, this occurred within 15 days, with the first participant consenting on the 13th June 2018 (Table 1).

The planned recruitment window was due to close on 1st October 2019 which left 17 months to recruit the target of 20 participants. Due to unforeseen delays obtaining the magnetic resonance spectroscopy (MRS) protocol, recruitment had to be postponed. The SYNAPTIC protocol stated that all participants would be given the option of whether they would prefer to be scanned in one visit or over two visits taking place within the same week. Due to the MRS delays, this option could not be given. Therefore, it was decided to pause recruitment until the issues with the MRS protocol were resolved. Recruitment commenced again in November 2018, following a 6-month pause. This left 11 months to recruit the target of 20 participants. A breakdown of recruitment during this time is outlined in Table 1.

Participants were recruited to one of two groups based on a diagnosis of either central or peripheral vision loss, with an initial aim to recruit 10 participants to each group. Recruitment to the central vision loss group went relatively smoothly. The nature of the macular degeneration treatment clinics at York Teaching Hospital meant there were around 200 patients over 4 clinics each week. Recruitment focusing on the central vision loss group lasted 4 months, from November 2018 to February 2019 when the 10th participant was recruited.

Figure 1: *Timeline of the application process for conducting the SYNAPTIC study with York Teaching Hospital NHS Foundation Trust.*

Table 1: Key dates during the recruitment window.

Recruitment time point	Date
Study activation (green light issued)	29th May 2018
First participant recruited	13th June 2018
Recruitment paused	22nd June – 1st November 2018
Last participant recruited	20th August 2019
Recruitment window closed	1st October 2019
Total recruitment period (activation – last participant recruited)	448 days (approx. 14 months)

Unfortunately, recruitment to the peripheral vision loss group was not as straight forward. Recruitment focusing on this group commenced in February 2019, initially recruiting from the glaucoma clinics which review around 50 patients, one day a week. Many of the patients identified as eligible based on eye data alone declined to take part in the study, resulting in recruitment of just 2 participants in 2-months. A discussion with the clinical supervisor resulted in a change in target group. Based on the inclusion criteria of a bilateral overlapping scotoma, it was decided that potentially a better group to target would be individuals diagnosed with retinitis pigmentosa (RP). Although this would not yield the intended target of 10 recruits due to the small number of patients regularly receiving check-ups in the eye clinic, it was decided that the change in patient group would still provide an interesting avenue for investigation. Due to the smaller recruitment target in this group, it was also decided to increase the number of participants recruited to the central vision loss group.

The final breakdown of participants invited and consented to the study are outlined in Figure 2. From the 18 participants consented to the central vision loss group, 14 completed the whole study. 2 participants withdrew before any data was collected and 2 participants were unable to perform the magnetic resonance imaging (MRI) element of the study. In the peripheral vision loss groups, 1 participant recruited with glaucoma was unable to complete the MRI elements with the second participants data being withdrawn due to anomalies identified in the MRI scan. Of the 5 participants recruited with RP, 4 participants completed the whole study with 1 participant withdrawing before data collection.

Figure 2: Breakdown of the number of participants *approached to join the SYNAPTIC study stratified by disease type. The final cohort size is denoted by the last box in each column, outlined in bold.*

7.4. Reasons participants declined to take part

In total, 88 patients were approached to join the SYNAPTIC study, however 49 patients declined to take part (Figure 2). In an open-ended question, all patients were asked to expand on why they chose not take part in the study if they were willing to provide this information. It was interesting to assess the reasons behind this large number of declines to understand if the reasons were due to the study design or something else as this information could be used when designing future studies to help improve recruitment rates. Reasons why patients declined to join the study have been highlighted in Figures 3 and 4, separated by the group they would have been allocated to.

Those participants approached to join the central vision loss group, the most common reason why participants declined to take part was due to their ineligibility to undergo an MRI with 31% of patients stating this reason (Figure 3). This ranged from mobility issues, to not being able to lie down for the duration of the scan and having a pacemaker. The least common reason given by 15% of participants was that they felt they were attending the hospital for other problems quite frequently, so they felt they had enough appointments and did not want to take on more. When considering the participants approached to join the peripheral vision loss group, the most common reason given by 50% of those approached was that participants did not want to take part in research (Figure 4). Responses ranged from not wanting to know what happens in the brain, to simply not wanting to be part of research.

Upon reviewing the reasons given by participants for not wanting to join the study, I do not feel that in this particular study, any changes to the design of the study would have yielded a greater number of recruits. The purpose of the SYNAPTIC study was to investigate the changes in the brain in response to long-term vision loss. MRI is a vital part of the study design allowing such investigations which could not be removed or replaced. Therefore, no changes could be made to appeal to those participants who declined due to not wanting an MRI.

With regards to those who stated their reason for declining was due to the number of clinical visits to the hospital they already had, this study was designed with minimal need for increased or multiple appointments. The additional clinical assessments took place during the participants usual clinical appointment, with the only change being that their appointment was switched from a clinic on a Wednesday or Thursday (standard clinic days) to a Friday research clinic. Not only did this reduce the need for an additional visit but it also minimised any disruption to the extremely busy standard eye clinics. However, it is important to note this reason when designing future research studies to ensure that the need for multiple appointments is minimised where possible.

CENTRAL VISION LOSS GROUP:
REASONS WHY PATIENTS DECLINED TO TAKE PART

Felt they had too many appointments and didn't want any more = 6

Did not want to take part in research = 11

MRI ineligible = 12

Did not want an MRI = 10

Figure 3: Pie chart showing the reasons participants *who declined to take part gave when approached to join the SYNAPTIC study. Al responses are from those* participants *who were diagnosed with central vision loss. Each segment contains the response given by* participants *at the side along with the number of* participants *who gave that response.*

**PERIPHERAL VISION LOSS GROUP:
REASONS WHY PATIENTS DECLINED TO TAKE PART**

Figure 4: Pie chart showing the reasons participants *who declined to take part gave when approached to join the SYNAPTIC study. Al responses are from those* participants *who were diagnosed with peripheral vision loss. Each segment contains the response given by* participants *at the side along with the number of* participants *who gave that response.*

7.5. Participant Feedback

The final part of the SYNAPTIC study asked participants to complete a PPI (Patient and Public Involvement) questionnaire (Appendix A). The aim of this was to gather feedback from participants involved in the SYNAPTIC research study between York Teaching Hospital and the University of York. The questionnaires took between 15-20 minutes to complete with the researcher asking the questions and writing down the participants responses. Depending on the length of responses, the questionnaire may have taken slightly longer to complete. Completing the qustionnaire was not a compulsary element of the study. From the entire SYNAPTIC cohort, seven of the eighteen participants completed the questionnaire. Those who didn't complete the questionnire stated that this

"was their first study" and *"didn't have anything to complain about"* and they *"enjoyed taking part"*.

The questionnaire was split into six sub-sections which covered questions relating to why participants chose to join the study, whether enough information was given justifying why the study was taking place, confidentiality, knowing results of the study and their experiences of taking part in the SYNAPTIC study. Some questions required a response using a Likert scale ranging from 1-5, whereby 1 indicated strongly disagree and 5 indicating strongly agree. The final question in every section allowing participants to provide any additional information relevant to that section if they felt the need.

On the whole, responses from all participants were very positive. One consistent theme amongst participants for why they chose to join the SYNAPTIC study was that they felt this was their was of repaying the NHS for the care they have received, with 5 of the 7 participants also stating they wanted to help others:

"I want to give something back for the treatment I have – try to repay the NHS. I'm glad I volunteered as it's helping you and me"

"Personally, I'm happy to be able to give back and help eye research. I'm also happy that I know I'm helping the NHS further their research"

The second common theme amongst responses related to participant experiences of taking part in the SYNAPTIC study. Some participants commented that being recruited in the eye clinic at the hospital made them feel more confident in the study:

"The great thing was the first appointment being at the hospital. This built up confidence that there was a link between the hospital and the university"

Some participants also noted they felt taking part in the study was a valuable experience:

"Yes. It's made me realise what work is being done to find ways to help conditions"

A third theme focused on the results of the study. All participants expressed the importance to them in knowing the results of the study, with all participants confriming

they had been informed the results would be shared once they are available by the researcher. However, feedback from the participants highlights that they feel the results need to be very clear in what it means for them:

"Setting expectations is important. What is the importance of the results? What do they mean for me?"

"What the results mean is more important than just knowing the results"

The final theme relates to what should be focused on for future research studies; ideas for improvement. All participants stated they were not aware that York Teaching Hospital was a research active trust and that they were unaware there were research links between the hospital and the University of York. One participant also commented that the eye clinic does not advertise research studies clearly either, which is definitely an area to be improved:

"Adverts and notices regarding what studies are available in the clinic and what studies would be appropriate for me to take part in. Possibility for optoms to encourage research and discuss with patients. 1-to-1 briefing in the hospital regarding information on research"

Participants also stated they think it would be better to highlight the importance of research in how it links back to everyday life in the hospital, including what research studies may mean to them:

"Research – I understand all of that. I don't really understand how research links back to everyday life at the hospital though"

7.6. Summary

This chapter has summarised the overall process of applying to complete the SYNAPTIC study with York NHS, the recruitment process, reasons some participants declined to take part ending with feedback from the participants who completed the study.

Applying to conduct scientific research within the NHS was a relatively straight forward exercise. Having completed this process for other research studies, I knew the

teams to liaise with from the start to make the whole process streamlined. From creating the study documents, to obtaining the green light to recruit the first participant, the application process took 14 months. There are areas which could have been speeded up however, this process was conducted alongside applying for a second research study within the NHS and whilst co-supervising a third study at the University.

Once the green light had been activated, indicating the first participant could be recruited, it took approximately 14-months to recruit the SYNAPTIC cohort. The recruitment window lasted much longer than expected due to an unforseen problem with the MRI procedures. Once recruitment reopened, the main issue concerned recruiting participants diagnosed with peripheral vision loss. The initial plan was to target the glaucoma clinic. The problem faced was that patients with the inclusion criteria of a bilateral overlapping scotoma, were not seen regularly in clinic. The few patients who were seen in clinic unfortunately either were MRI ineligible or did not want to take part in research. This again haulted recruitment to this group until a decision was made to open the target participant group to include those diagnosed with retinitis pigmentosa. In future research, I would reconsider the inclusion criteria for participants diagnosed with peripheral vision loss, making sure not to restrict potential interested participants who fit the inclusion criteria.

Collecting participant feedback via a questionnaire was an extremely valuable element of the SYNAPTIC study. Overall, feedback was very positive on participant experiences of the study and why they wanted to join in the first place. Some participants were also very helpful in giving suggestions on ways to improve research in the future. Therefore, I would encourage the use of PPI discussions during the development stage of future research studies, something which appears to be increasing in popularity with ophthalmology clinical research (Dean et al., 2017). Finally, increasing the information available in the eye clinic to inform patients of the different research studies available to them and who they can speak to about joining a project may increase uptake to research studies in the future.

Chapter 8

Summary and Conclusions

8.1. Summary

Restoring visual input to those with profound blindness is of growing interest with techniques including gene and stem cell therapy (Acland et al., 2001; Beltran et al., 2015; Boye et al., 2013), antiangiogenics (D. M. Brown et al., 2006a; Rosenfeld et al., 2006) and retinal prostheses (Bloch, Luo, & da Cruz, 2019; Humayun, de Juan, et al., 1999; Marc et al., 2014; Weiland & Humayun, 2014). Whilst such techniques aim to restore visual input to the anterior visual pathway (the eye), it remains unclear what changes may occur to the function and structure of the posterior visual pathway (the brain) following long-term retinal disease. If changes to the posterior visual pathway result in an inability to retrieve and process re-established visual input, vision restoration will be unsuccessful. Consequently, understanding the impact of such changes is essential to ensure the success of the current and future restorative treatments.

The data presented in this thesis identify that longstanding unilateral vision loss from neovascular age-related macular degeneration (nvAMD) results in significant atrophy (cortical shrinkage) of the posterior visual pathway. However, there is a window – at least within 3-4 months post-diagnosis – during which no detectable atrophy was present. This finding indicates that detrimental changes to the posterior visual pathway emerge relatively slowly. We also show that long-term bilateral nvAMD results in significant atrophy of the posterior visual pathway. However, with progressing central retinal disease, significant atrophy occurs in cortical representations of both the central and peripheral retina, namely the occipital pole and calcarine sulcus respectively Moreover, pilot data from a small cohort of patients with peripheral retinal disease due to retinitis pigmentosa (RP) suggest some patients show signs of atrophy whilst others do not, although a larger sample is needed to draw definitive conclusions.

Understanding the driving force for cortical atrophy and whether such cortical reductions in fact reflect demyelination (reduced myelin) or degeneration (cell death) is essential in understanding the effects of retinal disease on the posterior visual pathway. Two novel magnetic resonance imaging (MRI) protocols were employed in this thesis

to quantify changes in cortical myelin levels and changes in neurochemical metabolites associated with cell death (apoptosis and necrosis). With central retinal disease, whilst there is a possibility that the visual cortex may remain plastic to restored visual input due to reduced GABA:Cr levels, mean levels of NAA:Cr were also reduced which may indicate neuronal loss/dysfunction. However, these changes were only showing trends rather than highlighting significant differences in this cohort. Nevertheless, with peripheral retinal disease, pilot ^{1}H-MRS results indicate a trend towards evidence of cortical degeneration via apoptosis. This may suggest that the reduced cortical volume could be a result of cortical degeneration rather than cortical atrophy due to the lack of reduced mean thickness observed. However, confirming this hypothesis on a larger RP cohort is required.

With no significant evidence of cortical degeneration or demyelination associated with either central or peripheral retinal disease, we suggest that the posterior visual pathway may remain viable to process re-established visual input, lending hope to the future of vision restoration techniques. Assessing this possibility in a candidate for implantation of the Argus II® retinal prosthesis, we reveal a very modest increase in cortical thickness of the occipital cortex 13-months post-surgery. Nevertheless, substantial atrophy remained compared to sighted controls. Unfortunately, stimulus-driven responses were diminished post-surgery in this patient. It may well be that our ability to restore vision in this patient is limited by the fact that the visual cortex, specifically the occipital pole, was severely degraded pre-surgery due to long-term retinal disease.

Identifying new biomarkers of disease progression is a fundamental element in ensuring the most suitable treatment options are provided to patients with retinal disease. This study highlights that macular thickness across all retinal layers can be contaminated by active oedemas, particularly with central retinal disease due to nvAMD. Therefore, assessing changes to specific retinal layers which may be less contaminated by oedema may provide a more sensitive biomarker of disease progression. With both central and peripheral retinal disease, this study shows significant reductions in thickness of the ganglion cell layer (GCL). With central retinal disease, such retinal changes are reflected in a reduction in peripapillary retinal nerve fibre layer (pRNFL) thickness in the inferior temporal quadrant, implying reduced projections from the macular to the optic nerve head. Conversely, in peripheral retinal disease, pRNFL thickness is reduced in more

nasal quadrants, suggesting there may be a reduction in projections from the far peripheral retina to the optic nerve head.

Reduced thickness of the GCL in both central and peripheral retinal disease suggests that retinal degeneration due to apoptosis is occurring, following reduced input from the photoreceptors. Monitoring changes to GCL thickness should therefore be considered a biomarker of disease progression and specifically used when identifying suitable patients for restorative treatments such as the Argus II® system, an epiretinal implant that sits on the inner retina and thus relies on a functioning GCL and RNFL to carry signals to the brain.

A further novelty of this thesis was the investigation of the relationship between changes to the anterior and posterior visual pathway, to establish possible predictors in one pathway to changes in the other. With central retinal disease, this study is the first to reveal that cortical structure predicts visual function. These results show that reduced thickness of the occipital pole, the cortical representation of the central retina, predicts reduced best corrected visual acuity (BCVA), suggesting that BCVA relies on maintained structure of both the anterior and posterior visual pathway.

Whilst we reveal no evidence that retinal structure predicts cortical structure with central retinal disease, with peripheral retinal disease, data point towards retinal structure predicting cortical structure, specifically reduced total macula thickness and global pRNFL thickness predicting reduced cortical volume of the entire occipital cortex. Interestingly, this data also suggest that retinal structure may predict visual function, with reduced central macula GCL thickness related to reduced BCVA and retinal sensitivity. Finally, longer disease duration in this cohort also appears to relate with reduced cortical volume of the entire occipital cortex. However, with such a small cohort, larger numbers are required to confirm this result.

With so many clinical measures from the anterior visual pathway, this study also allowed for investigations into the relationship between structure and function of the eye. In central retinal disease, this study reveals that within the anterior visual pathway, bilateral disease duration predicts GCL thickness in the better seeing eye and large lesion size predicts visual function. Similarly, with peripheral retinal disease, disease duration also appears to be related with both macular thickness and macula GCL thickness, such that the longer the disease, the thinner the macula. Moreover, it was only in the central

retinal disease cohort where the size of the lesion was found to significantly predict visual function, with larger lesions related with poor vision both in terms of BCVA and retinal sensitivity.

In conclusion, whilst we reveal significant atrophy of the posterior visual pathway occurs with central retinal disease, testing a larger cohort of peripheral retinal disease patients is required for a definitive conclusion. With central retinal disease, although we find significant cortical atrophy in the retinotopic representations of the central and peripheral retina, namely the occipital pole and calcarine sulcus, we found no significant correlation between lesion size and cortical thickness in the calcarine sulcus. This suggests that the cortical atrophy observed in the calcarine sulcus is in fact a secondary effect of simply having a macula retinal lesion, evidence of disease progression on the brain. Whilst we found no significant evidence of cortical degeneration in either patient cohort, this pilot data did highlight possible trends which warrant further investigation. There was also no significant evidence of demyelination in either cohort, which may simply suggest that myelin density in the visual cortex is rather robust despite other structural cortical alterations resulting from disease.

There are two exciting findings from this thesis. Firstly, reduced macula GCL thickness in both central and peripheral retinal disease suggest that retinal degeneration is occurring due to the loss of input from the photoreceptors. Considering that vision restoration techniques are being trialled in these two diseases currently, it is imperative to monitor changes to the GCL as retinal prostheses in particular rely on sending signals to the brain via the GCL. Secondly, reduced cortical thickness in the occipital pole is a significant predictor of reduced BCVA in central retinal disease. This suggests that maintaining structure of the occipital pole may be critical to maintain visual function and prevent BCVA declining in nvAMD. Together, this information is important in future research into patient selection for vision restoration techniques. The ability to measure the impact of long-term vision loss on the extent of cortical atrophy and/or degeneration of the posterior visual pathway is vital as the success of such restorative devices relies on the posterior visual pathway remaining viable to process restored visual input.

8.2. Limitations and Future Work

There are a number of limitations throughout this thesis which could be overcome in future research. Throughout the chapters, it is important to note that measures of cognitive function were not obtained for any participant recruited as a sighted control. Future research collecting this information could include the measures, educational level and exercise level for example, as co-variates in statistical analyses. Including such information will help to determine whether cortical changes observed are related to natural aging or effects of the retinal disease.Secondly, when measuring cortical affects of retinal disease, it would be preferrable to capture the exact cortical representation of the retinal lesion, namely the lesion projection zone, via techniques such as retinotopic mapping. Whilst employing such techniques would provide the direct representation, it relies on the participants ability to fixate during the fMRI scan. Such an inclusion criteria will impact the number of participants recruited to the study and the extent of vision loss they experience. The nature of age-related macular degeneration is that the central visual field is affected which in turn impacts the participants ability to fixate on a centrally located target such as that used in retinotopic mapping. Recruiting participants with the ability to centrally fixate would prevent participants with advanced disease being able to partake in the study. However, not employing retinotopic mapping in this thesis allowed a wider recruitment pool of participants with varying levels of vision loss due to retinal disease. Future research would need to consider the pros and cons of using retinotopic mapping over the technique used in this thesis in relation to the potential number of eligible participants able to be recruited.

Thirdly, an interesting addition to future research investigating retinal implants would be the inclusion of behavioural measures such as motion, colour and contrast discrimination. Such measures could provide further detail on potential behavioural improvements associated with use of the retinal device. Including these measures would also eliminate possible distortion effects which may be affecting the quality of the cortical responses, although additional research into this is required for a definitive conclusion. However, incorporating MRI into future retinal device studies with larger sample sizes is important to establish the possibility of cortical changes associated with long-term use of the implants.

Appendix A – PPI Questionnaire

PATIENT PPI QUESTIONNAIRE

SYNAPTIC

STRUCTURAL, FUNCTIONAL AND CHEMICAL ASSESSMENTS OF THE VISUAL PATHWAY IN VISION LOSS

Patient ID number: ……………..   Name of Researcher: ………...………….

This questionnaire aims to gather feedback from participants involved in research studies between York Teaching Hospital NHS Foundation Trust and the University of York.

The researcher will complete this questionnaire with you, writing down your answers and it should take between 15-20 minutes to complete. Any information relating to your experience of taking part in a research study is welcome.

Section 1 - Introduction

a)   Is this the first research study you have taken part in? Please circle one

YES   NO

b) What made you decide to take part in research? (Tick all that apply)

To understand more about my condition

To help others

Felt pressured/obliged

Doctor recommended

Interested in research itself

Other (Please specify)

………

………

…………………………………………………………………

c) Do you have anything else to add to this section? Your explanation would be valuable to us to help us understand your answers to the previous questions.

………

………

………

………

Section 2 - Information

a) I was given all the information I needed in relation to the study, including the relevance of MRI in vision research. Please circle one number

Strongly disagree   1   2   3   4   5   Strongly agree

b) I had a good experience of taking part in the research study. Please circle one number

Strongly disagree   1   2   3   4   5   Strongly agree

c) Do you have anything else to add to this section? Your explanation would be valuable to us to help us understand your answers to the previous questions.

………
………
………
………

Section 3 – Relationship with Research Staff

a) My privacy and confidentiality were maintained during my research appointments. Please circle one number

Strongly disagree   1   2   3   4   5   Strongly agree

b) I was able to contact someone appropriate to ask questions throughout the study. Please circle one number

Strongly disagree   1   2   3   4   5   Strongly agree

c) The research staff were friendly and professional at all times. Please circle one number

Strongly disagree   1   2   3   4   5   Strongly agree

d) Do you have anything else to add to this section? Your explanation would be valuable to us to help us understand your answers to the previous questions.

………
………
………
………

Section 4 – Time

a) The times and dates of my research appointments have been acceptable. Please circle one number

Strongly disagree   1   2   3   4   5   Strongly agree

b) Waiting times during my research appointments have been acceptable. Please circle one number

Strongly disagree   1   2   3   4   5   Strongly agree

c) Do you have anything else to add to this section? Your explanation would be valuable to us to help us understand your answers to the previous questions.

………
………
………
………

Section 5 – Knowing Results

a) It is important to me to know the results of a research study. Please circle one number

Strongly disagree   1   2   3   4   5   Strongly agree

b) I have been told I will receive the results of the research study when they are available. Please circle one number

Strongly disagree   1   2   3   4   5   Strongly agree

c) Do you have anything else to add to this section? Your explanation would be valuable to us to help us understand your answers to the previous questions.

………
………

……
……

Section 6 – General Questions

a) Before you entered this research study, did you know that York Hospital was a research active trust?

YES   NO

b) If yes, how did you know this? What sources of information have you seen to inform you?

……
……
………………………………………………………………

c) Before you entered this research study, did you know that collaborative research between York Hospital and the University of York took place?

YES   NO

d) If yes, how did you know this? What sources of information have you seen to inform you?

……
……
………………………………………………………………

e) Would you say you understand why research looking at changes to the brain is also important in vision loss research? Why?

……
……
………………………………………………………………

f) Would you say taking part in this research study was a valuable experience? Why?

………

………

…………………………………………………………………

g) Do you have any suggestions on ways we can improve our research study?

………

………

…………………………………………………………………

h) Having experienced being part of a research study, would you repeat this experience? Why?

………

………

…………………………………………………………………

Thank you for taking time to complete this questionnaire

Abbreviations/Glossary

AMD	Age related macular degeneration
Anti-VEGF	Anti-vascular endothelial growth factor
BCVA	Best corrected visual acuity
CI	Chief investigator
Cr	Creatine
CRN	Clinical Research Network
CRT	Central retinal thickness
fMRI	Functional magnetic resonance imaging
GABA	γ-aminobutyric acid
GCL	Ganglion cell layer
Glu	Glutamate
HVA	Humphrey visual field analyser
IPZ	Intact projection zone
LPZ	Lesion projection zone
MRI	Magnetic resonance imaging
MRS	Magnetic resonance spectroscopy
NAA	N-acetyl-aspartate
NIHR	National Institute of Health Research
NHS	National Health Service
nvAMD	Neovascular age-related macular degeneration
OCT	Optical coherence tomography
PCh	Phosphocholine
PPI	Patient and Public Involvement
pRNFL	Peripapillary retinal nerve fibre layer
R&D	Research and Development
RNFL	Retinal nerve fibre layer
RP	Retinitis pigmentosa
SD-OCT	Spectral domain optical coherence tomography
VA	Visual acuity
YNiC	York Neuroimaging Centre
YTH	York Teaching Hospital NHS Foundation Trust

References

Abdollahi, R. O., Kolster, H., Glasser, M. F., Robinson, E. C., Coalson, T. S., Dierker, D., … Orban, G. A. (2014). Correspondences between retinotopic areas and myelin maps in human visual cortex. *NeuroImage*, *99*(JANUARY), 509–524. https://doi.org/10.1016/j.neuroimage.2014.06.042

Acland, G. M., Aguirre, G. D., Ray, J., Zhang, Q., Aleman, T. S., Cideciyan, A. V., … Bennett, J. (2001). Gene therapy restores vision in a canine model of childhood blindness. *Nature Genetics*, *28*(1), 92–95. https://doi.org/10.1038/ng0501-92

Adams, D. L., Sincich, L. C., & Horton, J. C. (2007). Complete Pattern of Ocular Dominance Columns in Human Primary Visual Cortex. *Journal of Neuroscience*, *27*(39), 10391–10403. https://doi.org/10.1523/jneurosci.2923-07.2007

Aguirre, G. K., Datta, R., Benson, N. C., Prasad, S., Jacobson, S. G., Cideciyan, A. V., … Gennatas, E. D. (2016). Patterns of individual variation in visual pathway structure and function in the sighted and blind. *PLoS ONE*, *11*(11), e0164677. https://doi.org/10.1371/journal.pone.0164677

Ahuja, A. K., Dorn, J. D., Caspi, A., McMahon, M. J., Dagnelie, G., da Cruz, L., … Greenberg, R. J. (2011). Blind subjects implanted with the Argus II retinal prosthesis are able to improve performance in a spatial-motor task. *The British Journal of Ophthalmology*, *95*(4), 539–543. https://doi.org/10.1136/bjo.2010.179622

Airody, A., Venugopal, D., Allgar, V., & Gale, R. P. (2015). Clinical characteristics and outcomes after 5 years pro re nata treatment of neovascular age-related macular degeneration with ranibizumab. *Acta Ophthalmologica*, *93*(6), e511–e512. https://doi.org/10.1111/aos.12618

Anastasakis, A., Genead, M. A., McAnany, J. J., & Fishman, G. A. (2012). Evaluation of retinal nerve fiber layer thickness in patients with retinitis pigmentosa using spectral-domain optical coherence tomography. *Retina*, *32*(2), 358–363. https://doi.org/10.1097/IAE.0b013e31821a891a

Anurova, I., Renier, L. A., De Volder, A. G., Carlson, S., & Rauschecker, J. P. (2015). Relationship Between Cortical Thickness and Functional Activation in the Early Blind. *Cerebral Cortex*, *25*(8), 2035–2048. https://doi.org/10.1093/cercor/bhu009

Baker, C. I., Dilks, D. D., Peli, E., & Kanwisher, N. (2008). Reorganization of visual processing in macular degeneration: Replication and clues about the role of foveal loss. *Vision Research*, *48*(18), 1910–1919. https://doi.org/10.1016/j.visres.2008.05.020

Baker, C. I., Peli, E., Knouf, N., & Kanwisher, N. G. (2005). Reorganization of visual processing in macular degeneration. *The Journal of Neuroscience : The Official Journal of the Society for Neuroscience*, *25*(3), 614–618. https://doi.org/10.1523/JNEUROSCI.3476-04.2005

Baseler, H. a, Crossland, M. D., Leung, C., Tufail, A., Rubin, G. S., Morland, A. B., … Fletcher, A. E. (2011). Objective Visual Assessment of Antiangiogenic Treatment for Wet Age-Related Macular Degeneration. *Archives of Ophthalmology*, *88*(10), 1255–1261. https://doi.org/10.1016/j.cortex.2013.01.003

Baseler, H. a, Gouws, A., Haak, K. V, Racey, C., Crossland, M. D., Tufail, A., … Morland, A. B. (2011). Large-scale remapping of visual cortex is absent in adult humans with macular degeneration. *Nature Neuroscience*, *14*(5), 649–655. https://doi.org/10.1038/nn.2793

Bavelier, D., Levi, D. M., Li, R. W., Dan, Y., & Hensch, T. K. (2010). Removing Brakes on Adult Brain Plasticity: From Molecular to Behavioral Interventions. *Journal of Neuroscience*, *30*(45), 14964–14971. https://doi.org/10.1523/JNEUROSCI.4812-10.2010

Beatty, R., Sadun, A., Smith, L., Vonsattel, J., & Richardson, E. (1982). Direct demonstration of transsynaptic degeneration in the human visual system: a comparison of retrograde and anterograde changes. *Journal of Neurology Neurosurgery, and Psychiatry*, *45*(August 1981), 143–146. https://doi.org/10.1136/jnnp.45.2.143

Beck, M., Munk, M. R., Ebneter, A., Wolf, S., & Zinkernagel, M. S. (2016). Retinal Ganglion Cell Layer Change in Patients Treated with Anti-Vascular Endothelial Growth Factor for Neovascular Age-related Macular Degeneration. *American Journal of Ophthalmology*, *167*, 10–17. https://doi.org/10.1016/j.ajo.2016.04.003

Beltran, W. A., Cideciyan, A. V., Iwabe, S., Swider, M., Kosyk, M. S., McDaid, K., … Aguirre, G. D. (2015). Successful arrest of photoreceptor and vision loss expands

the therapeutic window of retinal gene therapy to later stages of disease. *Proceedings of the National Academy of Sciences of the United States of America*, *112*(43), E5844–E5853. https://doi.org/10.1073/pnas.1509914112

Benevento, L. A., Bakkum, B. W., & Cohen, R. S. (1995). Gamma-aminobutyric acid and somatostatin immunoreactivity in the visual cortex of normal and dark-reared rats. *Brain Research*, *689*(2), 172–182. https://doi.org/10.1016/0006-8993(95)00553-3

Bernabeu, A., Alfaro, A., García, M., & Fernández, E. (2009). Proton magnetic resonance spectroscopy (1H-MRS) reveals the presence of elevated myo-inositol in the occipital cortex of blind subjects. *NeuroImage*, *47*(4), 1172–1176. https://doi.org/10.1016/j.neuroimage.2009.04.080

Berson, E. L. (2007). Long-term visual prognoses in patients with retinitis pigmentosa: The Ludwig von Sallmann lecture. *Experimental Eye Research*, *85*(1), 7–14. https://doi.org/10.1016/j.exer.2007.03.001

Beyeler, M., Rokem, A., Boynton, G. M., & Fine, I. (2017). Learning to see again: Biological constraints on cortical plasticity and the implications for sight restoration technologies. *Journal of Neural Engineering*, *14*(5). https://doi.org/10.1088/1741-2552/aa795e

Bloch, E., Luo, Y., & da Cruz, L. (2019). Advances in retinal prosthesis systems. *Therapeutic Advances in Ophthalmology*, *11*(6), 251584141881750. https://doi.org/10.1177/2515841418817501

Block, W., Träber, F., Flacke, S., Jessen, F., Pohl, C., & Schild, H. (2002). In-vivo proton MR-spectroscopy of the human brain: Assessment of N-acetylaspartate (NAA) reduction as a marker for neurodegeneration. In *Amino Acids* (Vol. 23, pp. 317–323). Springer. https://doi.org/10.1007/s00726-001-0144-0

Boucard, C. C., Hernowo, A. T., Maguire, R. P., Jansonius, N. M., Roerdink, J. B. T. M., Hooymans, J. M. M., & Cornelissen, F. W. (2009). Changes in cortical grey matter density associated with long-standing retinal visual field defects. *Brain : A Journal of Neurology*, *132*(Pt 7), 1898–1906. https://doi.org/10.1093/brain/awp119

Boucard, C. C., Hoogduin, J. M., van der Grond, J., & Cornelissen, F. W. (2007).

Occipital proton magnetic resonance spectroscopy (1H-MRS) reveals normal metabolite concentrations in retinal visual field defects. *PLoS ONE*, *2*(2). https://doi.org/10.1371/journal.pone.0000222

Boye, S. E., Boye, S. L., Lewin, A. S., & Hauswirth, W. W. (2013). A comprehensive review of retinal gene therapy. *Molecular Therapy*, *21*(3), 509–519. https://doi.org/10.1038/mt.2012.280

Bridge, H., Cowey, A., Ragge, N., & Watkins, K. (2009). Imaging studies in congenital anophthalmia reveal preservation of brain architecture in "visual" cortex. *Brain*, *132*(12), 3467–3480. https://doi.org/10.1093/brain/awp279

Brown, D. M., Kaiser, P. K., Michels, M., Soubrane, G., Heier, J. S., Kim, R. Y., … Schneider, S. (2006a). Ranibizumab versus verteporfin for neovascular age-related macular degeneration. *The New England Journal of Medicine*, *355*(14), 1432–1444. https://doi.org/10.1056/NEJMoa062655

Brown, D. M., Kaiser, P. K., Michels, M., Soubrane, G., Heier, J. S., Kim, R. Y., … Schneider, S. (2006b). Ranibizumab versus Verteporfin for Neovascular Age-Related Macular Degeneration. *New England Journal of Medicine*, *355*(14), 1432–1444. https://doi.org/10.1056/NEJMoa062655

Brown, H. D. H., Woodall, R. L., Kitching, R. E., Baseler, H. A., & Morland, A. B. (2016). Using magnetic resonance imaging to assess visual deficits: A review. *Ophthalmic and Physiological Optics*, *36*(3), 240–265. https://doi.org/10.1111/opo.12293

Burge, W. K., Griffis, J. C., Nenert, R., Elkhetali, A., DeCarlo, D. K., ver Hoef, L. W., … Visscher, K. M. (2016). Cortical thickness in human V1 associated with central vision loss. *Scientific Reports*, *6*(September 2015), 23268. https://doi.org/10.1038/srep23268

Cassels, N. K., Wild, J. M., Margrain, T. H., Chong, V., Acton, J. H., & Casciano, M. (2017). The use of microperimetry in assessing visual function in age-related macular degeneration. *Survey of Ophthalmology*, *117*(0), 303. https://doi.org/10.1016/j.survophthal.2017.05.007

Castaldi, E., Cicchini, G. M., Cinelli, L., Biagi, L., Rizzo, S., & Morrone, M. C. (2016). Visual BOLD Response in Late Blind Subjects with Argus II Retinal

Prosthesis. *PLoS Biology*, *14*(10), 1–19. https://doi.org/10.1371/journal.pbio.1002569

Castaldi, E., Cicchini, G. M., Falsini, B., Binda, P., & Morrone, C. (2019). Residual Visual Responses in Patients With Retinitis Pigmentosa Revealed by Functional Magnetic Resonance Imaging, *8*(6).

Cehajic-Kapetanovic, J., Xue, K., Martinez-Fernandez de la Camara, C., Nanda, A., Davies, A., Wood, L. J., … MacLaren, R. E. (2020). Initial results from a first-in-human gene therapy trial on X-linked retinitis pigmentosa caused by mutations in RPGR. *Nature Medicine*, *26*(March). https://doi.org/10.1038/s41591-020-0763-1

Chang, E. E., & Goldberg, J. L. (2012). Glaucoma 2.0: neuroprotection, neuroregeneration, neuroenhancement. *Ophthalmology*, *119*(5), 979–986. https://doi.org/10.1016/j.ophtha.2011.11.003

Cheung, S.-H., & Legge, G. E. (2005). Functional and cortical adaptations to central vision loss. *Visual Neuroscience*, *22*(2), 187–201. https://doi.org/10.1017/S0952523805222071

Coullon, G. S. L., Emir, U. E., Fine, I., Watkins, K. E., & Bridge, H. (2015). Neurochemical changes in the pericalcarine cortex in congenital blindness attributable to bilateral anophthalmia. *Journal of Neurophysiology*, *114*(3), 1725–1733. https://doi.org/10.1152/jn.00567.2015

Cunningham, S. I., Shi, Y., Weiland, J. D., Falabella, P., Koo, C. O. De, Zacks, D. N., & Tjan, B. S. (2015). Feasibility of Structural and Functional MRI Acquisition with Unpowered Implants in Argus II Retinal Prosthesis Patients : A Case Study. *Translational Vision Science & Technology*, *4*(6), 1–13. https://doi.org/10.1167/tvst.4.6.6

Cunningham, S. I., Weiland, J. D., Bao, P., Lopez-Jaime, G. R., & Tjan, B. S. (2015). Correlation of vision loss with tactile-evoked V1 responses in retinitis pigmentosa. *Vision Research*. https://doi.org/10.1016/j.visres.2014.10.015

da Cruz, L., Coley, B. F., Dorn, J., Merlini, F., Filley, E., Christopher, P., … Dagnelie, G. (2013). The Argus II epiretinal prosthesis system allows letter and word reading and long-term function in patients with profound vision loss. *The British Journal of Ophthalmology*, *97*(5), 632–636. https://doi.org/10.1136/bjophthalmol-

2012-301525

da Cruz, L., Dorn, J. D., Humayun, M. S., Dagnelie, G., Handa, J., Barale, P. O., … Greenberg, R. J. (2016). Five-Year Safety and Performance Results from the Argus II Retinal Prosthesis System Clinical Trial. *Ophthalmology*, *123*(10), 2248–2254. https://doi.org/10.1016/j.ophtha.2016.06.049

Dean, S., Mathers, J. M., Calvert, M., Kyte, D. G., Conroy, D., Folkard, A., … Denniston, A. K. (2017). "The patient is speaking": Discovering the patient voice in ophthalmology. *British Journal of Ophthalmology*, *101*(6), 700–708. https://doi.org/10.1136/bjophthalmol-2016-309955

Deelchand, D. K., Berrington, A., Noeske, R., Joers, J. M., Arani, A., Gillen, J., … Öz, G. (2019). Across-vendor standardization of semi-LASER for single-voxel MRS at 3T. *NMR in Biomedicine*, (July), 1–11. https://doi.org/10.1002/nbm.4218

Destrieux, C., Fischl, B., Dale, A., & Halgren, E. (2010). Automatic parcellation of human cortical gyri and sulci using standard anatomical nomenclature. *NeuroImage*, *53*(1), 1–15. https://doi.org/10.1016/j.neuroimage.2010.06.010

Dilks, D. D., Baker, C. I., Peli, E., & Kanwisher, N. (2009). Reorganization of visual processing in macular degeneration is not specific to the "preferred retinal locus". *The Journal of Neuroscience : The Official Journal of the Society for Neuroscience*, *29*(9), 2768–2773. https://doi.org/10.1523/JNEUROSCI.5258-08.2009

Dilks, D. D., Julian, J. B., Peli, E., & Kanwisher, N. (2014). Reorganization of visual processing in age-related macular degeneration depends on foveal loss. *Optometry and Vision Science : Official Publication of the American Academy of Optometry*, *91*(8). https://doi.org/10.1097/OPX.0000000000000325

Dinc, U. A., Yenerel, M., Gorgun, E., & Oncel, M. (2008). Assessment of macular function by microperimetry in intermediate age-related macular degeneration. *European Journal of Ophthalmology*, *18*(4), 595–600. https://doi.org/10.1177/112067210801800416

Dinkin, M. (2017). Trans-synaptic Retrograde Degeneration in the Human Visual System: Slow, Silent, and Real. *Current Neurology and Neuroscience Reports*, *17*(2), 16. https://doi.org/10.1007/s11910-017-0725-2

Dobelle, W. H., Quest, D. O., Antunes, J. L., Roberts, T. S., & Girvin, J. P. (1999). Artificial vision for the blind by electrical stimulation of the visual cortex. *Neurosurgery*, *5*(4), 521–527. https://doi.org/10.1227/00006123-197910000-00022

Duncan, J. L., Richards, T. P., Arditi, A., da Cruz, L., Dagnelie, G., Dorn, J. D., … Greenberg, R. J. (2017). Improvements in vision-related quality of life in blind patients implanted with the Argus II Epiretinal Prosthesis. *Clinical and Experimental Optometry*, *100*(2). https://doi.org/10.1111/cxo.12444

Edden, R. A. E., Puts, N. A. J., Harris, A. D., Barker, P. B., & Evans, C. J. (2014). Gannet: A batch-processing tool for the quantitative analysis of gamma-aminobutyric acid-edited MR spectroscopy spectra. *Journal of Magnetic Resonance Imaging*, *40*(6), 1445–1452. https://doi.org/10.1002/jmri.24478

Edden, R. a E., Intrapiromkul, J., Zhu, H., Cheng, Y., & Barker, P. B. (2012). Measuring T2 in vivo with J-difference editing: application to GABA at 3 Tesla. *Journal of Magnetic Resonance Imaging : JMRI*, *35*(1), 229–234. https://doi.org/10.1002/jmri.22865

ETDRS. (1985). Photocoagulation for diabetic macular edema: Early treatment diabetic retinopathy study report number 1 early treatment diabetic retinopathy study research group. *Archives of Ophthalmology*, *103*(12), 1796–1806. Retrieved from http://dx.doi.org/10.1001/archopht.1985.01050120030015

Ettl, A., Fischer-Klein, C., Chemelli, A., Daxer, A., & Felber, S. (1994). Nuclear magnetic resonance spectroscopy - Principles and applications in neuroophthalmology. *International Ophthalmology*, *18*(3), 171–181. https://doi.org/10.1007/BF00915968

Ferreira, S., Pereira, A. C., Quendera, B., Reis, A., Silva, E. D., & Castelo-Branco, M. (2017). Primary visual cortical remapping in patients with inherited peripheral retinal degeneration. *NeuroImage: Clinical*, *13*, 428–438. https://doi.org/10.1016/j.nicl.2016.12.013

Fine, I., & Boynton, G. M. (2015). Pulse trains to percepts: the challenge of creating a perceptually intelligible world with sight recovery technologies. *Philosophical Transactions of the Royal Society of London. Series B, Biological Sciences*,

370(1677), 20140208. https://doi.org/10.1098/rstb.2014.0208

Fine, I., Cepko, C. L., & Landy, M. S. (2015). Vision research special issue: Sight restoration: Prosthetics, optogenetics and gene therapy. *Vision Research*, *111*, 115–123. https://doi.org/10.1016/j.visres.2015.04.012

Fine, I., Wade, A. R., Brewer, A. a, May, M. G., Goodman, D. F., Boynton, G. M., … MacLeod, D. I. a. (2003). Long-term deprivation affects visual perception and cortex. *Nature Neuroscience*, *6*(9), 915–916. https://doi.org/10.1038/nn1102

Fitzgibbon, T., & Taylor, S. F. (1996). Retinotopy of the human retinal nerve fibre layer and optic nerve head. *Journal of Comparative Neurology*, *375*(2), 238–251. https://doi.org/10.1002/(SICI)1096-9861(19961111)375:2<238::AID-CNE5>3.0.CO;2-3

Fjell, A. M., Westlye, L. T., Amlien, I., Espeseth, T., Reinvang, I., Raz, N., … Walhovd, K. B. (2009). High consistency of regional cortical thinning in aging across multiple samples. *Cerebral Cortex*, *19*(9), 2001–2012. https://doi.org/10.1093/cercor/bhn232

Flinn, N. A. P. (2017). Evaluation of contrast sensitivity and other visual function outcomes in neovascular age-related macular degeneration patients after treatment switch to aflibercept from ranibizumab, 715–721.

Fosse, V. M., Heggelund, P., & Fonnum, F. (1989). Postnatal development of glutamatergic, GABAergic, and cholinergic neurotransmitter phenotypes in the visual cortex, lateral geniculate nucleus, pulvinar, and superior colliculus in cats. *Journal of Neuroscience*, *9*(2), 426–435. https://doi.org/10.1523/jneurosci.09-02-00426.1989

Garafalo, A. V., Cideciyan, A. V., Héon, E., Sheplock, R., Pearson, A., WeiYang Yu, C., … Jacobson, S. G. (2020). Progress in treating inherited retinal diseases: Early subretinal gene therapy clinical trials and candidates for future initiatives. *Progress in Retinal and Eye Research*, (October), 100827. https://doi.org/10.1016/j.preteyeres.2019.100827

Glasser, M. F., Sotiropoulos, S. N., Wilson, J. A., Coalson, T. S., Fischl, B., Andersson, J. L., … Jenkinson, M. (2013). The minimal preprocessing pipelines for the Human Connectome Project. *NeuroImage*, *80*, 105–124.

https://doi.org/10.1016/j.neuroimage.2013.04.127

Glasser, M. F., & Van Essen, D. C. (2011). Mapping human cortical areas in vivo based on myelin content as revealed by T1- and T2-weighted MRI. *The Journal of Neuroscience : The Official Journal of the Society for Neuroscience*, *31*(32), 11597–11616. https://doi.org/10.1523/JNEUROSCI.2180-11.2011

Goesaert, E., Van Baelen, M., Spileers, W., Wagemans, J., & Op De Beeck, H. P. (2014). Visual space and object space in the cerebral cortex of retinal disease patients. *PLoS ONE*, *9*(2). https://doi.org/10.1371/journal.pone.0088248

Griffis, J. C., Burge, W. K., & Visscher, K. M. (2016). Age-dependent cortical thinning of peripheral visual field representations in primary visual cortex. *Frontiers in Aging Neuroscience*, *8*(OCT), 1–7. https://doi.org/10.3389/fnagi.2016.00248

Grover, S., Fishman, G. A., Anderson, R. J., Alexander, K. R., & Derlacki, D. J. (1997). Rate of visual field loss in retinitis pigmentosa. *Ophthalmology*, *104*(3), 460–465. https://doi.org/10.1016/s0161-6420(97)30291-7

Grover, Sandeep, Fishman, G. A., & Brown, J. (1998). Patterns of visual field progression in patients with retinitis pigmentosa. *Ophthalmology*, *105*(6), 1069–1075. https://doi.org/10.1016/S0161-6420(98)96009-2

Gujar, S. K., Maheshwari, S., Bjo, I., & Sundgren, P. C. (2005). Magnetic Resonance Spectroscopy, *25*(3), 217–226.

Haak, K. V, Morland, A. B., & Engel, S. A. (2015). Plasticity, and Its Limits, in Adult Human Primary Visual Cortex. *Multisensory Research*, *28*, 297–307. https://doi.org/10.1163/22134808-00002496

Hanson, R. L. W., Gale, R. P., Gouws, D., Airody, A., Martin, T. W., Akthar, F., … Morland, A. B. (2019). Following the Status of Visual Cortex Over Time in Patients With Macular Degeneration Reveals Atrophy of Visually Deprived Brain Regions. *Investigative Ophthalmology and Visual Science*, *60*(15), 5045–5051.

Hartong, D. T., Berson, E. L., & Dryja, T. P. (2006). Retinitis pigmentosa. *Lancet*, *368*(9549), 1795–1809. https://doi.org/S0140-6736(06)69740-7 [pii]\r10.1016/S0140-6736(06)69740-7

Heidelberg. (2016). Heidelberg Engineering Academy, *[Online]*(Available at https://academy.heidelbergengineering.com/course/view.php?id=356&lang=en), [Accessed 20th January 2020].

Hensch, T. K. (2005). Critical period plasticity in local cortical circuits. *Nature Reviews. Neuroscience*, *6*(11), 877–888. https://doi.org/10.1038/nrn1787

Hensch, T. K., & Fagiolini, M. (2005). Excitatory-inhibitory balance and critical period plasticity in developing visual cortex. *Progress in Brain Research*, *147*, 115–124. https://doi.org/10.1016/S0079-6123(04)47009-5

Hernowo, A. T., Boucard, C. C., Jansonius, N. M., Hooymans, J. M. M., & Cornelissen, F. W. (2011). Automated morphometry of the visual pathway in primary open-angle glaucoma. *Investigative Ophthalmology and Visual Science*, *52*(5), 2758–2766. https://doi.org/10.1167/iovs.10-5682

Hernowo, A. T., Prins, D., Baseler, H. a, Plank, T., Gouws, A. D., Hooymans, J. M. M., … Cornelissen, F. W. (2014). Morphometric analyses of the visual pathways in macular degeneration. *Cortex; a Journal Devoted to the Study of the Nervous System and Behavior*, *56*, 99–110. https://doi.org/10.1016/j.cortex.2013.01.003

Hirakawa, H., Iijima, H., Gohdo, T., Imai, M., & Tsukahara, S. (1999). Progression of defects in the central 10-degree visual field of patients with retinitis pigmentosa and choroideremia. *American Journal of Ophthalmology*, *127*(4), 436–442. https://doi.org/10.1016/S0002-9394(98)00408-5

Holmes, G. (1918). DISTURBANCES OF VISUAL ORIENTATION. *The British Journal of Ophthalmology*, *2*(9), 449–468. Retrieved from http://www.pubmedcentral.nih.gov/articlerender.fcgi?artid=513529&tool=pmcentrez&rendertype=abstract

Holopigian, K., Greenstein, V., Seiple, W., & Carr, R. E. (1996). Rates of change differ among measures of visual function in patients with retinitis pigmentosa. *Ophthalmology*, *103*(3), 398–405. https://doi.org/10.1016/S0161-6420(96)30679-9

Holz, F. G., Pauleikhoff, D., Klein, R., & Bird, A. C. (2004). Pathogenesis of lesions in late age-related macular disease. *American Journal of Ophthalmology*, *137*(3), 504–510. https://doi.org/10.1016/j.ajo.2003.11.026

Hood, D. C., Lin, C. E., Lazow, M. A., Locke, K. G., Zhang, X., & Birch, D. G. (2009). Thickness of receptor and post-receptor retinal layers in patients with retinitis pigmentosa measured with frequency-domain optical coherence tomography. *Investigative Ophthalmology and Visual Science*, *50*(5), 2328–2336. https://doi.org/10.1167/iovs.08-2936

Humayun, M. S., de Juan, E., Weiland, J. D., Dagnelie, G., Katona, S., Greenberg, R. J., & Suzuki, S. (1999). Pattern electrical stimulation of the human retina. *Vision Research*, *39*(15), 2569–2576. https://doi.org/10.1016/S0042-6989(99)00052-8

Humayun, M. S., Dorn, J. D., Ahuja, A. K., Caspi, A., Filley, E., Dagnelie, G., … Greenberg, R. J. (2009). Preliminary 6 month results from the argus^TM II epiretinal prosthesis feasibility study. *Proceedings of the 31st Annual International Conference of the IEEE Engineering in Medicine and Biology Society: Engineering the Future of Biomedicine, EMBC 2009*, 4566–4568. https://doi.org/10.1109/IEMBS.2009.5332695

Humayun, M. S., Prince, M., De Juan, E., Barron, Y., Moskowitz, M., Klock, I. B., & Milam, A. H. (1999). Morphometric analysis of the extramacular retina from postmortem eyes with retinitis pigmentosa. *Investigative Ophthalmology and Visual Science*, *40*(1), 143–148.

Humayun, M. S., Weiland, J. D., Fujii, G. Y., Greenberg, R., Williamson, R., Little, J., … De Juan, E. (2003). Visual perception in a blind subject with a chronic microelectronic retinal prosthesis. *Vision Research*, *43*(24), 2573–2581. https://doi.org/10.1016/S0042-6989(03)00457-7

Jansonius, N. M., Nevalainen, J., Selig, B., Zangwill, L. M., Sample, P. A., Budde, W. M., … Schiefer, U. (2009). A mathematical description of nerve fiber bundle trajectories and their variability in the human retina. *Vision Research*, *49*(17), 2157–2163. https://doi.org/10.1016/j.visres.2009.04.029

Jiang, J., Zhu, W., Shi, F., Liu, Y., Li, J., Qin, W., … Jiang, T. (2009). Thick visual cortex in the early blind. *Journal of Neuroscience*, *29*(7), 2205–2211. https://doi.org/10.1523/JNEUROSCI.5451-08.2009

Jindahra, P., Petrie, A., & Plant, G. T. (2009). Retrograde trans-synaptic retinal ganglion cell loss identified by optical coherence tomography. *Brain*, *132*, 628–

634. https://doi.org/10.1093/brain/awp001

Joukal, M. (2017). Anatomy of the Human Visual Pathway. *Homonymous Visual Field Defects*, (April), 1–16. https://doi.org/10.1007/978-3-319-52284-5_1

Keane, P. A., Liakopoulos, S., Chang, K. T., Wang, M., Dustin, L., Walsh, A. C., & Sadda, S. R. (2008). Relationship Between Optical Coherence Tomography Retinal Parameters and Visual Acuity in Neovascular Age-Related Macular Degeneration. *Ophthalmology*, *115*(12), 2206–2214. https://doi.org/10.1016/j.ophtha.2008.08.016

Keenan, T. D. L., Goldacre, R., & Goldacre, M. J. (2014). Associations Between Age-Related Macular Degeneration, Alzheimer Disease, and Dementia. *JAMA Ophthalmology*, *132*(1), 63. https://doi.org/10.1001/jamaophthalmol.2013.5696

Keller, J., Sánchez-Dalmau, B. F., & Villoslada, P. (2014). Lesions in the Posterior Visual Pathway Promote Trans-Synaptic Degeneration of Retinal Ganglion Cells. *PLoS ONE*, *9*(5), 97444. https://doi.org/10.1371/journal.pone.0097444

Kelly, K. R., Desimone, K. D., Gallie, B. L., & Steeves, J. K. E. (2015). Increased cortical surface area and gyrification following long-term survival from early monocular enucleation. *NeuroImage: Clinical*, *7*, 297–305. https://doi.org/10.1016/j.nicl.2014.11.020

Kelly, K. R., McKetton, L., Schneider, K. A., Gallie, B. L., & Steeves, J. K. E. (2013). Altered anterior visual system development following early monocular enucleation. *NeuroImage: Clinical*, *4*, 72–81. https://doi.org/10.1016/j.nicl.2013.10.014

Kim, J. H., Lee, D. W., Chang, Y. S., Kim, J. W., & Kim, C. G. (2016). Twelve-month outcomes of treatment using ranibizumab or aflibercept for neovascular age-related macular degeneration: a comparative study. *Graefe's Archive for Clinical and Experimental Ophthalmology*, *254*(11), 2101–2109. https://doi.org/10.1007/s00417-016-3353-7

Kim, Y. J., Joe, S. G., Lee, D. H., Lee, J. Y., Kim, J. G., & Yoon, Y. H. (2013). Correlations between spectral-domain OCT measurements and visual acuity in cystoid macular edema associated with retinitis pigmentosa. *Investigative Ophthalmology and Visual Science*, *54*(2), 1303–1309.

https://doi.org/10.1167/iovs.12-10149

Kuzniecky, R. (2004, August 1). Clinical applications of MR spectroscopy in epilepsy. *Neuroimaging Clinics of North America*. Elsevier. https://doi.org/10.1016/j.nic.2004.04.010

Lee, A. Y., Lee, C. S., Butt, T., Xing, W., Johnston, R. L., Chakravarthy, U., … Patel, P. J. (2015). UK AMD EMR USERS GROUP REPORT V: Benefits of initiating ranibizumab therapy for neovascular AMD in eyes with vision better than 6/12. *British Journal of Ophthalmology*, *99*(8), 1045–1050. https://doi.org/10.1136/bjophthalmol-2014-306229

Lee, E. K., & Yu, H. G. (2015). Ganglion cell–inner plexiform layer and peripapillary retinal nerve fiber layer thicknesses in age-related macular degeneration. *Investigative Ophthalmology and Visual Science*, *56*(6), 3976–3983. https://doi.org/10.1167/iovs.15-17013

Lemaitre, H., Goldman, A. L., Sambataro, F., Verchinski, B. A., Meyer-Lindenberg, A., Weinberger, D. R., & Mattay, V. S. (2012). Normal age-related brain morphometric changes: Nonuniformity across cortical thickness, surface area and gray matter volume? *Neurobiology of Aging*, *33*(3), 1–15. https://doi.org/10.1016/j.neurobiolaging.2010.07.013

Lim, L. S., Mitchell, P., Seddon, J. M., Holz, F. G., & Wong, T. Y. (2012). Age-related macular degeneration. *The Lancet*, *379*(9827), 1728–1738. https://doi.org/10.1016/S0140-6736(12)60282-7

Lin, A. P., Shic, F., Enriquez, C., & Ross, B. D. (2003). Reduced glutamate neurotransmission in patients with Alzheimer's disease - An in vivo 13C magnetic resonance spectroscopy study. *Magnetic Resonance Materials in Physics, Biology and Medicine*, *16*(1), 29–42. https://doi.org/10.1007/s10334-003-0004-x

Lunghi, C., Emir, U. E., Morrone, M. C., & Bridge, H. (2015). Short-Term Monocular Deprivation Alters GABA in the Adult Human Visual Cortex. *Current Biology*, *25*(11), 1496–1501. https://doi.org/10.1016/j.cub.2015.04.021

Luo, Y. H. L., Davagnanam, I., & Dacruz, L. (2013). MRI brain scans in two patients with the Argus II retinal prosthesis. *Ophthalmology*, *120*(8), 0–8.

https://doi.org/10.1016/j.ophtha.2013.04.021

Luo, Y. H. L., Zhong, J. J., & da Cruz, L. (2015). The use of Argus® II retinal prosthesis by blind subjects to achieve localisation and prehension of objects in 3-dimensional space. *Graefe's Archive for Clinical and Experimental Ophthalmology*, *253*(11), 1907–1914. https://doi.org/10.1007/s00417-014-2912-z

Malania, M., Konra, J., Jägle, H., Werner, J. S., & Greenlee, M. W. (2017). Compromised integrity of central visual pathways in patients with macular degeneration. *Investigative Ophthalmology and Visual Science*, *58*(7), 2939–2947. https://doi.org/10.1167/iovs.16-21191

Marc, R., Pfeiffer, R., & Jones, B. (2014). Retinal prosthetics, optogenetics, and chemical photoswitches. *ACS Chemical Neuroscience*, *5*(10), 895–901. https://doi.org/10.1021/cn5001233

Martin, W. R. W. (2007). MR spectroscopy in neurodegenerative disease. *Molecular Imaging and Biology*, *9*(4), 196–203. https://doi.org/10.1007/s11307-007-0087-2

Martinez-de-la-Casa, J. M., Ruiz-Calvo, A., Saenz-Frances, F., Reche-Frutos, J., Calvo-Gonzalez, C., Donate-Lopez, J., & Garcia-Feijoo, J. (2012). Retinal nerve fiber layer thickness changes in patients with age-related macular degeneration treated with intravitreal ranibizumab. *Investigative Ophthalmology and Visual Science*, *53*(10), 6214–6218. https://doi.org/10.1167/iovs.12-9875

Masuda, Y., Dumoulin, S. O., Nakadomari, S., & Wandell, B. a. (2008). V1 projection zone signals in human macular degeneration depend on task, not stimulus. *Cerebral Cortex*, *18*(11), 2483–2493. https://doi.org/10.1093/cercor/bhm256

Masuda, Y., Horiguchi, H., Dumoulin, S. O., Furuta, A., Miyauchi, S., Nakadomari, S., & Wandell, B. a. (2010). Task-dependent V1 responses in human retinitis pigmentosa. *Investigative Ophthalmology and Visual Science*, *51*(10), 5356–5364. https://doi.org/10.1167/iovs.09-4775

McGinnis, S. M., Brickhouse, M., Pascual, B., & Dickerson, B. C. (2011). Age-Related changes in the thickness of cortical zones in humans. *Brain Topography*, *24*(3–4), 279–291. https://doi.org/10.1007/s10548-011-0198-6

Mendola, J. D., Conner, I. P., Roy, A., Chan, S. T., Schwartz, T. L., Odom, J. V., &

Kwong, K. K. (2005). Voxel-based analysis of MRI detects abnormal visual cortex in children and adults with amblyopia. *Human Brain Mapping*, *25*(2), 222–236. https://doi.org/10.1002/hbm.20109

Mitchell, J. R., Oliveira, C., Tsiouris, A. J., & Dinkin, M. J. (2015). Corresponding Ganglion Cell Atrophy in Patients with Postgeniculate Homonymous Visual Field Loss. *Journal of Neuro-Ophthalmology*, *35*(4), 353–359. https://doi.org/10.1097/WNO.0000000000000268

Morland, A. B. (2015). Organization of the Central Visual Pathways Following Field Defects Arising from Congenital, Inherited, and Acquired Eye Disease. *Annual Review of Vision Science*, *1*(1), 329–350. https://doi.org/10.1146/annurev-vision-082114-035600

Natu, V. S., Gomez, J., Barnett, M., Jeska, B., Kirilina, E., Jaeger, C., … Grill-Spector, K. (2019). Apparent thinning of human visual cortex during childhood is associated with myelination. *Proceedings of the National Academy of Sciences of the United States of America*, *116*(41). https://doi.org/10.1073/pnas.1904931116

Neveu, M. M., von dem Hagen, E., Morland, A. B., & Jeffery, G. (2008). The fovea regulates symmetrical development of the visual cortex. *The Journal of Comparative Neurology*, *506*(5), 791–800. https://doi.org/10.1002/cne.21574

NICE. (2008). Ranibizumab and pegaptanib for the treatment of age-related macular degeneration., (Updated 2012), NICE technology appraisal guidance [TA155]. Retrieved from http://www.nice.org.uk/guidance/TA155

NICE. (2018). Age-related macular degener Age-related macular degeneration ation NICE guideline Y Your responsibility our responsibility. Retrieved from https://www.nice.org.uk/guidance/ng82/resources/agerelated-macular-degeneration-pdf-1837691334853

Nieves-Moreno, M., Martínez-de-la-Casa, J. M., Bambo, M. P., Morales-Fernández, L., Van Keer, K., Vandewalle, E., … García-Feijoó, J. (2018). New normative database of inner macular layer thickness measured by spectralis OCT used as reference standard for Glaucoma Detection. *Translational Vision Science and Technology*, *7*(1), 1–9. https://doi.org/10.1167/tvst.7.1.20

Nieves-Moreno, M., Martínez-De-La-Casa, J. M., Cifuentes-Canorea, P., Sastre-

Ibáñez, M., Santos-Bueso, E., Sáenz-Francés, F., … García-Feijoó, J. (2017). Normative database for separate inner retinal layers thickness using spectral domain optical coherence tomography in Caucasian population. *PLoS ONE*, *12*(7), 14–21. https://doi.org/10.1371/journal.pone.0180450

Noppeney, U., Friston, K. J., Ashburner, J., Frackowiak, R., & Price, C. J. (2005). Early visual deprivation induces structural plasticity in gray and white matter. *Current Biology*, *15*(13), R488–R490. https://doi.org/10.1016/j.cub.2005.06.053

Nowak, J. Z. (2006). Age-related macular degeneration (AMD): Pathogenesis and therapy. *Pharmacological Reports*, *58*(3), 353–363.

Ohno-Matsui, K. (2011). Parallel findings in age-related macular degeneration and Alzheimer's disease. *Progress in Retinal and Eye Research*, *30*(4), 217–238. https://doi.org/10.1016/j.preteyeres.2011.02.004

Oishi, A., Otani, A., Sasahara, M., Kurimoto, M., Nakamura, H., Kojima, H., & Yoshimura, N. (2009). Retinal nerve fiber layer thickness in patients with retinitis pigmentosa. *Eye*, *23*(3), 561–566. https://doi.org/10.1038/eye.2008.63

Ou, W. C., Brown, D. M., Payne, J. F., & Wykoff, C. C. (2017). Relationship Between Visual Acuity and Retinal Thickness During Anti–Vascular Endothelial Growth Factor Therapy for Retinal Diseases. *American Journal of Ophthalmology*, *180*, 8–17. https://doi.org/10.1016/j.ajo.2017.05.014

Öz, G., & Tkáč, I. (2011). Short-echo, single-shot, full-intensity proton magnetic resonance spectroscopy for neurochemical profiling at 4 T: Validation in the cerebellum and brainstem. *Magnetic Resonance in Medicine*, *65*(4), 901–910. https://doi.org/10.1002/mrm.22708

Park, H. J., Lee, J. D., Kim, E. Y., Park, B., Oh, M. K., Lee, S. C., & Kim, J. J. (2009). Morphological alterations in the congenital blind based on the analysis of cortical thickness and surface area. *NeuroImage*, *47*(1), 98–106. https://doi.org/10.1016/j.neuroimage.2009.03.076

Patel, P. J., Chen, F. K., Rubin, G. S., & Tufail, A. (2008). Intersession repeatability of visual acuity scores in age-related macular degeneration. *Investigative Ophthalmology and Visual Science*, *49*(10), 4347–4352. https://doi.org/10.1167/iovs.08-1935

Pezaris, J. S., & Reid, R. C. (2007). Demonstration of artificial visual percepts generated through thalamic microstimulation. *Proceedings of the National Academy of Sciences*, *104*(18), 7670–7675. https://doi.org/10.1073/pnas.0608563104

Plank, T., Frolo, J., Brandl-Rühle, S., Renner, A. B., Hufendiek, K., Helbig, H., & Greenlee, M. W. (2011). Gray matter alterations in visual cortex of patients with loss of central vision due to hereditary retinal dystrophies. *NeuroImage*, *56*(3), 1556–1565. https://doi.org/10.1016/j.neuroimage.2011.02.055

Prins, D., Jansonius, N. M., & Cornelissen, F. W. (2017). Loss of binocular vision in monocularly blind patients causes selective degeneration of the superior lateral occipital cortices. *Investigative Ophthalmology and Visual Science*, *58*(2), 1304–1313. https://doi.org/10.1167/iovs.16-20404

Prins, D., Plank, T., Baseler, H. A., Gouws, A. D., Beer, A., Morland, A. B., … Cornelissen, F. W. (2016). Surface-based analyses of anatomical properties of the visual cortex in macular degeneration. *PLoS ONE*, *11*(1), 1–14. https://doi.org/10.1371/journal.pone.0146684

Ramadan, S., Lin, A., & Stanwell, P. (2013). Glutamate and glutamine: A review of in vivo MRS in the human brain. *NMR in Biomedicine*, *26*(12), 1630–1646. https://doi.org/10.1002/nbm.3045

Ristau, T., Keane, P. A., Walsh, A. C., Engin, A., Mokwa, N., Kirchhof, B., … Liakopoulos, S. (2014). Relationship between Visual Acuity and Spectral Domain Optical Coherence Tomography Retinal Parameters in Neovascular Age-Related Macular Degeneration. *Ophthalmologica*, *231*, 37–44. https://doi.org/10.1159/000354551

Rita Machado, A., Carvalho Pereira, A., Ferreira, F., Ferreira, S., Quendera, B., Silva, E., & Castelo-Branco, M. (2017). Structure-function correlations in Retinitis Pigmentosa patients with partially preserved vision: A voxel-based morphometry study. *Scientific Reports*, *7*(1), 1–10. https://doi.org/10.1038/s41598-017-11317-7

Rizzo, S., Belting, C., Cinelli, L., Allegrini, L., Genovesi-Ebert, F., Barca, F., & Di Bartolo, E. (2014). The Argus II retinal prosthesis: 12-month outcomes from a single-study center. *American Journal of Ophthalmology*, *157*(6), 1282–1290.

https://doi.org/10.1016/j.ajo.2014.02.039

RNIB. (2018). The economic impact of sight loss and blindness in the UK, (December). Retrieved from www.deloitte.com/au/about

Rofagha, S., Bhisitkul, R. B., Boyer, D. S., Sadda, S. R., & Zhang, K. (2013). Seven-year outcomes in ranibizumab-treated patients in ANCHOR, MARINA, and HORIZON: A multicenter cohort study (SEVEN-UP). *Ophthalmology*, *120*(11), 2292–2299. https://doi.org/10.1016/j.ophtha.2013.03.046

Rosenfeld, P. J., Brown, D. M., Heier, J. S., Boyer, D. S., Kaiser, P. K., Chung, C. Y., … MARINA Study Group. (2006). Ranibizumab for Neovascular Age-Related Macular Degeneration. *New England Journal of Medicine*, *355*(14), 1419–1431. https://doi.org/10.1056/NEJMoa054481

Rostron, E., & Mckibbin, M. (2012). Visual impairment certification secondary to ARMD in Leeds, 2005–2010: is the incidence falling? *Eye*, *26*, 933–93661. https://doi.org/10.1038/eye.2012.61

Sabbah, N., Sanda, N., Authié, C. N., Mohand-Saïd, S., Sahel, J.-A., Habas, C., … Safran, A. B. (2017). Reorganization of early visual cortex functional connectivity following selective peripheral and central visual loss. *Scientific Reports*, *7*(February), 43223. https://doi.org/10.1038/srep43223

Sabouri, M. R., Kazemnezhad, E., & Hafezi, V. (2016). Assessment of Macular Thickness in Healthy Eyes Using Cirrus HD-OCT : A Cross-Sectional Study, *5*(3).

Sandberg, M. A., Brockhurst, R. J., Gaudio, A. R., & Berson, E. L. (2005). The association between visual acuity and central retinal thickness in retinitis pigmentosa. *Investigative Ophthalmology and Visual Science*, *46*(9), 3349–3354. https://doi.org/10.1167/iovs.04-1383

Santos, A., Humayun, M. S., De Juan, E., Greenburg, R. J., Marsh, M. J., Klock, I. B., & Milam, A. H. (1997). Preservation of the inner retina in retinitis pigmentosa:A morphometric analysis. *Archives of Ophthalmology*, *115*(4), 511–515. https://doi.org/10.1001/archopht.1997.01100150513011

Schumacher, E. H., Jacko, J. a, Primo, S. a, Main, K. L., Moloney, K. P., Kinzel, E. N.,

& Ginn, J. (2008). Reorganization of visual processing is related to eccentric viewing in patients with macular degeneration. *Restorative Neurology and Neuroscience*, *26*(4–5), 391–402.

Sereno, M. I., Lutti, A., Weiskopf, N., & Dick, F. (2013). Mapping the human cortical surface by combining quantitative T1 with retinotopy. *Cerebral Cortex*, *23*(9), 2261–2268. https://doi.org/10.1093/cercor/bhs213

Shafee, R., Buckner, R. L., & Fischl, B. (2015). Gray matter myelination of 1555 human brains using partial volume corrected MRI images. *NeuroImage*, *105*, 473–485. https://doi.org/10.1016/j.neuroimage.2014.10.054

Shintani, K., Shechtman, D. L., & Gurwood, A. S. (2009). Review and update: Current treatment trends for patients with retinitis pigmentosa. *Optometry*. https://doi.org/10.1016/j.optm.2008.01.026

Sijens, P. E., Mostert, J. P., Oudkerk, M., & De Keyser, J. (2006). 1H MR spectroscopy of the brain in multiple sclerosis subtypes with analysis of the metabolite concentrations in gray and white matter: Initial findings. *European Radiology*, *16*(2), 489–495. https://doi.org/10.1007/s00330-005-2839-1

Singer, M. A., Awh, C. C., Sadda, S., Freeman, W. R., Antoszyk, A. N., Wong, P., & Tuomi, L. (2012). HORIZON: An open-label extension trial of ranibizumab for choroidal neovascularization secondary to age-related macular degeneration. *Ophthalmology*, *119*(6), 1175–1183. https://doi.org/10.1016/j.ophtha.2011.12.016

Sivak, J. M. (2013). The aging eye: Common degenerative mechanisms between the Alzheimer's brain and retinal disease. *Investigative Ophthalmology and Visual Science*, *54*(1), 871–880. https://doi.org/10.1167/iovs.12-10827

Smirnakis, S. M., Brewer, A. A., Schmid, M. C., Tolias, A. S., Schüz, A., Augath, M., … Logothetis, N. K. (2005). Lack of long-term cortical reorganization after macaque retinal lesions. *Nature*, *435*(7040), 300–307. https://doi.org/10.1038/nature03495

Snell, R., & Lemp, M. (1998). *Clinical Anatomy of the Eye, 2nd ed. Blackwell Science* (Second Edi). Blackwell Science.

Soares, D. P., & Law, M. (2009). Magnetic resonance spectroscopy of the brain:

review of metabolites and clinical applications. *Clinical Radiology*, *64*(1), 12–21. https://doi.org/10.1016/j.crad.2008.07.002

SPAIDE, R. F., LAUD, K., FINE, H. F., KLANCNIK, J. M., MEYERLE, C. B., YANNUZZI, L. A., … COONEY, M. J. (2006). INTRAVITREAL BEVACIZUMAB TREATMENT OF CHOROIDAL NEOVASCULARIZATION SECONDARY TO AGE-RELATED MACULAR DEGENERATION. *Retina*, *26*(4), 383–390. https://doi.org/10.1097/01.iae.0000238561.99283.0e

Stone, J. L., Barlow, W. E., Milam, A. H., Juan, E., & Milam, A. H. (1992). Morphometric Analysis of Macular Photoreceptors and Ganglion Cells in Retinas with Retinitis Pigmentosa. *Archives of Ophthalmology*, *110*(11), 1634–1639. https://doi.org/10.1001/archopht.1992.01080230134038

Sudharsan, R., & Beltran, W. A. (2019). Progress in Gene Therapy for Rhodopsin Autosomal Dominant Retinitis Pigmentosa. In *Advances in Experimental Medicine and Biology* (Vol. 1185, pp. 113–118). Springer. https://doi.org/10.1007/978-3-030-27378-1_19

Sunness, J. S., Liu, T., & Yantis, S. (2004). Retinotopic mapping of the visual cortex using functional magnetic resonance imaging in a patient with central scotomas from atrophic macular degeneration. *Ophthalmology*, *111*(8), 1595–1598. https://doi.org/10.1016/j.ophtha.2003.12.050

Swienton, D. J., & Thomas, A. G. (2014). The Visual pathway-functional anatomy and pathology. *Seminars in Ultrasound, CT and MRI*, *35*(5), 487–503. https://doi.org/10.1053/j.sult.2014.06.007

Tedeschi, G., Litvan, I., Bonavita, S., Bertolino, A., Lundbom, N., Patronas, N. J., & Hallett, M. (1997). Proton magnetic resonance spectroscopic imaging in progressive supranuclear palsy, Parkinson's disease and corticobasal degeneration. *Brain*, *120*(9), 1541–1552. https://doi.org/10.1093/brain/120.9.1541

Thambisetty, M., Wan, J., Carass, A., An, Y., Prince, J. L., & Resnick, S. M. (2010). Longitudinal changes in cortical thickness associated with normal aging. *NeuroImage*, *52*(4), 1215–1223. https://doi.org/10.1016/j.neuroimage.2010.04.258

Vámos, R., Tátrai, E., Németh, J., Holder, G. E., DeBuc, D. C., & Somfai, G. M. (2011). The structure and function of the macula in patients with advanced retinitis pigmentosa. *Investigative Ophthalmology and Visual Science*, *52*(11), 8425–8432. https://doi.org/10.1167/iovs.11-7780

Von Dem Hagen, E. A. H., Houston, G. C., Hoffmann, M. B., Jeffery, G., & Morland, A. B. (2005). Retinal abnormalities in human albinism translate into a reduction of grey matter in the occipital cortex. *European Journal of Neuroscience*, *22*(10), 2475–2480. https://doi.org/10.1111/j.1460-9568.2005.04433.x

Voss, P., & Zatorre, R. J. (2012). Occipital cortical thickness predicts performance on pitch and musical tasks in blind individuals. *Cerebral Cortex*, *22*(11), 2455–2465. https://doi.org/10.1093/cercor/bhr311

Vujosevic, S., Smolek, M. K., Lebow, K. A., Notaroberto, N., Pallikaris, A., & Casciano, M. (2011). Detection of Macular Function Changes in Early (AREDS 2) and Intermediate (AREDS 3) Age-Related Macular Degeneration. *Ophthalmologica*, *225*(3), 155–160. https://doi.org/10.1159/000320340

Walia, S., Fishman, G. A., Edward, D. P., & Lindeman, M. (2007). Retinal nerve fiber layer defects in RP patients. *Investigative Ophthalmology and Visual Science*, *48*(10), 4748–4752. https://doi.org/10.1167/iovs.07-0404

Wandell, B. A., Dumoulin, S. O., & Brewer, A. A. (2007). Visual Field Maps in Human Cortex. *Neuron*, *56*(2), 366–383. https://doi.org/10.1016/j.neuron.2007.10.012

Weaver, K. E., Richards, T. L., Saenz, M., Petropoulos, H., & Fine, I. (2013). Neurochemical changes within human early blind occipital cortex. *Neuroscience*, *252*, 222–233. https://doi.org/10.1016/j.neuroscience.2013.08.004

Weiland, J. D., Faraji, B., Greenberg, R. J., Humayun, M. S., & Shellock, F. G. (2012). Assessment of MRI issues for the Argus II Retinal Prosthesis. *Magnetic Resonance Imaging*, *30*(3), 382–389. https://doi.org/10.1016/j.mri.2011.12.005

Weiland, J. D., & Humayun, M. S. (2014). Retinal prosthesis. *IEEE Transactions on Biomedical Engineering*, *61*(5), 1412–1424. https://doi.org/10.1109/TBME.2014.2314733

Wilson, M., Reynolds, G., Kauppinen, R. A., Arvanitis, T. N., & Peet, A. C. (2011). A constrained least-squares approach to the automated quantitation of in vivo ^{1} H magnetic resonance spectroscopy data. *Magnetic Resonance in Medicine*, *65*(1), 1–12. https://doi.org/10.1002/mrm.22579

Wong, N. A., Rafique, S. A., Kelly, K. R., Moro, S. S., Gallie, B. L., & Steeves, J. K. E. (2017). Altered white matter structure in the visual system following early monocular enucleation. *Human Brain Mapping*, *39*(1), 133–144. https://doi.org/10.1002/hbm.23831

Wong, W. L., Su, X., Li, X., Cheung, C. M. G., Klein, R., Cheng, C. Y., & Wong, T. Y. (2014). Global prevalence of age-related macular degeneration and disease burden projection for 2020 and 2040: A systematic review and meta-analysis. *The Lancet Global Health*. https://doi.org/10.1016/S2214-109X(13)70145-1

Woolrich, M. W., Ripley, B. D., Brady, M., & Smith, S. M. (2001). Temporal autocorrelation in univariate linear modeling of FMRI data. *NeuroImage*, *14*(6), 1370–1386. https://doi.org/10.1006/nimg.2001.0931

Yamashita, T., Miki, A., Goto, K., Araki, S., Takizawa, G., Ieki, Y., … Yagita, Y. (2016). Retinal Ganglion Cell Atrophy in Homonymous Hemianopia due to Acquired Occipital Lesions Observed Using Cirrus High-Definition-OCT. *Journal of Ophthalmology*, *2016*, 9. https://doi.org/10.1155/2016/2394957

Yoon, C. K., & Yu, H. G. (2018). Ganglion cell-inner plexiform layer and retinal nerve fibre layer changes within the macula in retinitis pigmentosa: a spectral domain optical coherence tomography study. *Acta Ophthalmologica*, *96*(2), e180–e188. https://doi.org/10.1111/aos.13577

Zhang, Yan, Chen, X., Wen, G., Wu, G., & Zhang, X. (2013). Proton magnetic resonance spectroscopy ((1)H-MRS) reveals geniculocalcarine and striate area degeneration in primary glaucoma. *PloS One*, *8*(8), e73197. https://doi.org/10.1371/journal.pone.0073197

Zhang, YueMei, & Bhavnani, B. R. (2005). Glutamate-induced apoptosis in primary cortical neurons is inhibited by equine estrogens via down-regulation of caspase-3 and prevention of mitochondrial cytochrome c release. *BMC Neuroscience*, *6*, 1–23. https://doi.org/10.1186/1471-2202-6-13

Zheng, J. J., Li, S. J., Zhang, X. Di, Miao, W. Y., Zhang, D., Yao, H., & Yu, X. (2014). Oxytocin mediates early experience-dependent cross-modal plasticity in the sensory cortices. *Nature Neuroscience*, *17*(3), 391–399. https://doi.org/10.1038/nn.3634

Zucchiatti, I., Parodi, M. B., Pierro, L., Cicinelli, M. V., Gagliardi, M., Castellino, N., & Bandello, F. (2015). Macular ganglion cell complex and retinal nerve fiber layer comparison in different stages of age-related macular degeneration. *American Journal of Ophthalmology*, *160*(3), 602-607.e1. https://doi.org/10.1016/j.ajo.2015.05.030